論文 / 著書情報
Article / Book Information

題目(和文)	水銀を含む超伝導銅酸化物における不可逆磁場の向上とピーク効果の解明
Title(English)	Elucidation of the mechanism for peak effect and control of the magnetic irreversibility of superconducting mercury copper oxides
著者(和文)	赤尾尚洋
Author(English)	
出典(和文)	学位:不明, 学位授与機関:東京工業大学, 報告番号:甲第4397号, 授与年月日:2000年3月26日, 学位の種別:課程博士, 審査員:山内 尚雄
Citation(English)	Degree:, Conferring organization: Tokyo Institute of Technology, Report number:甲第4397号, Conferred date:2000/3/26, Degree Type:Course doctor, Examiner:
学位種別(和文)	博士論文
Type(English)	Doctoral Thesis

Elucidation of the Mechanism for Peak Effect and Control of the Magnetic Irreversibility of Superconducting Mercury Copper Oxides

A Thesis Submitted to
the Interdisciplinary Graduate School of
Science and Engineering

Through the Department of Innovative and
Engineered Materials,

TOKYO INSTITUTE OF TECHNOLOGY

In Partial Fulfillment of the Requirements for the Degree of
Doctor of Engineering

by

Takahiro AKAO

97D28010

Supervisier : Professor Hisao YAMAUCHI

14th March, 2000

ABSTRACT

Superconducting mercury cuprates have superconducting transition temperatures (T_c) being higher than those of any other superconductors known to exist. However the mercury cuprates have not been considered as promising materials for applications. This is mainly because the magnetic irreversibility-field (H_{irr}) characteristics is not superb and their critical current density (J_c) still remains quite low, as compared to *e.g.* $CuBa_2YCu_2O_{7-\delta}$ ("Y-123"). It has been suggested that the H_{irr} characteristics may be improved by either (i) introducing appropriate lattice defects for pinning the quantized flux *i.e.* flux pinning centers , or (ii) reducing the electronic anisotropy in superconductivity parameters. So far no effective pinning centers have been established for the mercury cuprate superconductors. On the other hand for (ii) Yamauchi *et al.* recently proposed that the anisotropy could be reduced by controlling the hole distribution along the direction perpendicular to the CuO_2 planes such that it may be more homogeneous.

On the other hand, "peak effect" or "fish-tail phenomenon" has been known (as the secondary peak besides the zero-field peak) in the magnetization hysteresis curve for type-II superconductors. This peak effect is attractive from the view point of applications as the J_c value could be enhanced at high magnetic fields. Some origins for the effect have been discussed, but they still remain controversial.

In the present research, (a) enhancement in the irreversibility field of both the second (Hg-1212) and the third (Hg-1223) members, and (b) elucidation of the mechanism of peak effect in (Hg,Pb)(Ba,Sr)-1223, are focused.

Enhancement of Irreversibility field characteristics

Hg-1212

The second member of the Hg-12(n-1)n homologous series, *e.g.* $HgBa_2CaCu_2O_{6+\delta}$ (with T_c~125 K) has two possible sites for hole creation and/or annihilation, one being the Ca site in the bare (or oxygen-free) Ca layer between two adjacent CuO_2 planes and the other the oxygen site in the charge reservoir (CR) block, *i.e.* HgO_δ. In order to control the hole distribution, solid solutions $HgBa_2(Ca_{1-x}Y_x)Cu_2O_{6+\delta}$ ($0 \le x \le 0.5$) were H_{irr}-vsynthesized by a conventional encapsulation technique and then post-annealed by a high-pressure oxidization technique. The total amount of doped holes depends on both the amount of Y substitution for Ca, x, and that of excess oxygen in the HgO_δ layer, δ. The former would reduce and the latter would increase the total amount of holes. The H_{irr} -vs.- T/T_c characteristics was remarkably improved by heavy oxygen doping only, however, the suppression of T_c was accompanied with increasing of the heavy oxygen doping.

On the other hand, the most enhanced H_{irr} - T characteristics was obtained for the sample in which holes were doped from multiple sites by means of not only high-pressure oxidization but also light substitution of Y for Ca (by~10 %). Accordingly, these results indicate possible tailoring of HTSC materials by controlling the hole-density distribution.

Hg-1223

The magnetic irreversibility study was carried out for the Hg-1223 single crystals with Hg and Ba partially substituted by Pb and Sr, *i.e.* (Hg,Pb)(Ba,Sr)-1223. Significant enhancement in the irreversibility-field characteristics was achieved for a (Hg,Pb)(Ba,Sr)-1223 compound as compared with the Sr-free (Hg)(Ba)-1223 compound. The Sr substitution for Ba worked effectively to improve the magnetic irreversibility. This was in good agreement with previous works. Furthermore the bond valence calculation suggested the hole density distribution in a (Hg,Pb)(Ba,Sr)-1223 compound was more homogeneous than that in the Sr-free Hg(Ba)-1223 compound. This revealed that the hole density distribution is most likely responsible for the significant enhancement in the magnetic irreversibility field characteristics of the present sample in which Sr was partially substituted for Ba.

Elucidation of the mechanism of the peak effect in (Hg,Pb)(Ba,Sr)-1223

Single crystals of $(Hg,Pb)(Ba,Sr)_2Ca_2Cu_3O_{8+\delta}$ have been successfully grown and prominent peak effect has been observed for the magnetization hysteresis loops. H_{irr} property also improved higher than those for other (Hg or Tl)-1223 compounds due to the hole distribution homogenized by Pb and Sr substitutions. The structure of the single crystal was studied in order to elucidate the origin of the peak effect by means of various microscopic analysis techniques.

A typical HRTEM image of the (001) plane showed somewhat distorted structure. In a SAED pattern with incident beam parallel to [001] for the region corresponding to the HRTEM image, sharp streaks were observed along <110> at each spot. From the dimension of the streaks, some long-period irregularities of tens nanometer order can be expected to exist.

Compositional analysis on the (001) plane was carried out by TEM-EDS with a probing beam of 1 nm diameter along a <110> direction. A compositional modulation, i.e. periodic fluctuation in the Hg and Pb ratio have been observed, while no spatial variations were seen for other cations. The distribution of Hg and Pb can be approximated by a sinusoidal curve with the period of ~18 nm. This value is in good agreement with the irregularity dimension (of tens nm) previously estimated from the SAED data. Considering, the Pb rich phase would have lower T_c than the matrix, the compositional modulation are supposed to act as "δT_c" pinning.

Taking into account the observed facts that (1) the ratio of Hg and Pb was nearly 1:1, (2) the distributions of Hg and Pb were approximated by sinusoidal curves, and (3) the streaks in the [001] SAED pattern indicated long-range modulations of tens nanometers, the observed modulated structure may be considered to be yielded via spinodal decomposition.

Consequently, such a spinodal-wave-like inhomogeneity is likely to yield mesoscopically distributed weak pinning centers to cause the peak effect.

Contents

Chapter I Introduction

In this chapter the basis of the present study is introduced. Firstly, the history of high-T_c superconductors (HTSC) is skimmed over. Then, some general features of HTSC with which this work is concerned are mentioned. Finally the objectives and significance of this study are stated.

1-1 Historical review of "high-T_c superconductivity"

1-1-1 Definition of "high-T_c superconductivity"

What definition is applied to "high-T_c superconductivity"? It must be distinguished from "low-T_c superconductivity" (or "conventional superconductivity") based on the value of T_c. One possible criterion concerning the value of T_c is obtained from the BCS theory [1] which predicted that the maximum T_c value should be 30~40 K in solid materials. This prediction worked for all the superconductors which had existed before the discovery of superconductivity at ~35 K in the "La-Ba-Cu-O" system by Bednorz and Müller [2]. From this point of view, one may say that high-T_c superconductivity is a phenomenon to which the BCS theory is not applicable. In other words, we may call the superconductivity above 30 K as "high-T_c superconductivity", though there are some exceptions. One of them is the case where a material initially exhibits high-T_c superconductivity but sometimes turns to show a T_c value lower than 30 K without any significant structural changes in the material. The presently most strict criterion to distinguish whether it is BCS-like or not is for the symmetry of the superconducting electron pair to be s-wave-like or not. This is, however, out of the scope of this thesis.

1-1-2 Brief introduction of HTSC

The discovery by Bednorz and Müller in 1986 broke the record high value of T_c (see Fig.1.1). Thereafter numbers of new HTSC materials have been synthesized. It is worthwhile to note that all of them are copper oxides. The value of the highest T_c has been raised year by year. Soon after the discovery, Wu *et al.* [3] synthesized an Y-Ba-Cu-O compound which showed a T_c above the boiling temperature of liquid nitrogen for the first time. In 1988, compounds in the "Bi-Sr-Ca-Cu-O" [4] and "Tl-Ba-Ca-Cu-O" [5, 6] systems achieved T_c's higher than 100 K. At present a compound of the "Hg-Ba-Ca-Cu-O" system [7, 8] has the record high T_c of 135.4 K under ambient pressure [9]. Furthermore, under a pressure higher than 11 GPa, T_c has been recorded at ~150 K or higher [10]. Although there have been a variety of progress in the field of HTSC, one may say the highest values of T_c seems to have

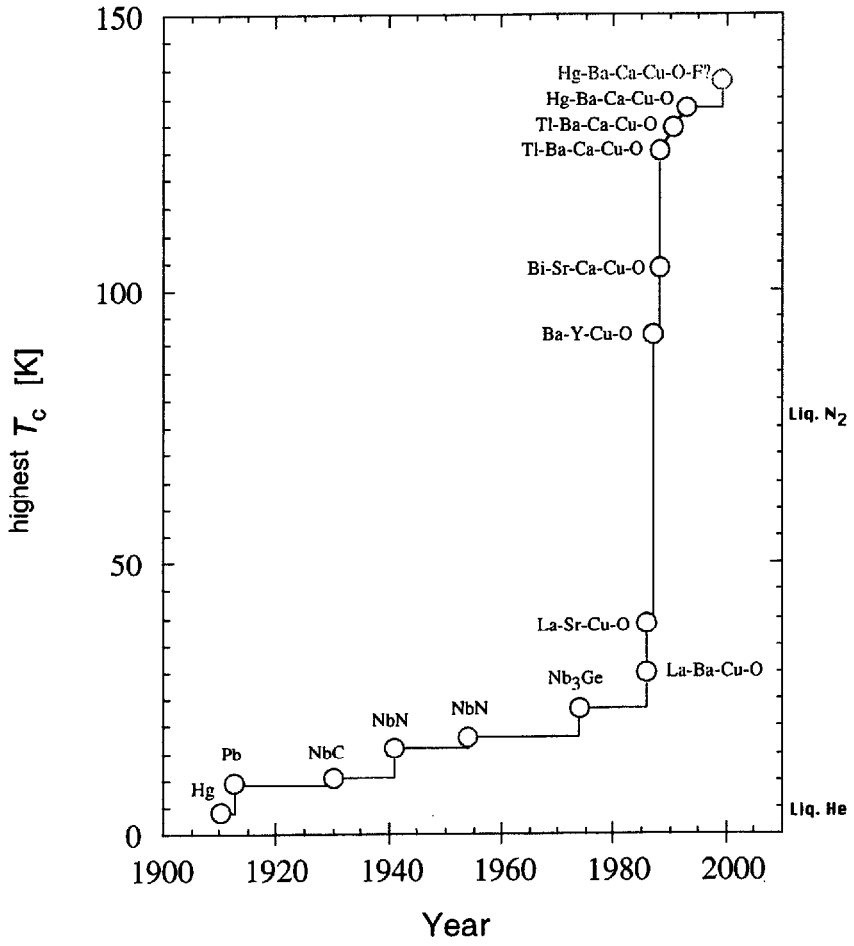

Fig. 1.1. The highest value of critical temperatures in year

been leveled off in recent years. Accordingly the stage of HTSC research has been shifting from "alchemy" to "chemistry". This means that the "real" chemical approaches have been recognized to be important and indispensable. Therefore, representative chemistry approaches to understanding the phenomenon of HTSC are overviewed in the following.

1-2 Structural classification of HTSC

1-2-1 Homologous series

High-T_c superconductors essentially have a layered structure with the block consisting of alternately stack of the CuO_2 layers ("superconductive" block) and the "blocking" block as shown in Fig.1.2. For tailoring novel materials, classification of the structures of superconductive cuprates is indispensable. From this point of view, the general classification based on the concept of "homologous series" advocated by Yamauchi *et al.* [11] is useful. Here the structure of a typical homologous series is explained as an example [11, 12].

In Fig.1.2., the crystal structure of high-T_c superconductive copper oxides is built up by piling $M_mO_{m\pm\delta}$ perovskite/rock-salt type block, a $Q_{n-1}Cu_nO_{2n}$ perovskite-type block and two AO rock-salt type planes. The $M_mO_{m\pm\delta}$ block is called "charge-reservoir" block because the block generally acts as a donator of holes generated by excess charge due to charge balance of cation (M) and anion (O) in the block. Note that most HTSC's have holes which carry the superconducting current. Therefore such HTSC's are of the "p-type". On the other hand, it has been empirically known that compounds of the "n-type" have electrons as charge carriers for superconducting current. The block, $Q_{n-1}Cu_nO_{2n}$, is commonly found in all p-type HTSC's. In this block, the CuO_2 planes are most likely responsible for the superconducting current. When the number, n, is higher than 1, a layer of "bare" alkaline-earth or rare-earth cations (Q) intercalates into two adjacent CuO_2 planes. The AO rock-salt type plane (where A represents an alkaline-earth or a rare-earth element) provides spacing between the charge-reservoir block and the $Q_{n-1}Cu_nO_{2n}$ block. Accordingly a general expression for the n-th member of a "homologous series" is given by $M_mA_2Q_{n-1}Cu_nO_{m+2+2n\pm\delta}$ or simply by an abbreviation, M-m2(n-1)n. The majority of the structures of HTSC's is represented by this formula which is valid for homologous series of "Category A" [13].

1-2-2 Universal relationship – T_c vs. number of CuO_2 planes –

In each homologous series known to exist, the maximum value of the critical temperature, $T_{c,max}$, shows a universal dependence on the number of CuO_2 planes, n, as shown in Fig. 1.3. [13, 14] The n = 3 member has the highest value of T_c in each series. Here, a question arises: why does the phase with n = 3 always mark the highest T_c in a homologous

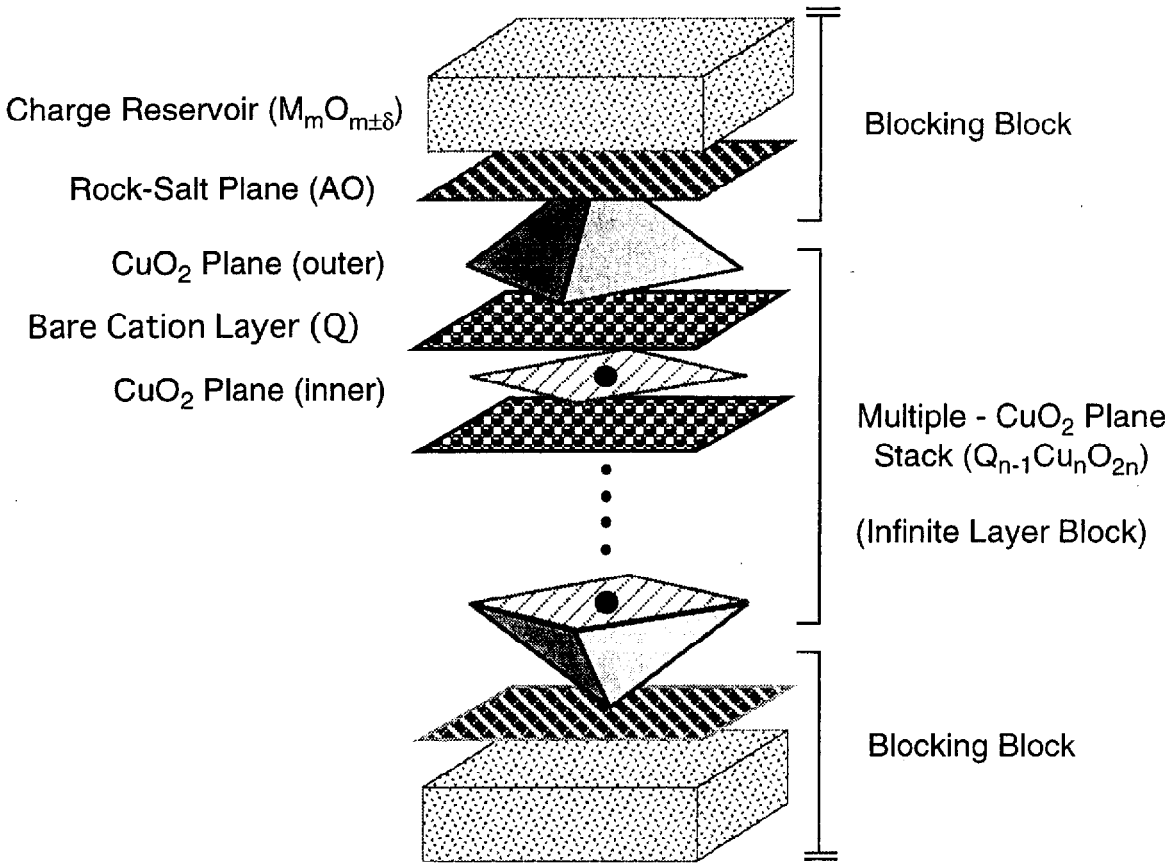

Fig. 1.2. Structure of M-m2(n-1)n homologous series of superconducting copper oxides. (After ref. 11)

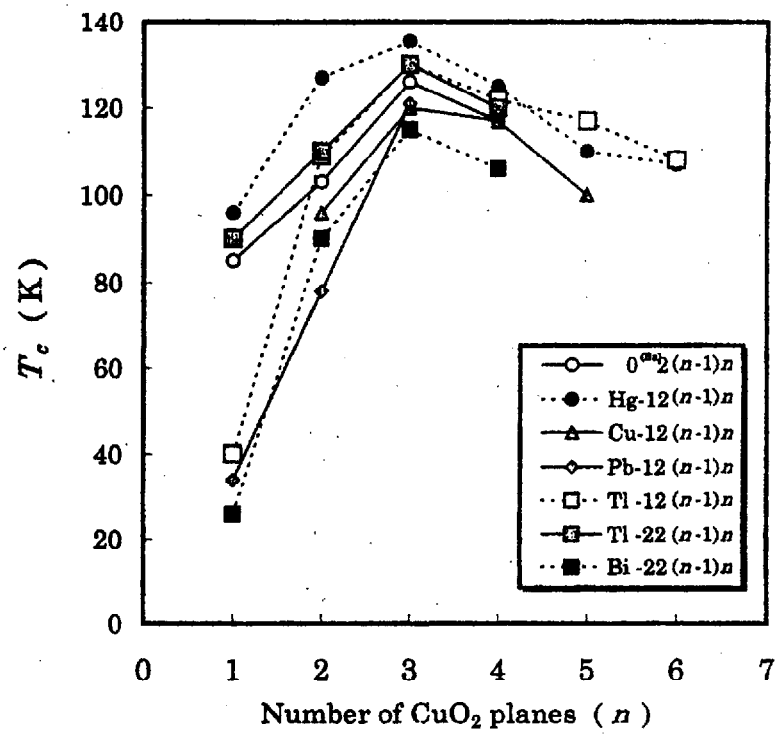

Fig. 1.3. Relationship between maximum T_c and number of CuO_2 planes, n for various homologous series, M-m2(n-1)n. The n=3 member of each homologous series most likely has the highest $T_{c,max}$ in the series.

series? It has been suggested that this is related with local confinement of the hole carriers [13].

1-3 Mercury based HTSC

As shown in Figs. 1.1 and 1.3, the mercury copper oxides have the record high values of T_c for the phases with n=1, 2 and 3 at present. Here general features of these fascinating materials are described in the following.

1-3-1 Introduction

In 1991, Putilin *et al.* synthesized mercury based 1212-type cuprates containing a rare earth element (*RE*), namely $HgBa_2RECu_2O_{6+\delta}$. [15]. However, due to low hole concentrations, no superconductivity was found in these compounds. Two years later, however, Putilin *et al.* [7] finally induced superconductivity of $T_c = 94$ K in $HgBa_2CuO_{4+\delta}$. It may be worthwhile to point out that the first superconductivity in mercury-containing copper oxides, in a broad sense of the word of mercury copper oxides, $(Pb,Hg)Sr_2(Ca,Y)Cu_2O_7$ was reported by Hu *et al.* [16] by substituting Hg for Pb in the Pb-1212 phase [17, 18]. However, the mercury-containing copper oxide showed a rather low value of T_c (~ 90 K) for a second member of the Hg-12(n-1)n homologous series.

The compound, $HgBa_2CuO_{4+\delta}$, reported by Putilin *et al.* is nothing but an n = 1 member of homologous series Hg-12(n-1)n, *i.e.* Hg-1201. Immediately it was anticipated that the higher T_c's would appear for the higher members of the series. In fact, soon after the discovery, a Hg-1223 sample with T_c of 133.5 K was reported by Schilling *et al.* [8]. At present members of the homologous series, Hg-12(n-1)n, have been confirmed to exist for n = 1, 2, 3, ···8 [19]. The value of T_c = 135.4 K [9] under ambient pressure has been the highest since 1994. It must be noted, however, that recently Putilin *et al.* [20] reported $T_c \cong 138$ K with a significantly strong Meissner signal for a fluorinated Hg-1223 compound. Moreover, the n-th member of the Hg-12(n-1)n series has the highest value of T_c among all the n-th members of other homologous series. This fact makes the members of the Hg-12(n-1)n series highly attractive from the view point of not only science but also engineering.

1-3-2 Crystal structure

Crystal structures of the n = 1, 2 and 3 members of homologous series, Hg-12(n-1)n, in the "Hg-Ba-Ca-Cu-O" system are shown in Fig. 1.4 [21]. The oxygen site in the HgO_δ layers is represented by lighter colored circles to indicate relatively high oxygen deficiency at the site. Each Hg forms a "dumbbell-type" bonds like O-Hg-O along the c-axis. This provides the

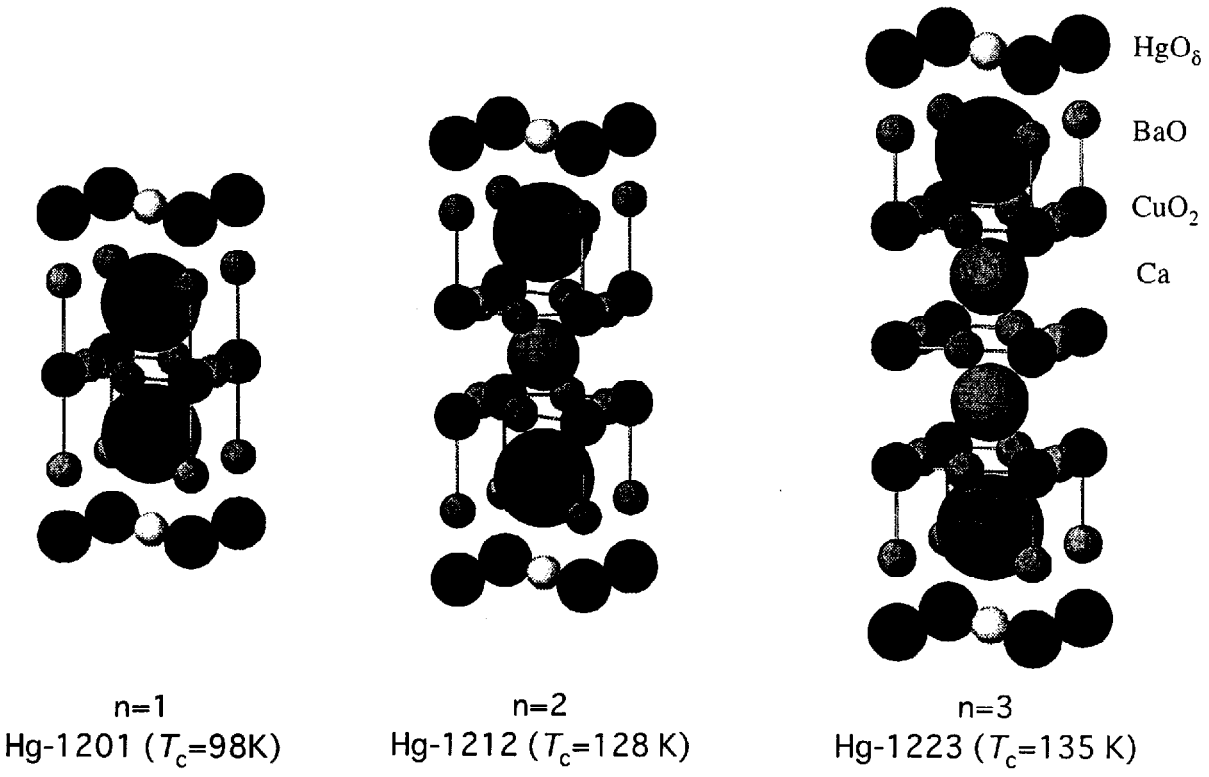

Fig. 1.4. Crystal structures of $HgBa_2Ca_{n-1}Cu_nO_{2(n+1)+\delta}$ [Hg-12(n-1)n] (n= 1, 2, 3)

members of Hg-12(n-1)n with a distinct feature, *i.e.* a the long $Cu_{(pyramidal\text{-}plane)}$-$O_{(pyramidal\text{-}apical)}$ bond length. This is likely responsible to their higher T_c's. The Cu-O bonds are emphasized by rods in this figure because they should have higher degree of covalency than other bonds.

1-3-3 Synthesis

High-purity mercury based copper oxides have not been obtained by conventional synthesis methods including solid-state reaction. The synthesis procedure is rather more complicated than those for other HTSC's mainly because of high vapor pressure of mercury and its toxicity. This situation has caused a large variation in the sample preparation technique. Even only for bulk-sample preparation, there have been reported various techniques which may be generally classified into two major categories:

(I) Encapsulation Techniques

(1) Precursor method [8, 22-24]

In this method the precursor(s) which contains two or more metallic elements except for mercury is calcined prior to sintering when mixed with HgO. The activity of a precursor which contains Ba source is extremely high against humidity and carbon dioxide. Most of the precursors are prepared by decomposing a nitrate mixture or by a sol-gel method [25, 26].

(2) Single-firing method [9, 27-29]

Simple oxides (usually mono-oxides) of all the cations (including HgO) are mixed at once. This method allows us to obtain relatively high-purity samples when sintered at a low temperature (625~665 °C) for a long period (~70h). The phase purity of the final product strongly depends on the purity of BaO.

(II) High-Pressure Methods [22, 30-33]

Sintering is carried out at a relatively high temperature (800~1100 °C) under an ultra-high-pressure of 1.8~5.0 GPa generated by means of a belt-type or a cubic-anvil-type high-pressure apparatus. Sometimes, a high-pressure up to 1.1 GPa is applied through an argon gas pressure [33]. Usually, the purity of precursor does not strongly affect the phase formation. The product usually has high density and less superconductivity weak links.

In the type-(I) methods, high sensitivity of the Ba source to carbon dioxide is due to unstable Ba-O bonds. Moreover the humid environment tends to promote this type of instability. The $(CO_3)^{2-}$ groups brought into the capsule prevents the formation of the aimed

phase, whereas in the high-pressure synthesis the phase is possible to form because the $(CO_3)^{2-}$ can be incorporated into the matrix [34, 35].

1-3-4 Cation substitution

Since the preparation of superconductive compounds of the Hg-Ba-Ca-Cu-O system is rather difficult, there have been a number of attempts to improve the chemical process by cation substitutions. Some of the attempts made previously are listed below.

(i) Cation substitution for Hg : In [36], Re [37], Au [38], Tl [39, 40], Pb [41-43] and Bi [44, 45]

(ii) Simultaneous cation substitutions : M for Hg and Sr for Ba where M = V [46], Cr [47, 48], Ga [49], Mo [50, 51], Re [37, 50, 52] and Pb [16, 53, 54].

Note that all of these substituents have a higher valence than that of Hg^{2+}, yielding extra oxygen which partially fills vacantsites around the Hg site. This works effectively to stabilize the phase. Furthermore, remarkable improvements in the magnetic characteristics have been reported in particular for the substitution of Sr for Ba [37, 55, 56].

(iii) Substitution of *RE* for Ca (only for the case of the Hg-1212 structure): where *RE* = Y [16, 49-51], Dy [57], Sm [58], Nd [59] and other *RE*'s [15, 60]
To control the amount of carriers / hole concentration, cation substitution of this type is useful since the $HgBa_2(Ca_{1-x}RE_x)Cu_2O_{6+\delta}$ system usually has a wide solid-solution region.

Additionally, for the study on phase formation, the substitution of C [34, 35] and S [35] for Hg has been investigated.

1-3-5 Single crystal growth

Single crystals of the Hg-12(n-1)n phases (with n = 1, 2 and 3) have been obtained by mechanically separating large grains from the bulk samples prepared by an encapsulation technique [45, 46, 61-63]. Another effective technique for growing large single crystals (especially of the higher n-th members) is the application of a high-pressure synthesis using argon gas [33, 64-66].

With single crystals, more specified (in terms of the orientation) data for various physical properties such as the structure [62, 64, 65] and the magnetic characteristics [45, 46, 67, 68] etc. may be obtained.

1-4 Hole doping

1-4-1 Backgrounds

For the HTSC copper oxide system, the temperature -vs.- hole concentration diagram shows common features [69, 70] as schematically shown in Fig. 1.5 (a). The parent phase usually shows an anti-ferromagnetic ordering with a Néel temperature (T_N) of several hundred K. As the hole concentration increases, T_N drops and the bulk anti-ferromagnetism disappears, being replaced almost immediately by superconductivity. In the so-called "under-doped" region, T_c rises up to a maximum value at which the amount of holes per unit cell is said to be optimized. Then T_c falls again toward zero in the "over-doped" region. Empirically it is known that the curve of T_c vs. hole concentration shows a parabolic/"bell" shape [71]. This phase diagram is extremely important in controlling T_c as a function of the average hole concentration in a HTSC. The values of such average hole concentration are usually defined from the charge-balance between the hole amount and the excess oxygen determined by chemical titrations such as thermogravimetry, iodometry and coulometry [72].

In the chemical approach, the hole concentration in the CuO_2 plane is regarded as a mixed valence as value of Cu based on the assumption that all other elements including O have a nominal valence as appears in the steric environment. Even if the structure has multiple CuO_2 planes in the unit cell, the Cu valence should be determined commonly for each inequivalent Cu site. In such a calculation scheme, the Cu valence is directly connected with the O content, namely δ in the charge-reservoir, $M_mO_{m\pm\delta}$ (see Fig. 1.2.). Thus the "nominal Cu valence" may be given as follows [72]:

$$V_{Cu,nom} = 2 + [\,-C_{CR} - 2C_{RS} - (n-1)V_Q + 2n] / n\,, \qquad (1.1)$$

where C_{CR}, C_{RS} and V_Q, are the nominal charges of the charge-reservoir block, the rock-salt AO plane and the "bare" cation Q (Ca^{2+} and/or Y^{3+}), respectively. The nominal charge of the charge-reservoir block depends on the nominal valence $V_{M,nom}$ of the metal constituent M and the excess oxygen δ, *i.e.* $C_{CR} = mV_{M,nom}-2(m\pm\delta)$. The nominal charge of the rock-salt plane, C_{RS} is equal to zero in most of the cases. Furthermore, the average nominal hole concentration is defined by :

$$p_{nom} = V_{Cu,nom} - 2\,. \qquad (1.2)$$

Quantity p_{nom} can be used as the variable in the horizontal axis of the phase diagram shown in Fig. 1.5.(a). However p_{nom} is far from being the universal variable to control most of the superconducting properties. Then there have been many attempts to establish the

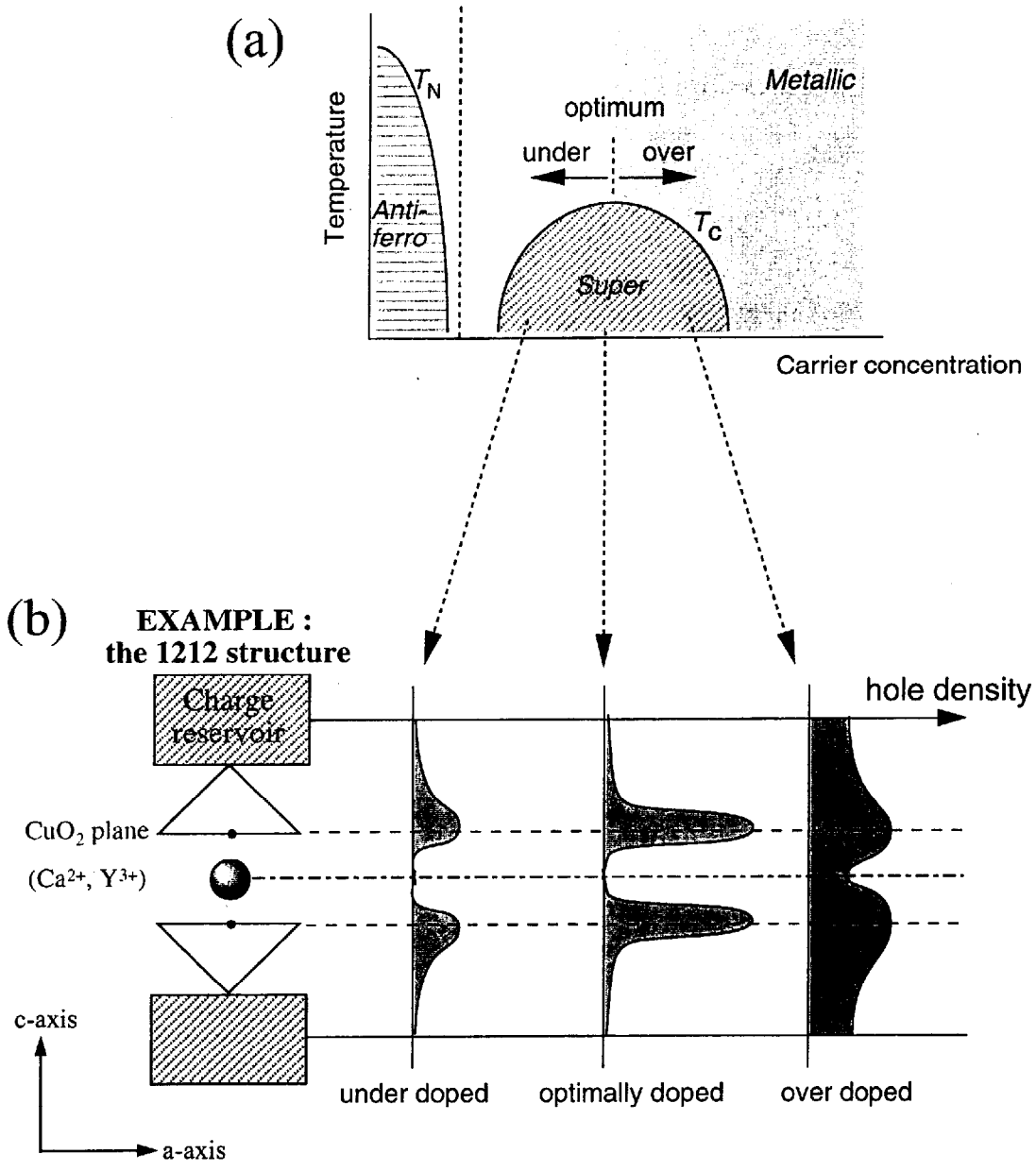

Fig. 1.5. Schematic pictures of correlation between (a) a typical electric phase diagram and (b) projective hole density distributions along layers in the unit cell (the 1212 structure is chosen for example) of the high-T_c superconductors.

universal factors determining the superconducting properties. Some examples of such efforts are:

(i) Bond valence sum (BVS):

The distinct valence values at different atomic sites estimated through the BVS method [71, 73-77] provides us with the knowledge of how the excess charge is redistributed over different sites

(ii) Cu-O bond length (in-plane):

The in-plane Cu-O bond length is closely related to the amount of hole concentration in the CuO_2 planes [71, 78]. The main relation is that, the higher is the hole concentration in the CuO_2 plane, the shorter is the Cu-O bond length since hole doping removes the anti-bonding electrons from the bond. This relationship seems to be meaningful as long as the "A" element remains the same (*e.g.* Sr, Ba or La).

(iii) Muon-spin relaxation (μSR):

The superconducting carrier concentration, n_s, can be estimated by a μSR study [79]. The precession of muons in a solid constituents a microscopic probe of the distribution of local magnetic fields, and in particular the width of the muon spin relaxation signal from a superconductor provides an estimate of this field distribution and the penetration depth λ. From this penetration depth, the value of n_s is evaluated by this relation:

$$\sigma \propto 1/\lambda^2 \propto n_s/m^* . \qquad (1.3)$$

Here, σ is the muon relaxation rate and m^* is effective mass of the superconducting carrier. A universal relation between T_c vs. n_s/m^* was first given by Uemura *et al.* [79]. More μSR studies have been reported for the Bi-2212 single crystal [80], Re-doped Hg-12(n-1)n [81, 82], etc.

(iv) Lower critical field (H_{c1}):

The superconducting carrier concentration, n_s may be estimated from the lower critical field H_{c1} [83, 84], *via* following relationship:

$$H_{c1} = (\Phi_0/4\pi\lambda^2) \ln\kappa \propto n_s \qquad (1.4)$$

where Φ_0 is a flux quantum and κ is a Ginzburg-Landau parameter [85]. Here, the proportionality of H_{c1} to n_s is valid only if κ and m^* are constants.

(v) Thermo-electronic power (TEP):

The TEP signal could show the type of carriers and the degree of carrier concentration [86-90].

1-4-2 The concept of "hole density distribution"

Yamauchi and Karppinen previously proposed the concept of "net holes" as calculated through a BVS method [14]. This concept allows us to consider the distribution of hole density across the unit cell. Furthermore, concerning the way how "net holes" are doped into the CuO_2 planes, it is enough to deal only with three different types of hole doping route [91, 92]. Concerning the crystal structure around the CuO_2 planes (Fig.1.2), the in-plane Cu has two different kinds of Cu-O bond: one with an apical oxygen (O_{api}) and the other with a neighboring in-plane oxygen (O_{pl}). Accordingly, the three doping routes work for inducing holes into the CuO_2 plane [92],

(1) by shortening the Cu_{pl}-O_{api} bond (only into the outer CuO_2 plane),

(2) by elongating the effective O_{pl}-A bond (only into the outer CuO_2 plane), and

(3) by elongating the O_{pl}-Q bond (only into the inner CuO_2 plane).

Whole holes are doped only through these doping routes into the CuO_2 plane, as previously mentioned. Especially, the concentrations of holes at inequivalent CuO_2 planes in the superconductive block are needed to be distinguished.

Examining the distribution of holes over the crystals of M-m2(n-1)n (M = Cu, Ga, Tl, Hg ; m = 1, 2 ; n = 3, 4, 5) phases, Karppinen and Yamauchi found that the "net hole" concentration in the inner CuO_2 plane(s) is significantly higher than that of the outer ones [14, 92]. For the sake of quantitative analysis, the degree of hole confinement in the inner plane(s) may be defined as follows [92]:

$$\text{"hole confinement"} \equiv p(CuO_2)_{inner} - p(CuO_2)_{outer} \cdot \qquad (1.5)$$

They found a relationship between quantities, "hole confinement" and T_c, such that T_c is roughly proportional to "hole confinement". This result provides us with a significant conjecture that the higher "hole confinement" can realize the higher T_c value. Furthermore, it is worthwhile to point out that cuprates of the "infinite-layer" structure doped with holes, in which holes cannot be confined in principle do show no superconductivity [93, 94], implying that the hole confinement is necessary for high-T_c superconductivity to occur. Judging from the above mentioned framework, schematic images of the hole density distribution along the c-axis for three different doping states are drawn in Fig. 1.5 (b) for the case of the 1212 structure. So far, however, there have been no direct measuring methods of hole density in

inequivalent CuO_2 planes because of low resolutions of any techniques known to exist. Thus further progress is required in the techniques for detecting the distribution of hole density. Possible candidates for such techniques are given in the following:

- Nuclear magnetic resonance (NMR) including nuclear quadrupolar resonance (NQR) spectra are sensitive to the immediate chemical environment of the nucleus being observed, to the local magnetic field and field gradient, and in the case of quadrupolar nuclei ($I > 1/2$), to the crystal field symmetry. Relaxation time measurements determine the efficiency of spin-energy transfer to the lattice. Many investigations have been carried out in the field of high-T_c superconductivity, examples are for Hg-1223 [95, 96], for Bi- [97, 98] and Tl- [99] systems with ^{17}O which provides a more site specific sensitivity.
- Electron energy loss spectroscopy (EELS) [100] has been utilized to observe an unoccupied state in O-*K* edge and/or Cu-L_3 edge. Particularly, the O-*K* edge fine structure shows pre-edge peaks. By combining the results of band-structure calculations [101, 102], these pre-edge peaks have been assigned to holes in different orbitals which are constituents of the valence band [103-105].
- X-ray absorption near edge structure (XANES) using synchrotron radiation provides basically same knowledge as that obtained in EELS study, however, the XANES investigation has more advantages for precise analysis especially as to the signal / noise ratio. Furthermore the XANES studies using polarized photon have been quite successful in measuring the electronic structure near the Cu-O bonds for the single crystals of HTSC's [106-109]. Additionally, the XANES spectrum of the constituent metal is also utilized for determination of the metallic valence state in the solid [110-112]. The Cu-L_3 [106-108, 113] and Cu-*K* [111, 112, 114, 115] edges also show the hole characteristics as the shoulder of the edges.
- Convergent beam electron diffraction (CBED) method has been utilized to study a precise crystallographic symmetry so far. In recent years, however it becomes possible to determine the charge distribution in the crystal by comparing with the calculated intensity based on the dynamical theory of Bloch-wave. Although some investigations have been carried out to develop the technique which can determine the hole distribution in HTSC crystals [116, 117, 118,], there are still some obstacles before establishment as the method.

1-5 Magnetic irreversibility field characteristics

Superconductors possess characteristic critical values for the three major variables, temperature (T_c), magnetic field (H_c) and supercurrent density (J_c), as schematically shown in Fig.1.6. In this figure, the superconducting state appears in the region surrounded by the three critical boundaries. Note that in most HTSC materials, magnetic upper critical field, H_{c2} cannot be directly detected because it is not an experimentally detectable quantity anymore.

For a conventional type-II superconductor the supercurrent disappears very sharply at an applied field just below the upper critical field (H_{c2}). However, the HTSC copper oxides behave differently: the supercurrent gradually diminishes with increasing the applied field strength and then it vanishes at a certain field well below H_{c2}. This means that there is a region where the material shows a substantial resistance corresponding to energy dissipation due to flux flow, being separated from the region in the H-T plane at lower fields where the resistance is zero. The boundary between the regions is now usually referred to as the irreversibility line [85]. The boundary is represented by a specific field called the magnetic irreversibility field (H_{irr}) which is a function of temperature (often normalized by T_c).

The irreversibility field can be determined by several methods, for example, transport measurement, magnetization measurement and AC susceptibility measurements. Moreover, as for the magnetization measurement, a variety of methods using, *e.g.* a superconducting quantum interference device (SQUID) magnetometer, a vibrating sample magnetometer (VSM) and magnetic torque measurements, yield slightly inconsistent results originating from the difference in the time constant of measurement [119].

Quantity H_{irr} is defined as the value of magnetic field at which the current density equals to zero;

$$H_{irr} \equiv \mathrm{H} \mid_{J_c \to 0} \ . \tag{1.6}$$

This determination method for H_{irr} value, namely "extrapolation criterion method", was established by Yamauchi *et al.* [120-122]. Now, as long as the intra-grain current density is concerned, J_c can be evaluated from the magnetization hysteresis width (ΔM) and the grain size (d) via the well-known critical-state model, *i.e* Bean's model [123] (for a slab shaped superconductor):

$$J_c = 20\ \Delta M/d \ . \tag{1.7}$$

Then, H_{irr} is defined as the value of magnetic field at which the difference between increasing

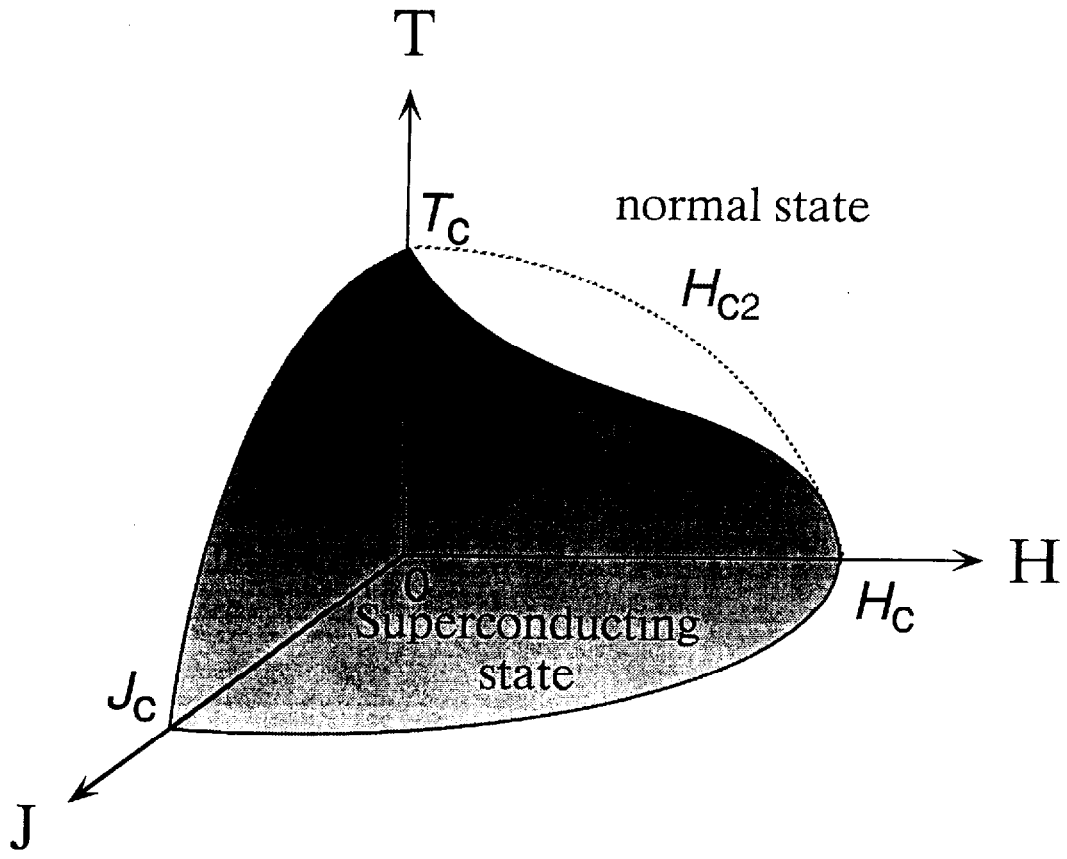

Fig. 1.6. 3 D correlation among three critical values, the H_c, J_c and T_c in the HTSC's.

and decreasing branches of the magnetization hysteresis loops are extrapolated to zero [121, 122, 124],

$$H_{irr} \equiv H \mid_{\Delta M \to 0} \cdot \tag{1.8}$$

By using this method, we can avoid the uncertainty which comes from estimation of the *d* value, as Nakane *et al.* pointed out [122]. The procedure to determine H_{irr} is illustrated in Fig. 1.7. It is worthwhile to point out that the values of H_{irr} measured by different techniques are not always agreeable and also the H_{irr} value depends on the sample size [125, 126].

Although a great deal of efforts have been made on the theoretical interpretation for the magnetic irreversibility phenomenon, it still remains unsettled. Some of the causes include (1) the vortex phase transformation from glass [127] to liquid [128], (2) thermally activated de-pinning [129, 130], and (3) vortex-lattice melting [131]. Accordingly, it is hard to construct a universal phase diagram for all the HTSC's because of various factors originated from individuality of the materials.

Figure. 1.8. shows the irreversibility lines for typical HTSC's, all of which show linearity in the log(H) - log(1-T/T_c) plot, indicating the relation:

$$H_{irr} = A(1-T/T_c)^{\alpha}, \tag{1.9}$$

where A is a constant and α is an exponent. Here, constant A corresponding to the value of H_{irr} at T$\rightarrow$ 0 K might be influenced by the vortex pinning strength [132]. In the log(H) - log(1-T/T_c) plot, the superior irreversibility-field characteristic curve generally lies at the upper left region showing the milder gradient, *i.e.* with the lower value of α. This empirical rule implies the strong relation between H_{irr} and the dimensionality of the superconductivity [125]. The typical values of α for representative HTSC materials are: ~1.5 for Cu-1212:P , 2~3 for Hg-1212 [133] and Hg-1223 [133], 4~5 for Bi-2212 [134].

From the application point of view, the higher J_c under the higher field is desired. As for the mercury based superconducting copper oxides, there have been reported many investigations of the magnetic irreversibility characteristics not only for pristine materials of Hg-12(n-1)n with n = 1 [68, 135, 136], = 2 [133, 137] and = 3 [132, 137], but also for those with cation substitution of Hg by Pb [42, 138, 139], Bi [45] and Re [37, 140, 141], and of Ba by Sr [55, 56, 142]. In the latter case, the Sr substitution has caused drastic improvement in the irreversibility field characteristics at higher temperature regions. A conventional explanation that the large enhancement has been interpreted as caused by an enhanced inter-

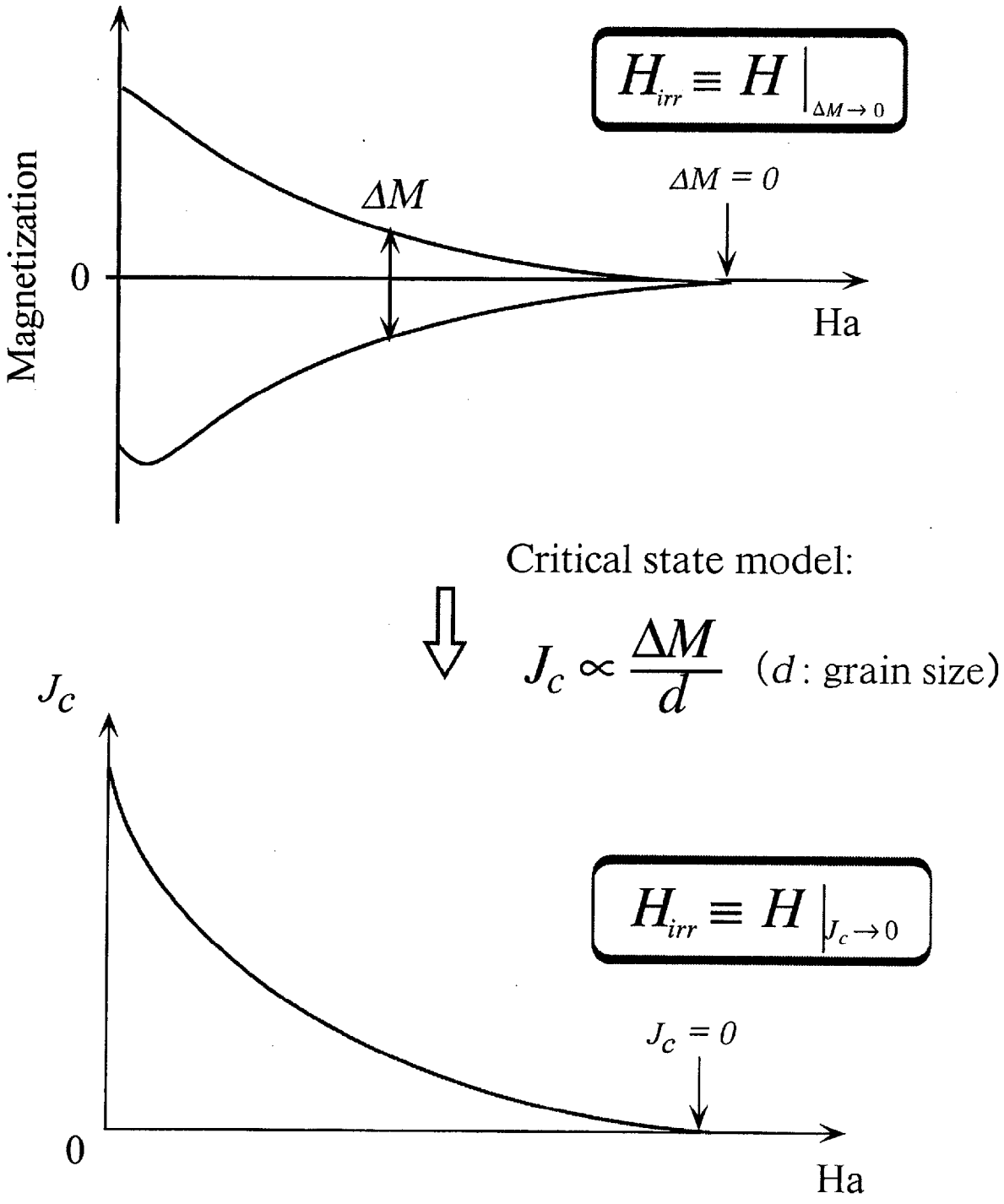

Fig. 1.7. Determination of the H_{irr} from M-H curve and from corresponding J_c-H characteristics derived through the critical state model.

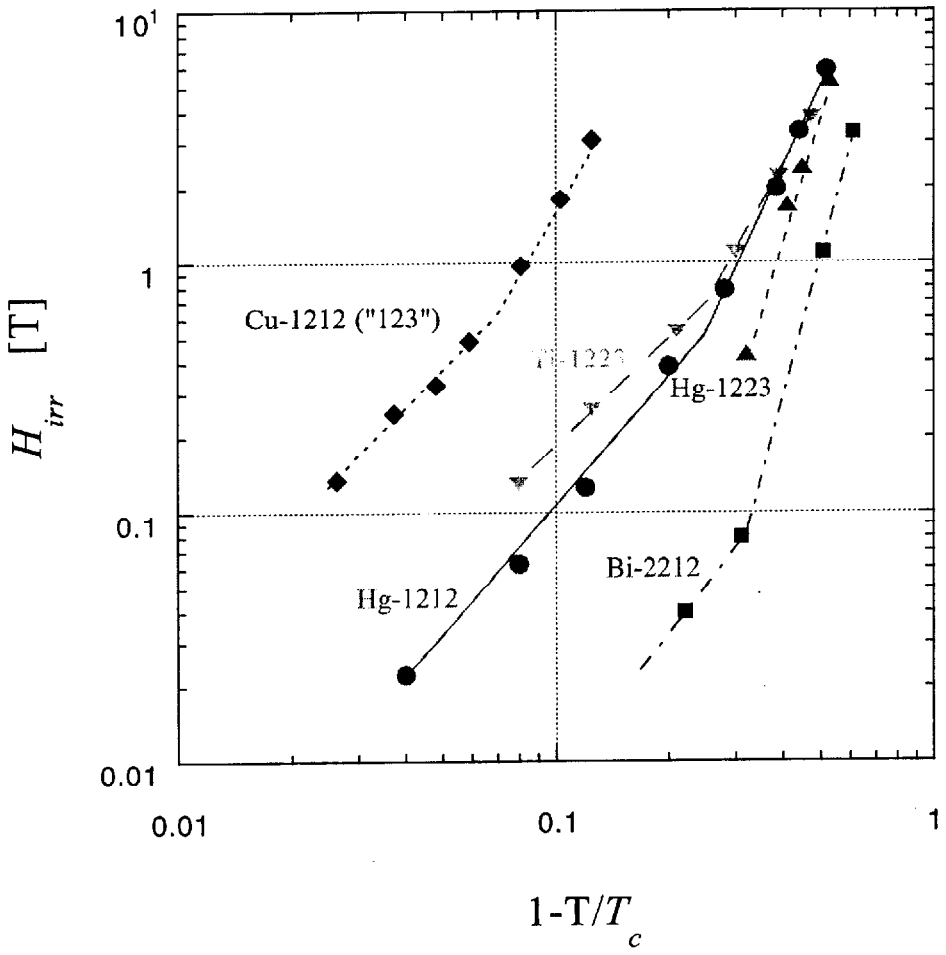

Fig. 1.8. The log-log plot pf irreversibility lines for conventional HTSC's.

layer coupling influenced by shortening of the blocking layers [142-145] is certainly not always true.

Another powerful method to improve the vortex-pinning property is to introduce strong pinning centers by irradiations (by heavy ions or neutrons, high energy electrons). Drastic improvements in the J_c property after irradiation were reported for Hg-1201 [146], Hg-12(n-1)n (n = 2,3) [147], and Bi-2212 [134, 148]. However, T_c was suppressed proportionally to the density of defects [149]. Moreover, the suppression of T_c was often accompanied with a broadening of the superconducting transition due to the local damages in the CuO_2 planes.

From the intensive works aiming for the enhancement of the magnetic characteristics, it was reported that the distance between two blocks of the CuO_2 plane stacking, namely the thickness of "blocking" block, correlated to the irreversibility field [55, 143, 145, 150]. However, in these works, little attention was paid to the hole density distribution in the whole crystal. The oxygenation of the sample has been known to improve the magnetic irreversibility [67, 83, 120, 133]. Also electronic anisotropy was considered as to play a role that governed the magnetic irreversibility characteristics [83, 144]. Furthermore, it was pointed out that the irreversibility field characteristics would be significantly enhanced if the charge-reservoir was metallized [81].

Apparently, the electronic anisotropy is related to the hole density distribution. Yamauchi *et al.* [13, 92, 121] has demonstrated that the magnetic irreversibility characteristics is improved by controlling the hole density distribution along the direction perpendicular to the CuO_2 planes such that it may be more homogeneous. It is important to note that controlling the hole density distribution has a potential to provide us not only with an improvement in the magnetic irreversibility characteristics, but also with optimization of both T_c and H_{irr} characteristics [13, 92].

1-6 Peak effect

1-6-1 General feature

The peak effect or "fishtail phenomenon" is often observed in the magnetization -vs.- applied field (H_a) curves, especially in HTSC single crystals, as shown in Fig.1.9. Usually, the values of J_c decreases with increasing the field (like $\propto H_a^{-1}$). However, for materials which show the peak effect, J_c first decreases and starts to increase on the way of increasing the magnetic field strength, and then shows a secondary peak at a certain magnetic field.

The advantages of using peak effect from the engineering point of view are listed below:

1. Enhancement in the J_c value at high magnetic fields and at relatively high temperatures.
2. High stability of the superconducting current in the low field range just below the peak field (see Fig. 1.9)
3. Simple processing for enhancing the J_c value as compared to other methods such as high-energy particle radiation.

Thus peak effect is extremely useful. Some origins for the effect have been discussed for long time. However no essential understanding has been achieved yet. Here, possible origins of peak effect are overviewed.

1-6-2 Possible origins for peak effect

Various models have been proposed for the mechanism of peak effect:

(I) Flux lattice matching effect
(II) Low T_c phase (or region)
(III) Decrease in the elastic constant for vortex lattice
(IV) Softening of the vortex lattice

(I) Flux lattice matching effect

When the spacing between vortices becomes comparable to the spacing between pinning centers, the J_c value could be maximized. At low fields, the vortices are less dense than the pinning centers and the vortex can move because these are many other equivalent sites open for jump. As the field increases, the spacing of the vortex becomes nearly equal to that of the pinning site. This increases the nominal pinning strength because there are fewer vacant sites where the extra vortex can settle in. This matching effect leads to stronger pinning with increasing field. It is known that the matching mechanism works only when the pinning force is weak and the arrangement of pinning centers is relatively regular [151, 152]. It is worth to note that the field strength of the secondary peak position ($H_{s.p}$ as shown in Fig.1.9.) due to

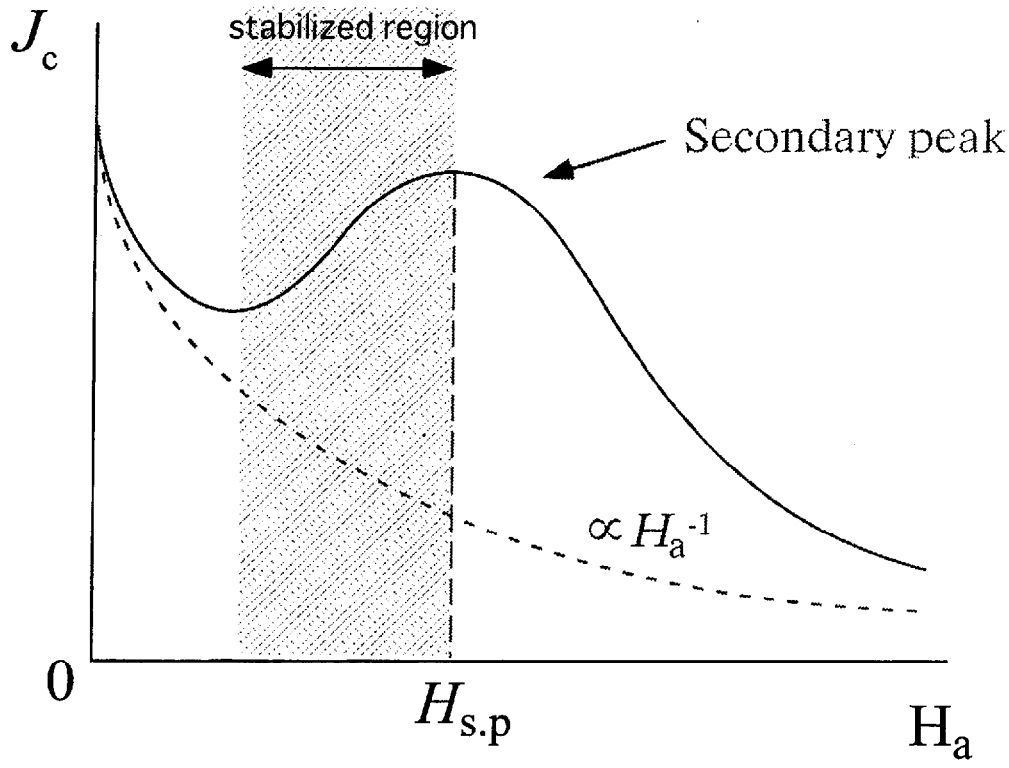

Fig. 1.9. Schematic picture of the peak effect on a dependence of J_c on applied field, H_a. $H_{s.p}$ represents the field at secondary peak position. Broken line shows a typical curve without peak effect. Hached region shows the stabilized region where the J_c is to increase with increasing of H_a.

this mechanism dose not move with the change in temperature [153]. This type of peak effect has been observed in the Bi-2212 phase [154]. However the $H_{s.p}$ commonly depends on temperature [155].

(II) Low T_c phase

When the pinning centers are superconductive with T_c lower than that of the matrix superconductor, peak effect may be expected to occur. A defect in the crystal may give rise to a small local depression of the order parameter at low field so that pinning is relatively weak at low fields. As the field increases, the local order parameter near the defect becomes depressed faster with increasing field than the suppression of matrix's order parameter, thus turning the nominal pinning strength from weak to stronger with increasing field. The oxygen deficient region in the Cu-1212:P ["*RE*(Y)-123"] phases may work as such a pinning center. However it is difficult to observe oxygen deficient regions, though some positive indications has been obtained for a Cu-1212:P, *i.e.* Sm-123 [156].

The other hand, the defect caused by cation disorder may also work as an above mentioned pinning center. In this case, the dominant effect of controlling the oxygen content is to alter the bulk order parameter and the temperature dependence of irreversibility fields [157].

(III) Decrease in the elastic constant for vortex lattice

Larkin and Ovchinikov predicted that the decrease in the size of flux bundle (which is determined as the elastic correlation length) may cause the peak effect [158]. The elastic constants of vortex lattice (c_{11} and c_{44} for uniaxial compression and tilt, respectively) sufficiently decrease when the applied magnetic field increase as near upper critical field, H_{c2}, causing each vortex plastically deforming the flux bundle in order to obtain the full value of pinning force. However, this mechanism may work only when the applied field near H_{c2}. Therefore it is hard to explain the peak effect in a high κ superconductor such as HTSC in which the peak effect is observed at the relatively low magnetic field. (here, κ means the Ginzburg-Landau parameter [85])

(IV) Softening of vortex lattice

When the tilt modulus of the flux line lattice , c_{44}, softens as the magnetic field increases and allows the vortices to bend and relax to the most favorable pinning configuration, the rise in J_c may occur. This is the classic explanation for the peak in J_c that occurs very close to upper critical field , H_{c2} in transition metal alloys. Ordinarily this effect would occur in a

region where the bulk order parameter changes rapidly with field or temperature and hence, close to H_{c2}. The other hand, when shear modulus (c_{66}) for magnetic vortices is deteriorated by increasing the applied magnetic field, the vortices are re-arranged to fit the arrangement of the pinning center optimally. Such a re-arrangement can also induce a peak effect under such a condition.

So far, as aforementioned, to mechanism for the unusual feature of peak effect still remains unelucidated.

1-7 Objectives of the present work

Superconductive mercury cuprates form a homologous series, $HgBa_2Ca_{n-1}Cu_nO_{2(n+1)+\delta}$ or Hg-12(n-1)n. The members with n = 1, 2 and 3 of the series have intensively been investigated for both scientific and technical interests, since their superconducting transition temperatures (T_c) are higher than those of any other superconductors known to exist (the highest value of $T_c \sim 135.4$ K for Hg-1223 under ambient pressure). However the mercury cuprates have not been considered as promising materials for applications. This is mainly because the magnetic irreversibility-field (H_{irr}) characteristics is not superb and their critical current density (J_c) characteristics is rather poor, as compared to *e.g.* $CuBa_2YCu_2O_{7-\delta}$ ("Y-123"). It has been suggested that the H_{irr} characteristics may be improved by either (i) introducing appropriate lattice defects for pinning vortices *i.e.* flux pinning centers or (ii) reducing the electronic anisotropy.

Yamauchi *et al.* recently proposed that not only the critical temperature but the magnetic irreversibility could be maximized by controlling the hole density distribution along the direction perpendicular to the CuO_2 planes [92, 121]. Thus in this work, (1) enhancement in the irreversibility-field strength in the second and third members of the Hg-12(n-1)n homologous series is pursued by controlling the hole density distribution .

Now, peak effect or fish-tail phenomenon has been known as the secondary peak besides the zero-field peak in the magnetization-vs.-field curve for type-II (high-κ) superconductors. This effect is extremely attractive as the J_c value could be enhanced at high magnetic fields. Some origins of the effect have been proposed, but still remain controversial [155, 159-161],. For example, it has been pointed out that the presence of weak pinning defects in the superconducting matrix is crucial to get the pronounced peak effect. However, no such defects have been established for the mercury cuprate superconductors so far. Thus, (2) the mechanism of peak effect in (Hg,Pb)(Ba,Sr)-1223 superconductors is investigated in this work particularly in terms of the microstructure of atomic to "deca-nanoscopic" scales.

Chapter II Enhancement in the Irreversibility Field of Mercury Copper Oxides

2-1 Introduction

As mentioned in the Chapter I, though Tc of members of Hg-12(n-1)n series are higher than those of other HTSC series, the mercury copper oxides have not been considered as promising materials for applications. This is mainly because the magnetic irreversibility-field (H_{irr}) characteristics is not superb (see Fig.1.8) [133, 135-137] and their critical current density (J_c) characteristics are rather poor, as compared to *e.g.* $CuBa_2YCu_2O_{7-\delta}$ ("Y-123"). It has been suggested that the H_{irr} characteristics may be improved by either (i) introducing appropriate lattice defects for pinning the vortices *i.e.* flux pinning centers [134, 146, 147], or (ii) reducing the electronic anisotropy [144, 150], which usually acquired in over-doped state [83, 120]. So far no effective pinning centers have been established for the mercury cuprate superconductors. On the other hand concerning (ii), Yamauchi *et al.* recently proposed that the magnetic irreversibility could be improved by controlling the hole density distribution along the direction perpendicular to the CuO_2 planes such that it would be more homogeneous [121]. Nakane *et al.* already found that such approach was effective in the Cu-1212:P compound [122]. Furthermore, not only the magnetic irreversibility, but also the T_c is reported to be governed by the distribution [92], suggesting that a higher confined hole density in the CuO_2 plane could make the value of T_c higher than that of lower confinement.

2-1-1 Hg-1212

Comparing to other members of Hg-12(n-1)n series, only Hg-1212 has two possible crystallographic sites for hole creation and/or annihilation, one being the Ca site in the oxygen-free Ca layer between two adjacent CuO_2 planes and the other the oxygen site in the charge reservoir (CR) block, *i.e.* HgO_δ. Note that the substitution for Ca by trivalent cations are generally allowed only for the 1212 structure. In order to control the hole density distribution, solid solutions $HgBa_2(Ca_{1-x}Y_x)Cu_2O_{6+\delta}$ ($0 \le x \le 0.5$) have been synthesized by an encapsulation technique and then post-annealed by a high-pressure oxidization (HPO) technique. The total amount of doped holes depends on both the amount of Y substitution for Ca, x, and that of excess oxygen in the HgO_δ layer, δ. The former would reduce the hole density in the neighborhood of the CuO_2 planes and the latter would increase the amount of holes especially in the CR block. Thus the hole density distribution could be changed in this system by applying both the Y and O dopings simultaneously.

The H_{irr} characteristics was predicted to be maximized in the optimally distributed hole density by aforementioned method.

2-1-2 Hg-1223

The Hg-1223 has been supposed as one of the most promising materials because of its high-T_c. For promising applications of the material in high magnetic fields, it is crucial to improve the irreversibility field. Until now, it has been reported that the partial substitutions for Hg and/or Ba were quite effective to improve not only the magnetic behavior but also the chemical stability [37, 56, 138, 141]. Especially, by substituting Sr to Ba the extreme enhancements were observed on the irreversibility field [37, 56, 142]. In this study the effect of the cation substitutions is investigated with single crystals. More noteworthy is that the Sr substituted Hg-1223 samples have been synthesized only by the high-pressure technique so far, however, Lee *et al.* [56] recently succeeded to prepare the material without high-pressure but with a modified encapsulation technique. In their case, the Pb substitution was considered to play a crucial role for the phase formation under ambient pressure. Moreover, the single crystals with relatively large size were found in the synthesized polycrystalline samples. Then by using such single crystals, the investigation for the better irreversibility characteristics in this compounds was of interest to verify the effect of Sr substitutions.

2-2 Experimental

2-2-1 Synthesis

(1) Encapsulation technique

$HgBa_2(Ca_{1-x}Y_x)Cu_2O_{6+\delta}$ (Hg-1212) polycrystalline samples were synthesized by the encapsulation technique [9, 162], where the simple oxides HgO (≥99.9 %), BaO (≥99 %) and CaO, Y_2O_3, CuO (≥99.99 %) were employed as the starting materials (these reagents were purchased from High purity chemical laboratory Co. Ltd.). They were subsequently mixed and pelletized in dried nitrogen atmosphere, and sealed into an evacuated quartz tube and sintered at 680~720 °C for 20 hrs. Figure 2.1 shows the typical configuration of the encapsulated sample, where a sealed quartz tube enclosed in a surrounding stainless steel protector. This protector works for keeping the furnace from a physical damage when the tube explodes by inner pressure.

(2) High-pressure oxidation technique

A part of the as-sintered sample was subjected to the high-pressure oxidization (HPO) technique developed by T. Ito *et al.* [163]. Following this method, the sample with 25 mol% of $KClO_3$ as an external oxidizing agent, was heat treated under a pressure of 5 GPa, and at 500 °C for 2 hours in order to introduce the excess oxygen into the crystal without any

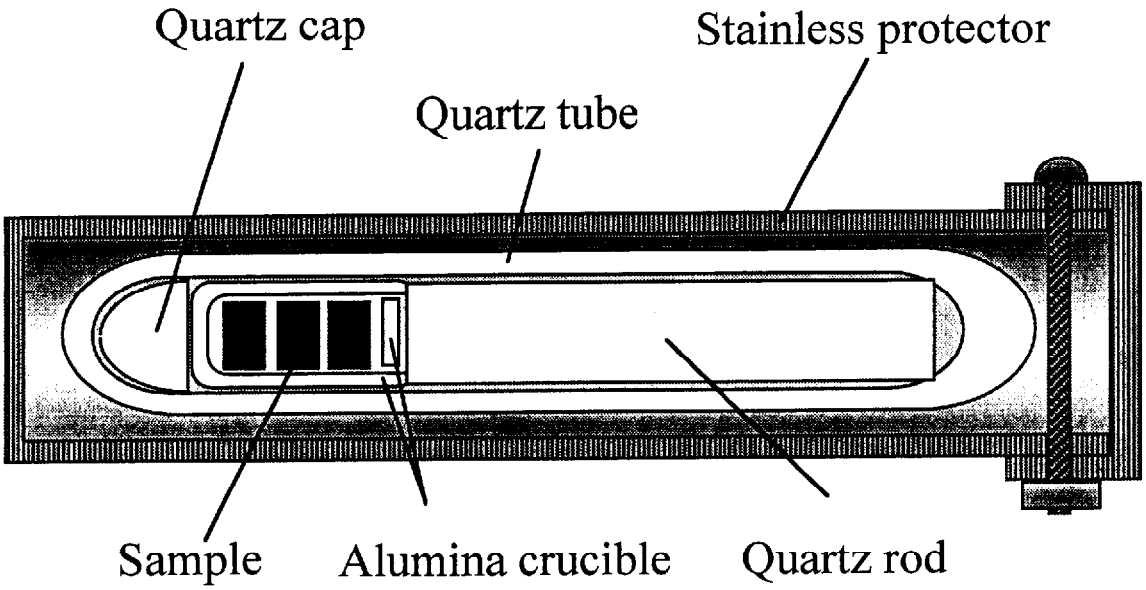

Fig. 2.1. Schematic diagram of an ampoule configuration for the encapsulation technique.

serious phase decomposition. Figure 2.2 shows a illustration of experimental procedure of the high-pressure oxidizing technique.

$(Hg_{1-x}Pb_x)(Ba_{1-y}Sr_y)_2Ca_2Cu_3O_{8+\delta}$ {(Hg,Pb)(Ba,Sr)-1223} single crystals were obtained by extracting from the polycrystalline samples synthesized by the encapsulation technique as mentioned above, except for the starting materials which prepared from nitrates solution. The nitrates solution including Ba-Sr-Ca-Cu elements was spray dried into very fine and homogeneous powder [54]. The nitrate powder was decomposed in vacuum at 600~700 °C and then the obtained oxides powder was further mixed with HgO and PbO powders. The final mixture was compacted into pellets and sintered in 850 ~ 875 °C for 15 hrs by means of encapsulation method. It must be noticed that in some cases relatively large single crystals were grown. Particularly the larger crystals (~100×100×30μm^3) were able to extracted from the pellet surface.

2-2-2 Estimations

(1) Phase composition

The phases in the samples were identified by powder XRD study with Cu K_α radiation (M18XHF, MAC Science). A typical condition for the measurement was as followings; operating power : 45 kV×200 mA, scanning range : 3~70 ° (2θ) , sampling width : 0.02 ° , scanning rate : 5 ° / min.

(2) Chemical composition

Compositional analyses were carried out by means of an energy dispersive X-ray spectrometry detector (EDX; Sigma, Kevex) mounted on a transmission electron microscope (TEM) operating at 300 kV (H-9000NAR, Hitachi).

For the analysis, the TEM-EDX combination allows us to neglect the absorption effect of X-ray (thin film approximation or Cliff-Lorimer method). On the other hand, to improve an accuracy of analysis, the k-factors were calibrated using standard materials for all elements of which the sample consisted. Furthermore, to reduce the occasional error, more than a dozen spectra from different sampling points were collected for averaging the data. Note that such TEM-EDX combination based on standard materials calibration gives us the correct chemical composition within an accuracy of about 2 %.

For TEM study, a specimen was prepared by a conventional crushing method. In the crushing method, the sample was crushed in an agate mortar and dispersed into ethanol. The dispersed grains were scooped up with a carbon microgrid supported by a molybdenum mesh.

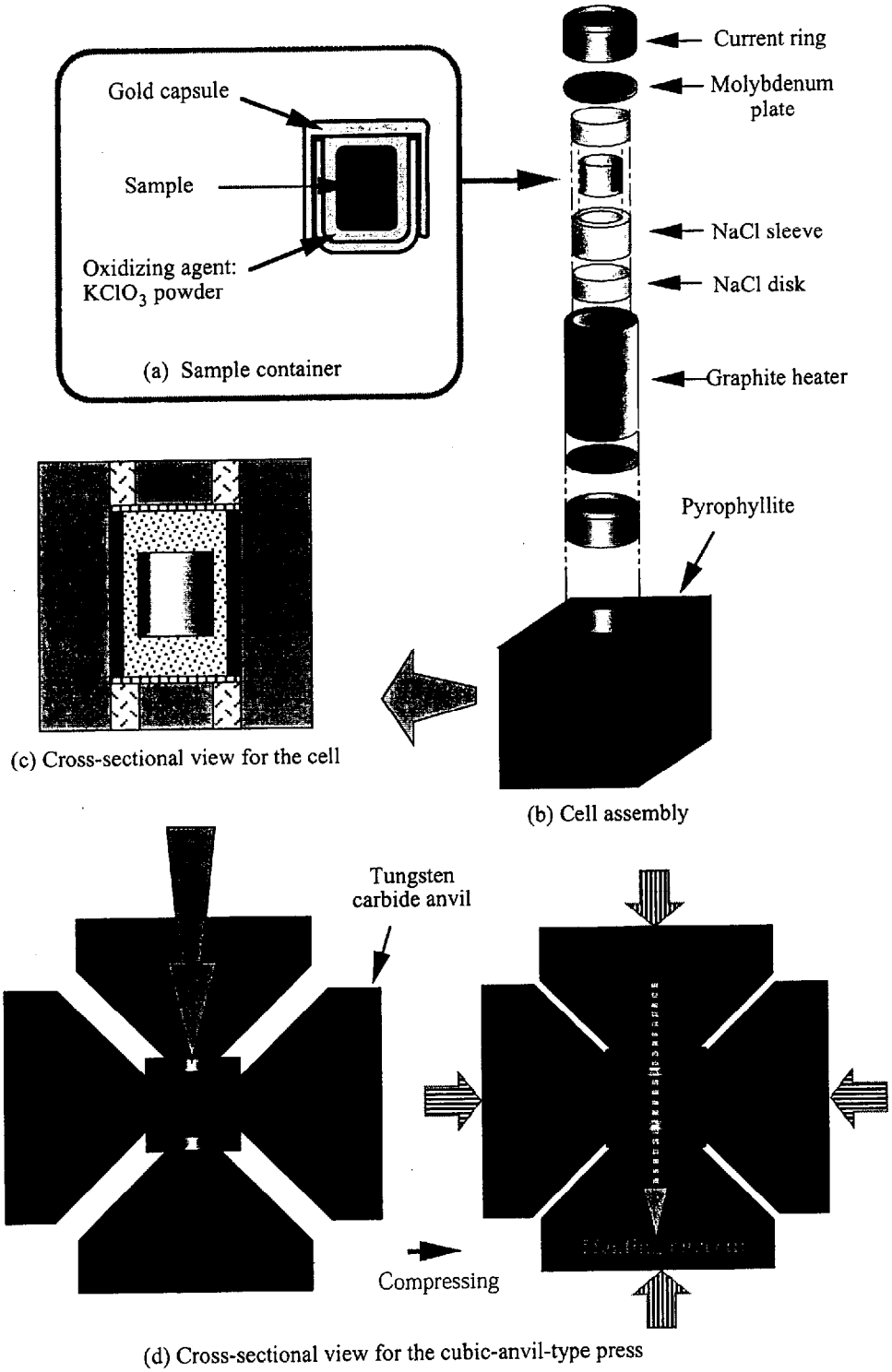

Fig. 2.2. Illustration of a procedure for the high-pressure oxidization technique.

(3) Oxygen content

Oxygen content of the as-sintered sample was estimated by coulometric Cu(+I)/Cu(+II) titration method [72]. In this method, the possible trivalent copper, *i.e.* $(CuO)^+$, is reduced by Cu(+I) when dissolving the sample into HCl solution (1N) with a known amount of excess (γ) Cu(+I) [in Eq.(2-1)]. The other hand, if the sample contains monovalent copper, *i.e.* $(CuO)^-$, Cu(+I) is increased with the corresponding amount [Eq.(2-2)]. Finally, when the resulting amount of Cu(+I) is titrated by anodic oxidation, the quantity of electricity [$Q = (\beta-\alpha+\gamma)/F$] is detected, where F means Faraday's constant. From this titration result, the oxygen content of the sample can be determined simply by the charge balance, as long as the valence state in the acidic solution for each element is known. The actual titration process was carried out in a reactor cell (Fig. 2.3) at room temperature under flowing argon gas. In all measurement, CuCl (99.99%, High-Purity Chem. Lab. Co. Ltd.) was employed as a reductant agent.

$$\alpha(CuO)^+ + \gamma Cu^+ + 2\alpha H^+ \rightarrow 2\alpha Cu^{2+} + (\gamma-\alpha)Cu^+ + \alpha H_2O \quad (2\text{-}1)$$

$$\beta(CuO)^- + 2\beta H^+ \rightarrow \beta Cu^+ + \beta H_2O \quad (2\text{-}2)$$

$$(\beta-\alpha+\gamma)Cu^+ \rightarrow (\beta-\alpha+\gamma)Cu^{2+} + (\beta-\alpha+\gamma)e^- \text{ (coulometry).} \quad (2\text{-}3)$$

In contrast to above, the oxygen content of high-pressure oxidized sample was roughly evaluated by spectrometry using electron energy loss spectroscopy (EELS) [100]. The latter mentioned was chosen because the amount of the high-pressure treated sample was too small to obtain a accurate results by coulometric titration. The EELS data were acquired by the spectrometer (GIF, Gatan) mounted beneath the TEM (as mentioned above). During the measurement, an incident beam was fixed parallel to [001] of the 1212 structure and the radiation-induced degradation of the sample was carefully avoided. The detailed determination scheme for oxygen content in present samples through EELS data is mentioned below.

(4) Magnetic characteristics

Magnetic studies were performed by a DC SQUID magnetometer (MPMS-S5, Quantum Design) under applied field up to 5 T, and in temperature range from 5 K to 130 K. The DC susceptibility was measured in both zero-field cooled mode and field cooled mode under applied field of 10 Oe.

The values of H_{irr} were given as the value of field at which the difference between increasing and decreasing branches of magnetization hysteresis loops are extrapolated to zero [121, 124] (see, Fig. 1.7). This determination scheme allows us to estimate the value of H_{irr}

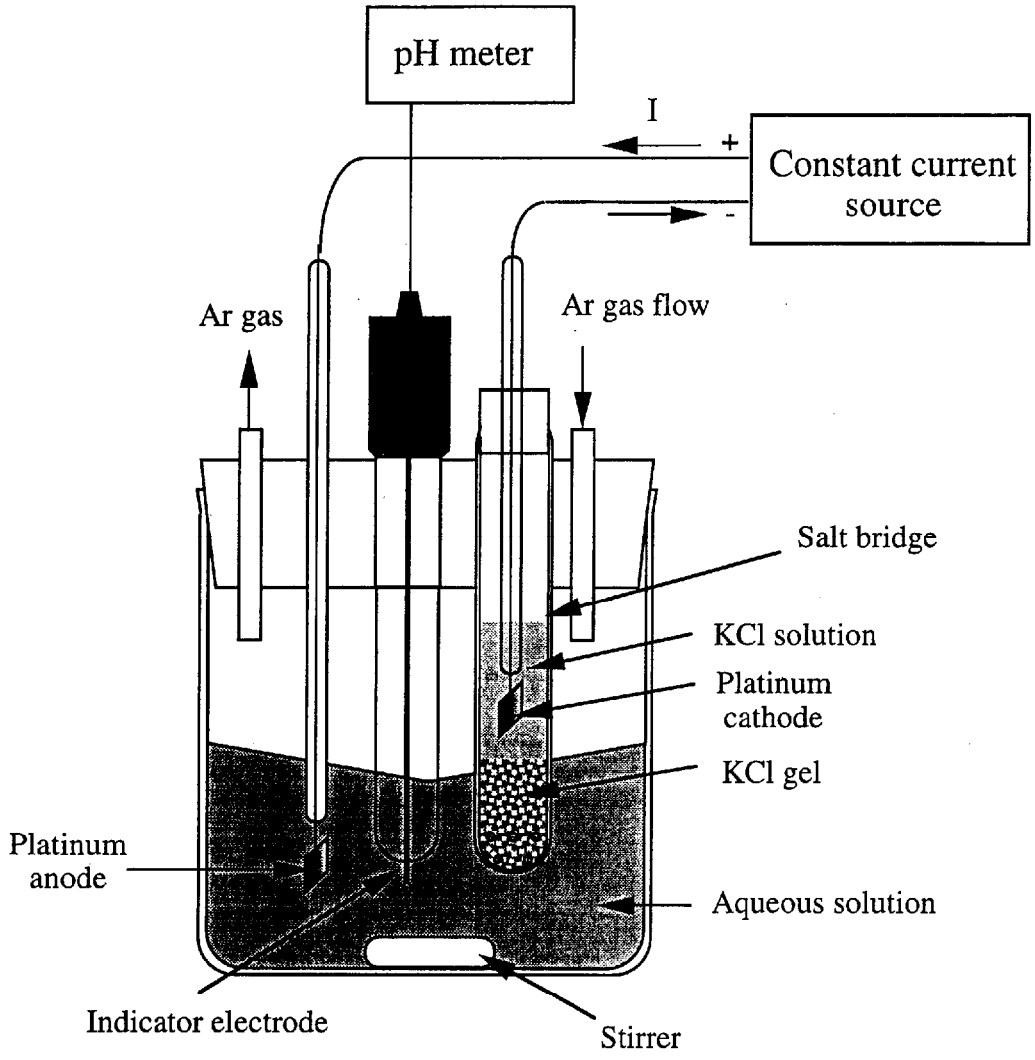

Fig. 2.3. Cell assembly for coulometric titration

without the J_c values derived from the critical state model which requires the rather correct grains size and the width of magnetization hysteresis loops.

2-2-3 Determination of oxygen content by EELS spectrometry

For the sample of high-pressure oxidized (HPO) Hg-1212(Y), EELS measurements were carried out in order to determine the oxygen content. It should be important that the large number of data is required because this attempt will give us only relative value. Generally, if the case of the specimen thickness is enough less than mean-free-path (usually many microns), the EELS intensity integrated under "raw" ionization edge (*K* shell), $I_k(\Delta)$ is given as following [100],

$$I_k(\Delta) \approx N \sigma_k(\Delta) I_l(\Delta) \tag{2-1}$$

where, Δ is energy window for integration, N is the number of atoms per a unit area, σ_k is cross section per the atom and $I_l(\Delta)$ is the intensity present in the low-loss region, integrated up to an energy loss Δ and including the zero-loss peak. In practice, an aperture is present between the specimen and spectrometer to exclude electrons which are scattered through angles greater than a certain value β. Then, Eq. (2-1) can be written as

$$I_k(\beta, \Delta) \approx N \sigma_k(\beta, \Delta) I_l(\beta, \Delta) \tag{2-2}$$

where $\sigma_k(\beta, \Delta)$is a "partial" cross section (this can be calculated). These equations are only rough approximations, because if we want to know the absolute quantity of N, we have to evaluate the each edge of any element with sufficient accuracy. Therefore, often we can estimate the ratio N_x/N_y of a given elemental pair (x and y) as

$$\frac{N^x}{N^y} \approx \frac{\sigma_k^x(\beta,\Delta)}{\sigma_j^y(\beta,\Delta)} \cdot \frac{I_l^x(\beta,\Delta)}{I_j^y(\beta,\Delta)} \tag{2-3}$$

The shell index can be different for each edge ($j = K, L, M\cdots$). Now, to evaluate the oxygen contents of the samples, the Ba-*M* edge was employ as the counter element because its energy difference from the O-*K* edge is not so large, furthermore it is easily expected that the Ba contents hardly change so much in the Hg-1212.samples.

By utilizing the Eq. (2-3), the compositional ratio of the elemental pair, R_{OB} which can be written as N^O / N^{Ba} $\{\propto I^O(\beta, \Delta) / I^{Ba}(\beta, \Delta)\}$, should give the absolute ratio of oxygen contents of each Hg-1212 samples. In order to determine the absolute oxygen content of high-

pressure oxidized samples, the oxygen contents which have been obtained previously for as-sintered samples by coulometric titration can be a standard. In this estimation, the Ba contents in the samples are assumed to be fixed. The results are listed in Table 2.1, showing that a rough relation between the oxygen content (6+δ) and the compositional ratio of the elemental pair, oxygen and barium, *i.e* R_{OB}.

2-3 Results and Discussion

Hg-1212

Identification of the phase purity

In Fig. 2-4(a),(b), XRD patterns for the sample series of as-sintered (AS) by encapsulation technique and post-annealed by high-pressure oxidized (HPO) $HgBa_2(Ca_{1-x}Y_x)Cu_2O_{6+\delta}$ ($0 \le x \le 0.5$) are shown, respectively. In both series, samples with higher Y content than $x > 0.1$ seem to be single phases, while the samples with low x value include some impurity phases such as $CaHgO_2$ and CuO, reflecting that Y(*RE*) substituted phases [15] can form more stably than Y(*RE*)-free phase. Although HPO samples have small amounts of impurities compared with AS samples, these phases exhibit certain crystalline inhomogeneity because the width of each peak is relatively larger compared to the AS samples. In all samples studied here, there are no traces of other superconducting phases except Hg-1212. This allows us to regard the Hg-1212 phase as the representative superconducting phase.

2. Elemental compositions

The average cationic composition evaluated by TEM-EDX analysis over a dozen grains for each sample is listed in Table 2.1 and also shown in Figs. 2.5(a), (b) for AS and HPO samples, respectively. The ratio of cations is normalized by fixing the cationic composition of Ba to be 2.0 because the composition of other elements could easily change due to the presence of deficiency and/or the forming other member of homologous series like Hg-1201 or Hg-1223. Despite some deviations from the nominal values of the Hg and Cu compositions the Ca/Y ratios are proportional to the nominal ones. Thus the degree of Y substitution for Ca was changed successfully in all present samples. The contents of excess oxygen, δ for AS samples were determined by coulometric titration as listed in Table 2.1. As for the HPO samples, oxygen content was estimated only by the ratio of integrated EELS spectra for O-*K* with that respect to Ba-*M* edges as mentioned in Section 2-2-3. Based on the relationship between oxygen content and R_{OB} for AS samples, $\sigma^O(\beta, \Delta) / \sigma^{Ba}(\beta, \Delta)$ in Eq.(2-3) was found to be 0.515. By using this result, the values of δ for the HPO samples were obtained as

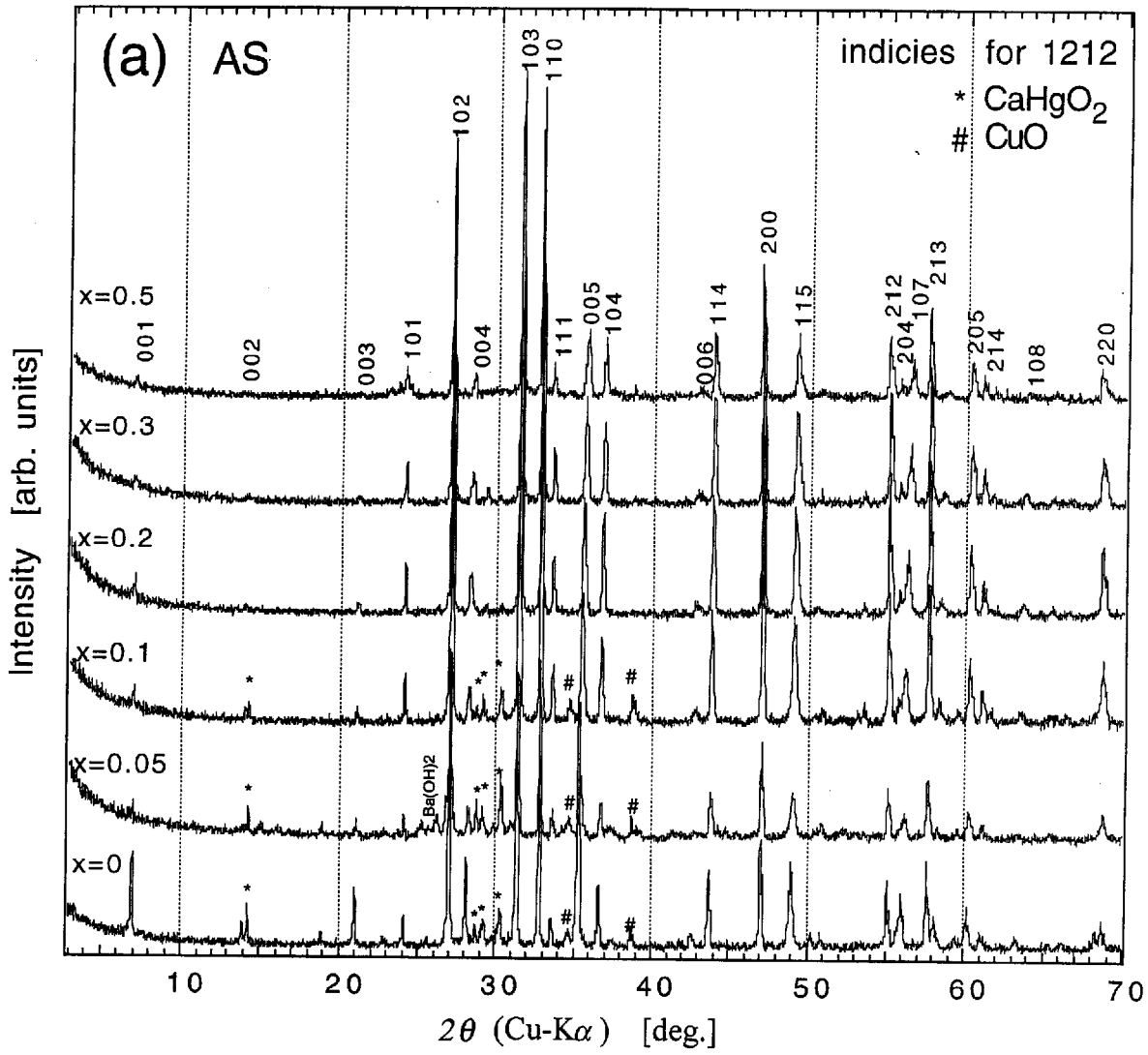

Fig. 2.4 (a) XRD patterns for as-sintered (AS) samples of $HgBa_2(Ca_{1-x}Y_x)Cu_2O_{6+\delta}$ ($0 \le x \le 0.5$). The indicies are for 1212 phase, and marked peaks are for impurity phases, (+) for $CaHgO_2$ and (#) for CuO.

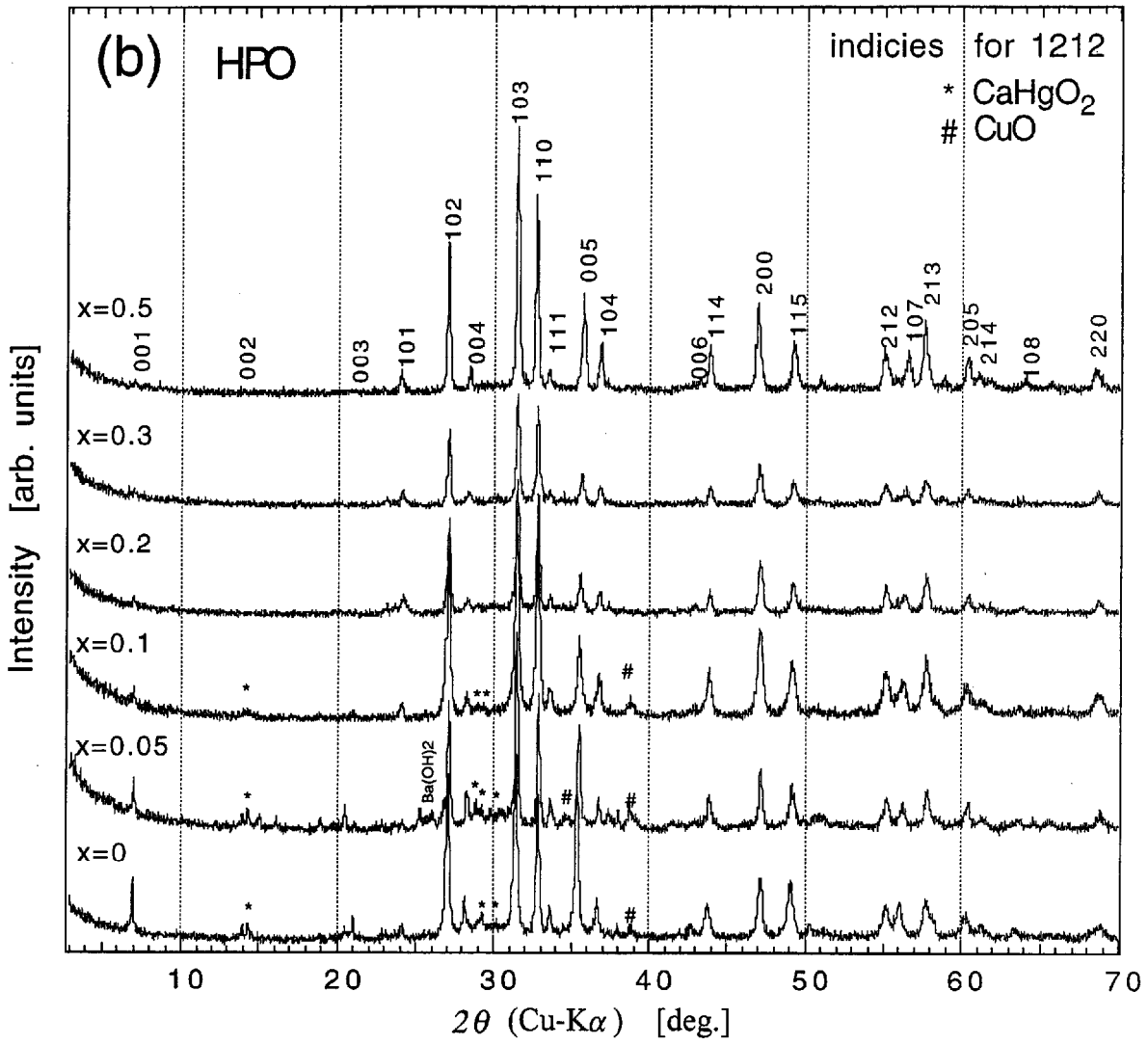

Fig. 2.4 (b) XRD patterns for high-pressure oxidized (HPO) samples of $HgBa_2(Ca_{1-x}Y_x)Cu_2O_{6+\delta}$ ($0 \le x \le 0.5$). The indicies are for 1212 phase, and marked peaks are for impurity phases, (+) for $CaHgO_2$ and (#) for CuO.

Table 2.1 Results of chemical composition and T_c for both as-sintered (AS) and high-pressure oxidized (HPO) $HgBa_2(Ca_{1-x}Y_x)Cu_2O_{6+\delta}$ samples

Sample	x	Cationic composition [a]					T_c^{eff} [K]	δ [b]	p_{nom}	R_{OB} [c] (=I^O/I^{Ba})
		Hg	Ba	Ca	Y	Cu				
AS	0	0.99	2.00	0.92	0.00	1.86	120	0.32	0.32	12.2
	0.1	1.02	2.00	0.75	0.13	1.79	110	0.31	0.26	12.2
	0.2	0.85	2.00	0.72	0.18	1.92	110	0.31	0.21	12.3
	0.3	1.00	2.00	0.63	0.28	2.04	106	0.34	0.19	12.3
	0.5	0.95	2.00	0.45	0.47	1.97	82	0.40	0.15	12.5
HPO	0	1.01	2.00	0.83	0.00	1.93	68	0.8	0.83	13.3
	0.1	0.94	2.00	0.78	0.11	1.83	102	1.0	0.95	13.6
	0.2	0.92	2.00	0.74	0.16	1.89	96	1.0	0.86	13.5
	0.3	0.85	2.00	0.60	0.32	1.85	93	1.0	0.82	13.5
	0.5	0.85	2.00	0.43	0.43	1.85	92	1.1	0.86	13.8

[a] evaluated from the results of TEM-EDX by fixing the Ba content to be 2.0.

[b] determined by coulometric titration and EELS spectrometry for AS and HPO samples, respectively.

[c] ratio of integrated EELS intensities of O-K and Ba-M edges with a certain energy window.

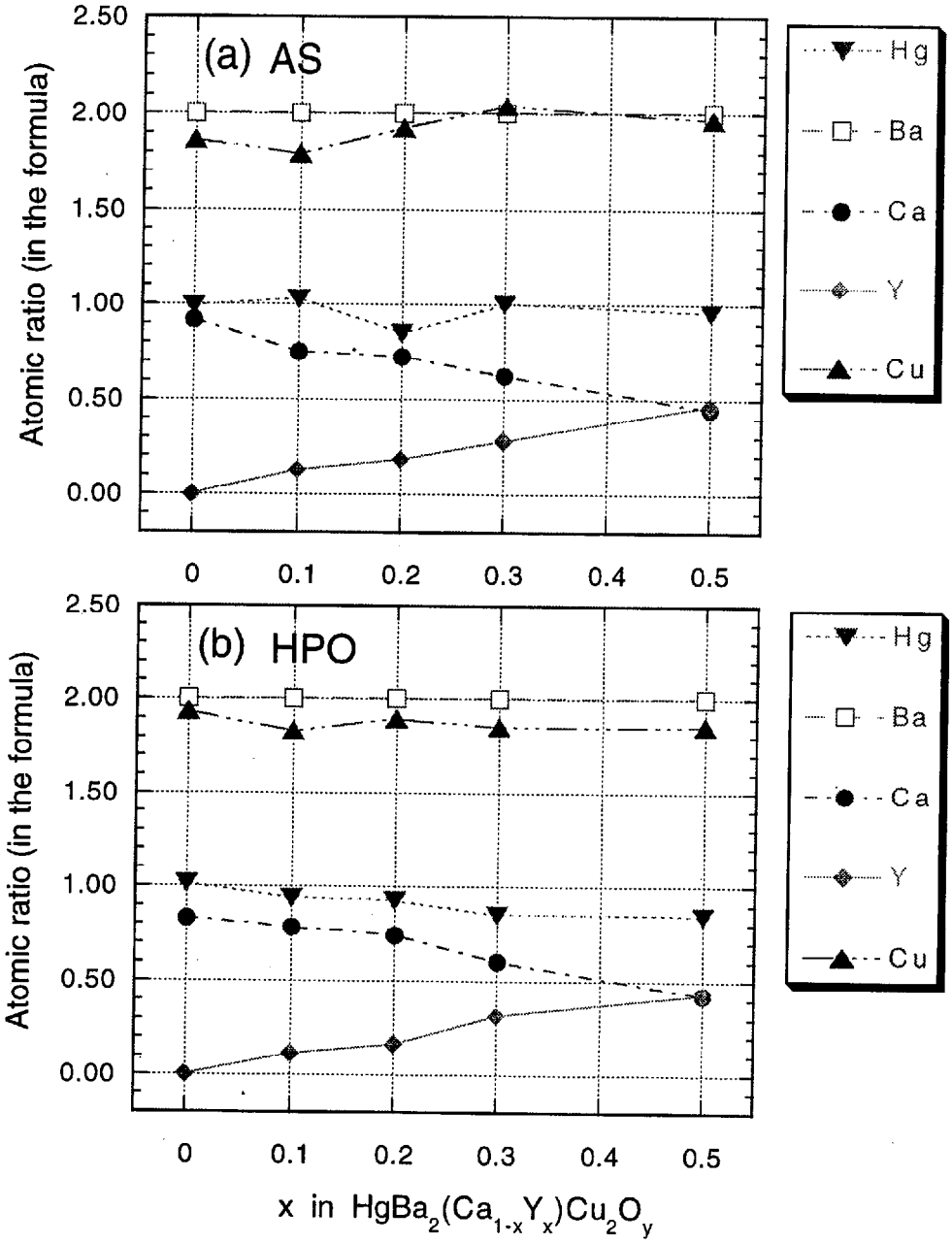

Fig.2.5 Results of TEM-EDX analysis for (a) as-sintered (AS) and (b) high-pressure oxidized (HPO) samples of $HgBa_2(Ca_{1-x}Y_x)Cu_2O_{6+\delta}$ ($0 \leq x \leq 0.5$). These compositions are normalized by fixing the Ba content to be 2.0.

listed in Table 2.1. Figure 2.6 shows the oxygen contents of both AS and HPO samples. In the estimation for the HPO sample, the barium contents are assumed to be the same for all the samples used here. Since the values of oxygen content for the HPO samples were obtained only from the spectrometry based on the EELS measurement, the values have a maximum accuracy of ± 10 %. Nevertheless, at least one can say that the oxygen contents of the HPO samples are larger than that of the AS samples. Furthermore, it makes sense that the oxygen contents of the HPO samples hardly exceed 7.0. This means that the oxygen site of the charge-reservoir block (HgO_δ), which is rock-salt structure, should be fully occupied. Anyhow, it is hard to think that too much mobile holes are generated from such a large amount of excess oxygen (the concentrations of these so-called "nominal holes"[92] are also shown in Table 2.1 as p_{nom}). Thus a certain amount of the excess charge is likely to be localized on the Hg site and/or the oxygen site of HgO_δ layer not only because the position is near by the excess oxygen site, but because the Hg^{3+} state [164] and the O^{1-} state [165, 166] may occur in the layer as reported. Assuming the formal valence of the excess oxygen equals to be -1 as reported by Loureiro et al. [166], the values of p_{nom} for HPO samples acceptably shift down to ~0.4. However, it is still higher than commonly expected to be seen in high-T_c superconductors.

3. Critical Temperature, T_c

The temperature dependencies of DC susceptibility (normalized by the value at 5 K) typically measured for both the AS and HPO samples are shown in Fig. 2.7 (only for x=0.0). For the HPO sample, the diamagnetic transition seems to be spread over the wide temperature region below T_c, whereas a sharp transition is observed for the AS sample. Strictly speaking, it is necessary to take an exact mean value of T_c into account when a bulk properties are discussed [167]. Therefore, at present time, the effective transition temperature, T_c^{eff} was determined as the point at which a tangent line drawn from mid-point of the transition is extrapolated to $\chi = 0$ line. The values of T_c^{eff} for each sample are listed in Table 2.1. In following part, the symbol, T_c will be used in stead of T_c^{eff} for the sake of convenience. The Y content dependence of T_c is shown in Fig. 2.8. For the AS samples, the value of T_c decreases monotonically with increasing the Y content, originating from the doping state gotten to more under-doped region. For the HPO samples , however, the Y content dependence of T_c shows a maximum around x ~ 0.1 like a optimum of the parabolic shape, implying the doping state goes toward over-doped region from under-doped region by the high-pressure oxidization. In Fig. 2.9, the T_c values are also potted as a function of the "nominal hole" concentration, p_{nom} only for the AS samples. The relation apparently confirms that the doping state of the whole AS samples is in under-doped region, as

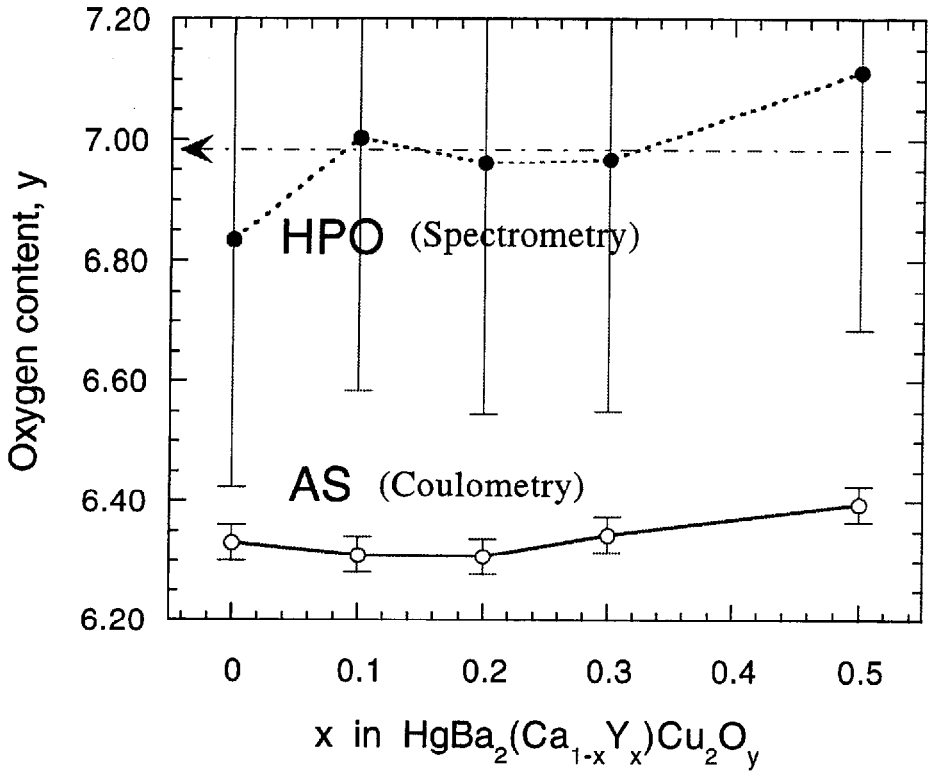

Fig.2.6 Oxygen content for (a) as-sintered (AS) and (b) high-pressure oxidized (HPO) samples of $HgBa_2(Ca_{1-x}Y_x)Cu_2O_{6+\delta}$ ($0 \leq x \leq 0.5$). Oxygen contents for these samples were determien by the coulometric titrarion and the EELS spectrometry, respectively.

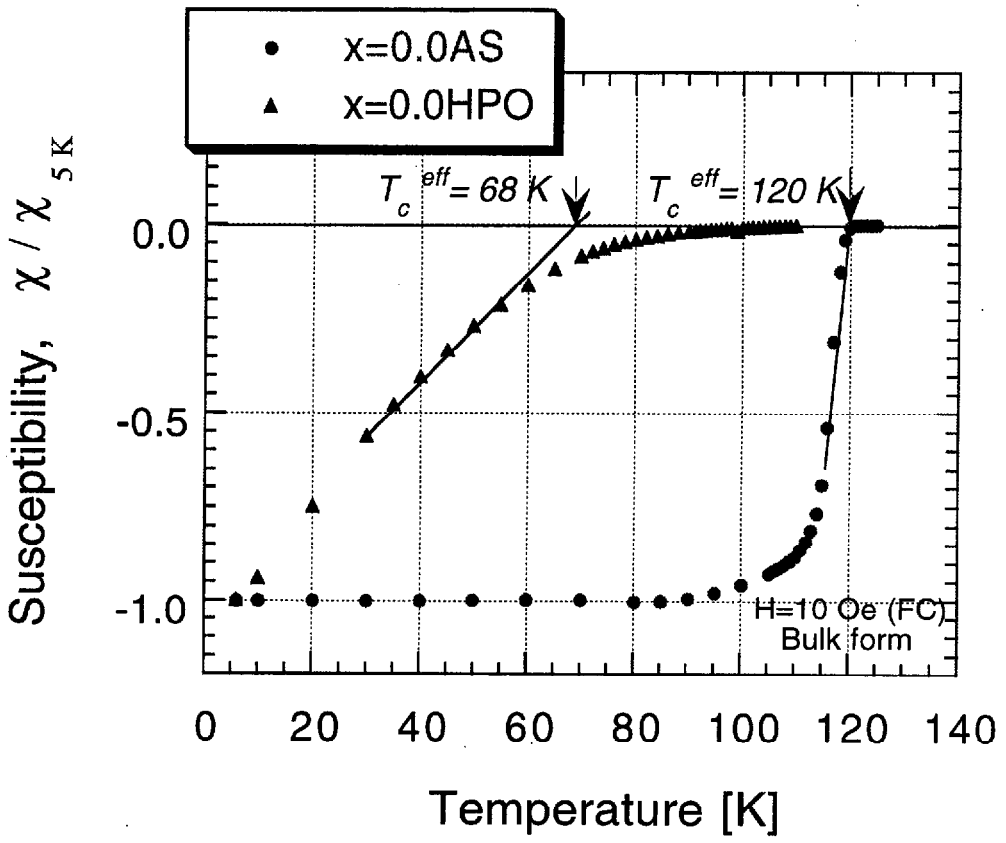

Fig. 2.7 Normalized temperature dependence of DC susceptibility for as-sintered (AS) and high-pressure oxidized (HPO) $HgBa_2(Ca_{1-x}Y_x)Cu_2O_{6+\delta}$ samples (in field cooled mode; Ha= 10 Oe). The arrows indicate the effective critical temperatures (T_c^{eff}) for each samples (see text).

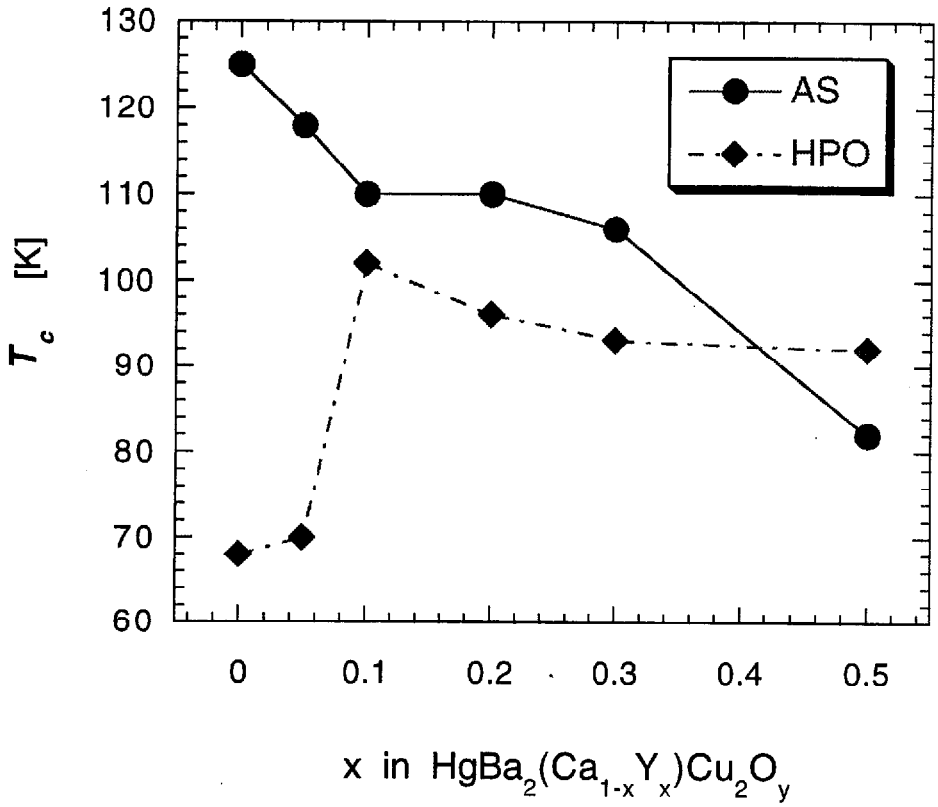

Fig. 2.8 Y content dependence of critical temperature, T_c, for as-sintered (AS) and high-pressure oxidized (HPO) $HgBa_2(Ca_{1-x}Y_x)Cu_2O_{6+\delta}$ samples.

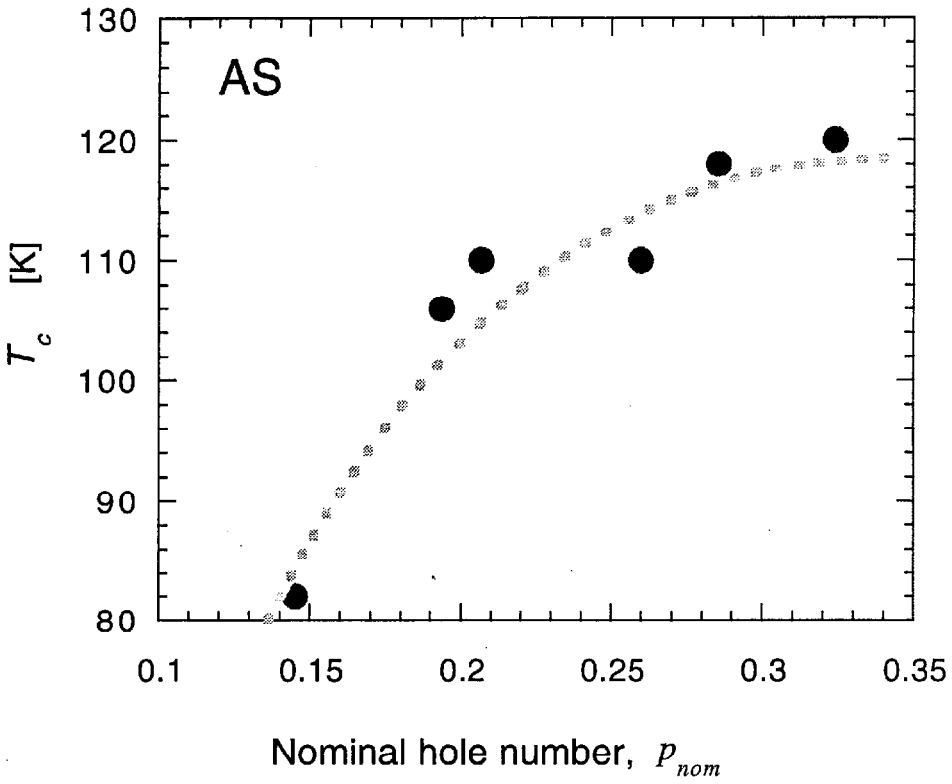

Fig. 2.9 Correlation between the critical temterature, T_c, and the nominal holes for as-sintered $HgBa_2(Ca_{1-x}Y_x)Cu_2O_{6+\delta}$ samples.

supposed above. Furthermore, the relationship between the values of T_c and the a-axis lattice parameters generally shows a clear relationship with doping state [21, 71, 90]. The lattice parameters derived from XRD study for all samples are plotted in Fig. 2.10. In the figure, for both AS and HPO samples, the c-axis lattice parameter decreases with increasing the Y content, whereas the a-axis lattice parameter increase with increasing the Y content. Based on the general relationships of a-axis lattice parameter and doping state, the lattice parameter behavior implies the lower Y substitution may give the higher doping state. Furthermore, all the HPO samples have shorter a-axis lattice parameter than AS samples, indicating that the higher degree of doping should be achieved by the HPO process. Figure 2.11 shows the relationship between T_c and a-axis lattice parameter for both the AS and the HPO samples, accompanying with reference data reported by Antipov *et al.* [21]. The plot roughly shows a parabolic shape, indicating that the degree of doping states of the samples are successfully varied from under to over-doped states. Although, the T_c's of the HPO samples seem to be suppressed probably due to changing of the doping mechanism under high-pressure oxidizing as mentioned above, the over-doped state was achieved in samples with lower Y content.

4. Irreversibility field characteristics

To investigate the H_{irr} characteristics precisely, the grain alignment of the sample is generally preferred because the value of H_{irr} strongly depends on the direction of applied field. Nevertheless in present study, all magnetic measurements for the polycrystalline samples were carried out without any grain alignments. It is possible to compare the value of H_{irr} among all the bulk samples which should consist of randomly oriented grains.

In Fig. 2.12, H_{irr} are plotted as a function of $(1\text{-}T/T_c)$ for both the AS and HPO samples with x = 0.0 and x = 0.50, which just indicate a boundary of the present data for the whole composition in this work. The H_{irr}-vs.-$(1\text{-}T/T_c)$ characteristics was well enhanced by the HPO process in all samples, moreover, the best characteristics was obtained for the x = 0.0 / HPO sample. This result simply points out that the best characteristics is achieved in the most over-doped state, showing good agreement with results reported for Hg-1201 [83] and Hg-1223 [120]. In such over-doped sample, however, the T_c tends to decrease with the increase in hole doping state, which is a general feature of high-T_c superconductors. On the other hand, the sample with both low Y and high oxygen content showed remarkably improved H_{irr} characteristics without a large suppression of the T_c value. A plot of H_{irr} as a function of temperature for the present samples is shown in Fig. 2.13. In this plot which is more important from the application point of view, H_{irr} of the sample with x = 0.10 / HPO is higher than that of the other samples in the region below 100 K. It seems reasonable to think that the best H_{irr}-vs.-T characteristics should be obtained in the case with well balanced H_{irr}

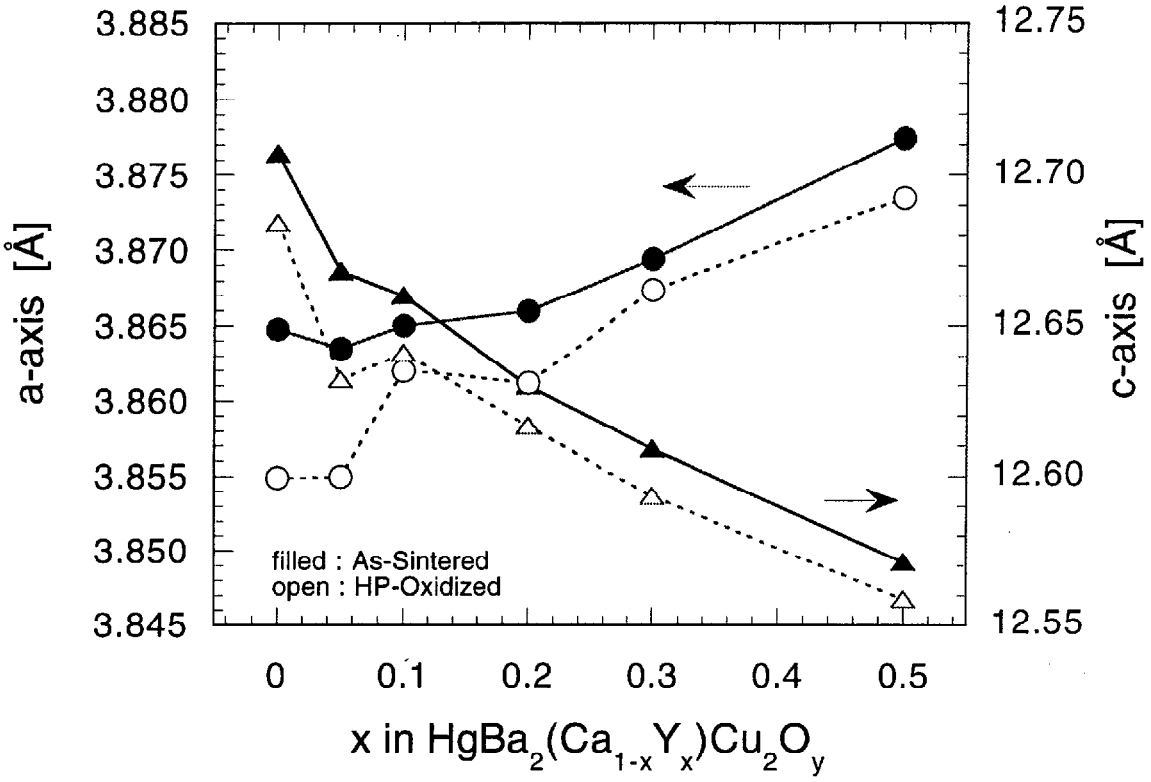

Fig. 2.10 Y content dependence of lattice parameters for as-sintered (AS) and high-pressure oxidized (HPO) samples of $HgBa_2(Ca_{1-x}Y_x)Cu_2O_{6+d}$ ($0 \leq x \leq 0.5$).

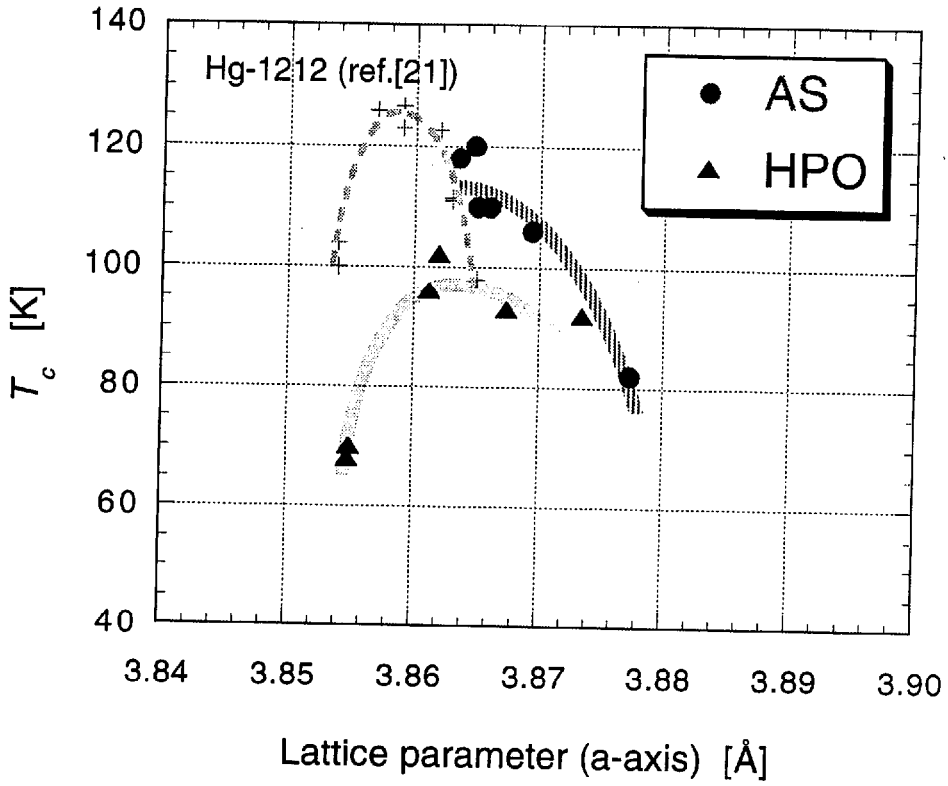

Fig. 2.11 Correlation between a-axis lattice parameters and critical temperature, T_c, for as-sintered (AS) and high-pressure oxidized (HPO) samples of $HgBa_2(Ca_{1-x}Y_x)Cu_2O_{6+d}$ ($0 \leq x \leq 0.5$), being compared with reported data.

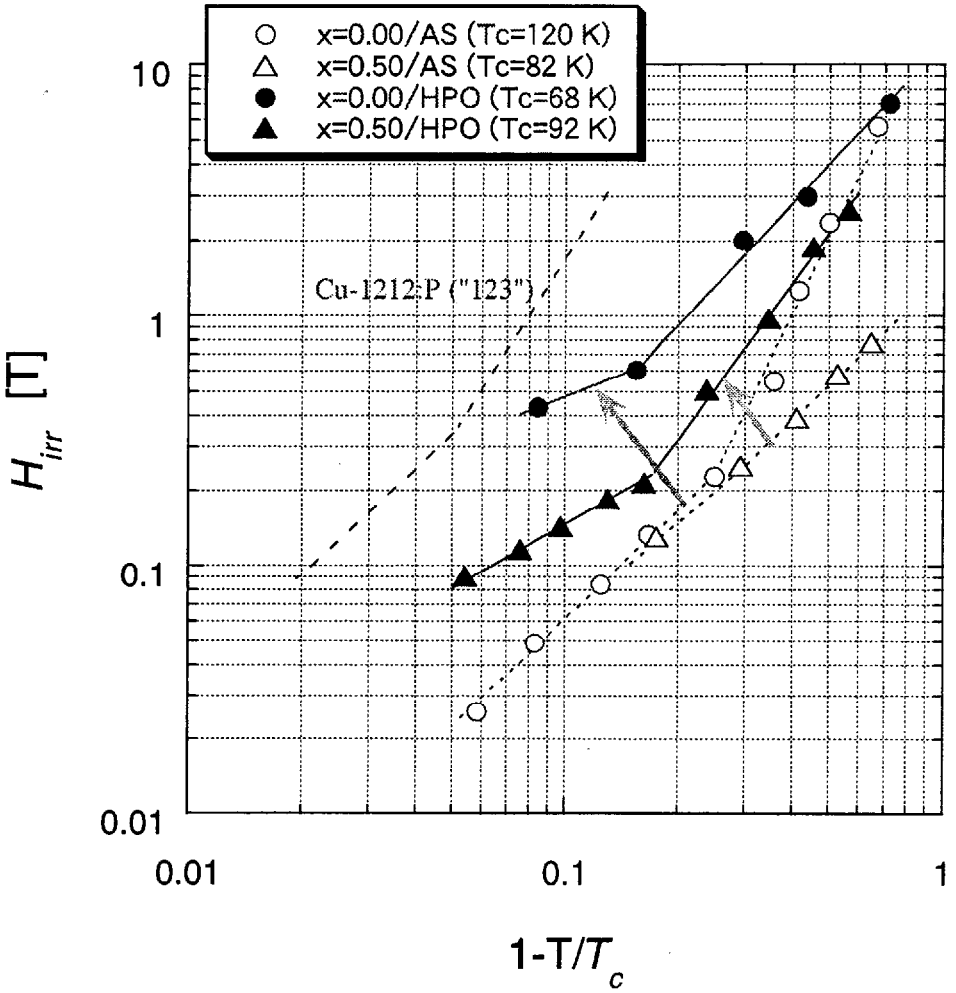

Fig. 2.12 Irreversibility field vs. (1-T/T_c) characteristics for as-sintered (AS) and high-pressure oxidized (HPO) samples with both x = 0.0 and x = 0.50 in $HgBa_2(Ca_{1-x}Y_x)Cu_2O_{6+d}$. A broken line exhibit a reference for Cu-1212 (so called a "123") material. Arrows are only guides for the eye.

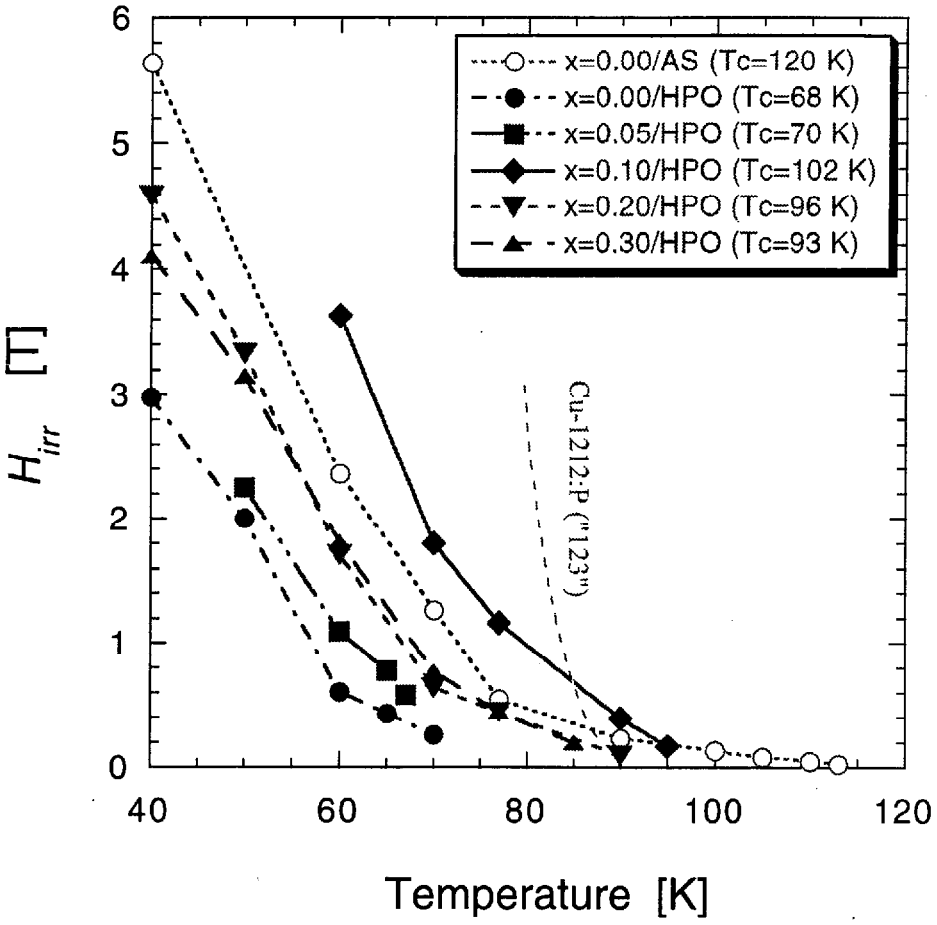

Fig. 2.13 Irreversibility field vs. T characteristics of high-pressure oxidized samples of $HgBa_2(Ca_{1-x}Y_x)Cu_2O_{6+d}$ ($0 \le x \le 0.5$). A broken line exhibit a reference for Cu-1212 (so called a "123") material.

and T_c. Previously, Nakane *et al.* [122] studied the correlation between the H_{irr} characteristics and hole density distribution in the Cu-1212:P compound in detail. They claimed that it was possible to obtain the optimization of both T_c and H_{irr} characteristics by controlling the hole density distribution which had been estimated from neutron powder diffraction data by BVS method (see Section 1-4-1). The present result is in agreement with their result.

Therefore we can conclude that the resulting optimized H_{irr}-vs.-T characteristics was achieved by controlling the hole density distribution in the present samples. This result agree with reported

5. Hole density distributions

In order to explain the results obtained above, it is worth while to examine the hole density distribution which in fact, should be a key for understanding the variance of high-T_c superconductors [13, 92]. A schematic image for the projective hole density distributions along the layers in the unit cell is shown in Fig. 2.14. In the figure, the upper three diagrams correspond to hole density distribution of the AS samples with x = 0.0, 0.1, 0.5, respectively. These distributions show that the hole density on the CuO_2 planes is getting gradually decreased by increasing Y content. In other words, higher content of Y substituting for Ca makes the sample more under-doped. In contrast to this, the three lower diagrams correspond to hole density distribution of the HPO samples. Many holes are produced by excess oxygen and these tend to remain in the CR block. The resulting distributions of holes are more homogeneous than those of the AS samples. Especially, in the case of x = 0.1 / HPO, the decrease of T_c caused by over-doped state is suppressed by selective annihilation of the hole adjacent to the CuO_2 planes. We believe there is considerable validity to this assumption, though it should not be driven too far, as we have no direct information about the real hole density distribution. Thus other experimental procedure for detecting the real distribution such as bond-valence-sum calculation [92], XANES measurement [168], TEM-CBED observation [118] *etc.*, is needed for further confirmation of the above results.

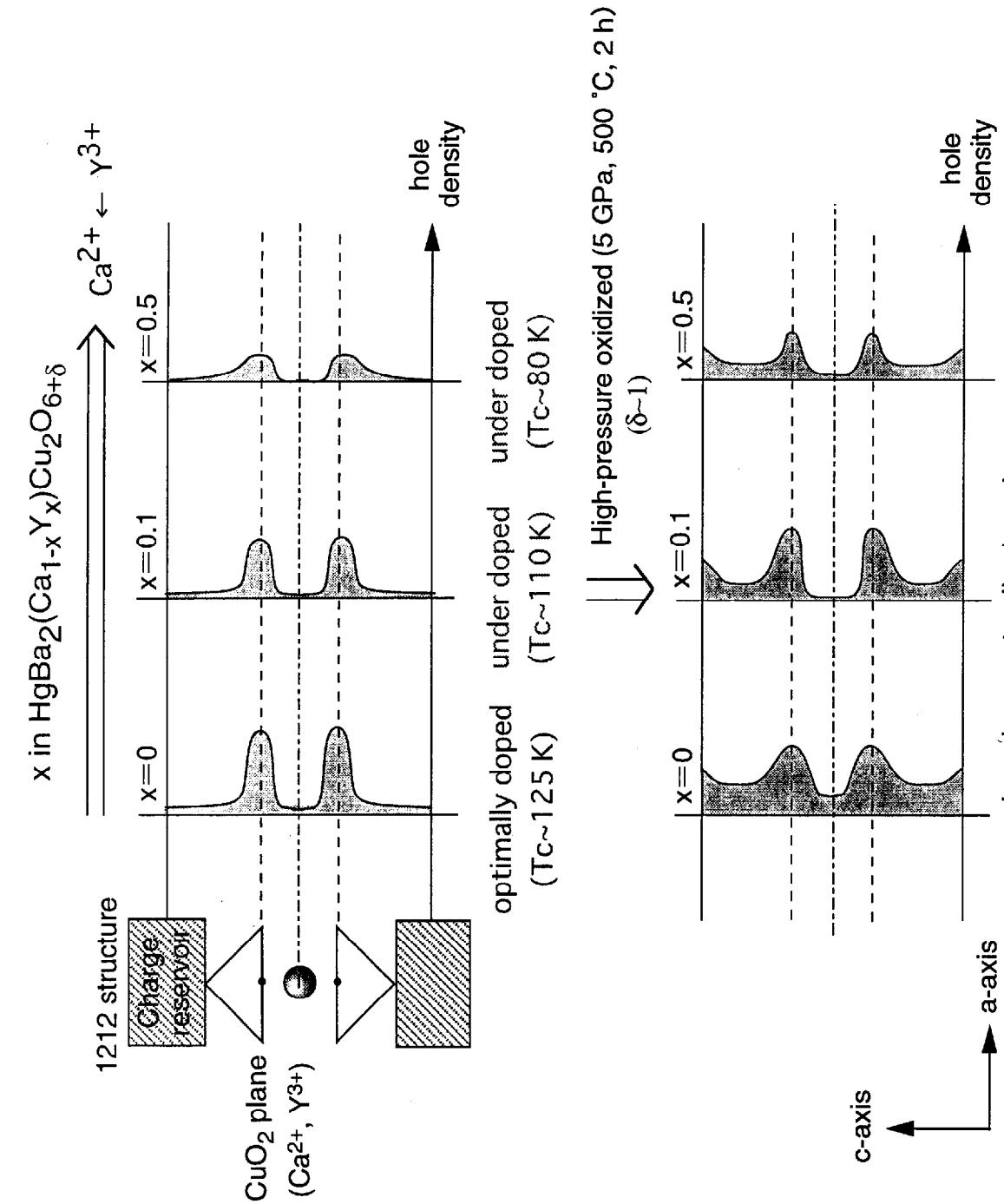

Fig. 2.14 Schematic image for projective hole density distributions along the layers in the unit cell of samples used in present study.

Hg-1223

1. Single crystals

The cationic substituted Hg-1223 $\{(Hg_{1-x}M_x)(Ba_{1-y}Sr_y)_2CaCu_3O_{8+\delta}\}$ has been successfully synthesized for M = Pb; x = 0 ~ 0.5; y = 0 ~ 1.0 [56]. Here, the large single crystals were obtained in the composition of x = 0.3, y = 0.75. A typical SEM image of the single crystals is shown in Fig. 3.7(a). The TEM-EDX analysis revealed the cationic composition of single crystals as $[Hg_{0.46}Pb_{0.46}][Ba_{0.54}Sr_{1.14}][Ca_{1.68}][Cu_{3.08}]$, indicating a large enrichment of Pb, and large decrease in Sr and Ca contents, compared with the nominal ratio. This implies that such ratio is favorable for growth of large crystals. Thus it should be hard to change the composition of the single crystals in this compound.

For the magnetic measurements, 25 single crystals were mechanically aligned on a surface of an epoxy-resin sample holder. The degree of grain alignment checked by XRD was pretty good as shown in Fig. 2.15. In the figure, only 00*l* peaks corresponding to the (Hg,Pb)(Ba,Sr)-1223 structure were detected. Consequently we found the crystals were well aligned even by the simple mechanical method.

Figures 2.16 (a), (b) show the magnetization hysteresis loops for the single crystals measured with the applied magnetic field parallel to both c-axis and a-axis, respectively. In the figure, the hysteresis measured with the applied magnetic field parallel to c-axis shows an obvious peak effect, while no peaks appear on that parallel to a-axis. The angular dependence on the peak effect is commonly observed in other superconductors [169, 170].

2. Irreversibility field characteristics

Figure. 2.17 shows the reduced temperature dependence of irreversibility field characteristics for the present (Hg,Pb)(Ba,Sr)-1223 single crystals and other results reported for typical HTSC single crystals. It is important to note that the (Hg,Pb)(Ba,Sr)-1223 possess the large enhancement in terms of the H_{irr}-vs.-$(1-T/T_c)$ characteristics compared with the pure Hg-1223 [67]. Moreover, the characteristics of (Hg,Pb)(Ba,Sr)-1223 is comparable to the Tl-1223 [171]. This means the such substitution is quite effective to improve the magnetic behavior. Nevertheless it is also found that the enhanced H_{irr} characteristics of (Hg,Pb)(Ba,Sr)-1223 cannot be comparable to that of Cu-1212:P ("Y-123"), reflecting the Cu-1212:P has better electronic anisotropy than (Hg,Pb)(Ba,Sr)-1223. The result shows a fairly good agreement with previous results found in the polycrystalline samples [56].

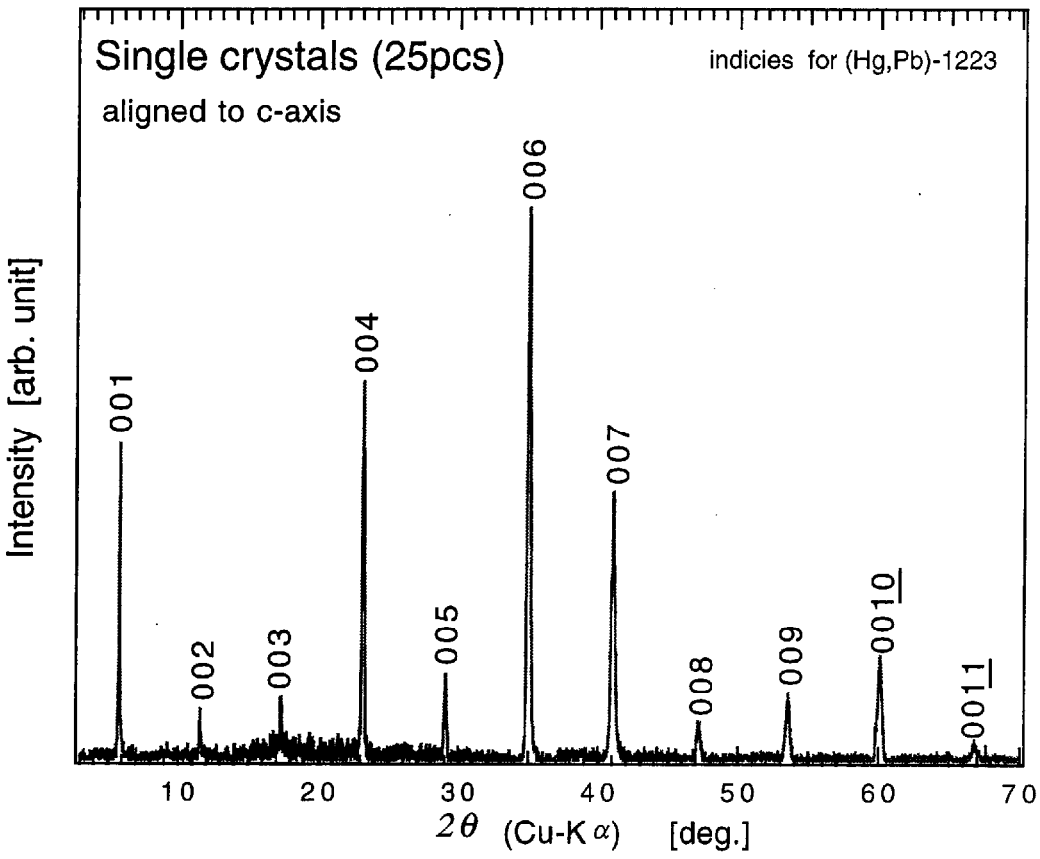

Fig. 2.15 XRD pattern for (Hg,Pb)(Ba,Sr)-1223 single cryatal samples with mechanically aligned to c-axis direction. Only 00*l* refrections are observed , indicating a degree of crystal alignment was good.

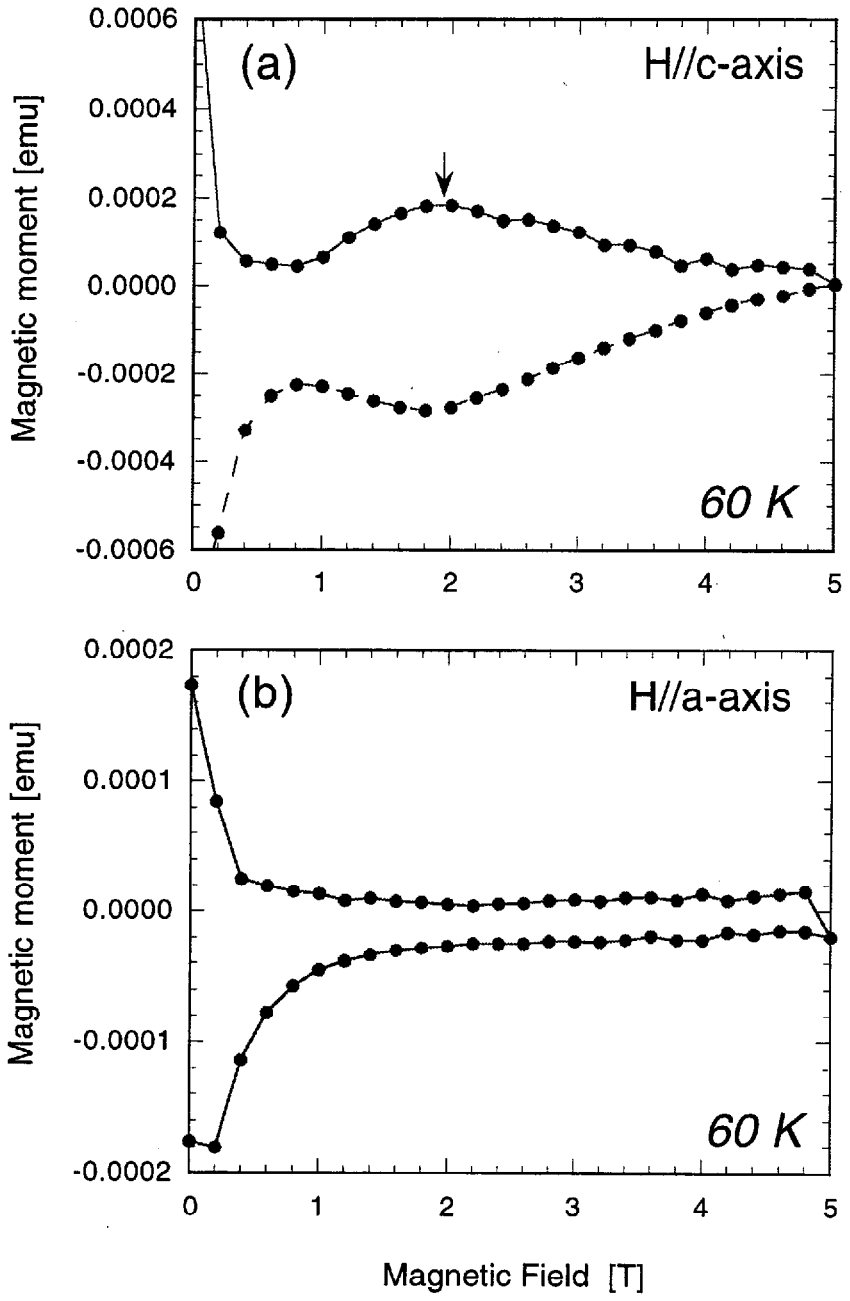

Fig. 2.16 Magnetization hysteresys loops (a) with applied field parallel to c-axis, and (b) to a-axis for (Hg,Pb)(Ba,Sr)-1223 single cryatal samples with mechanically aligned to c-axis direction. A large angular dependence was observed.

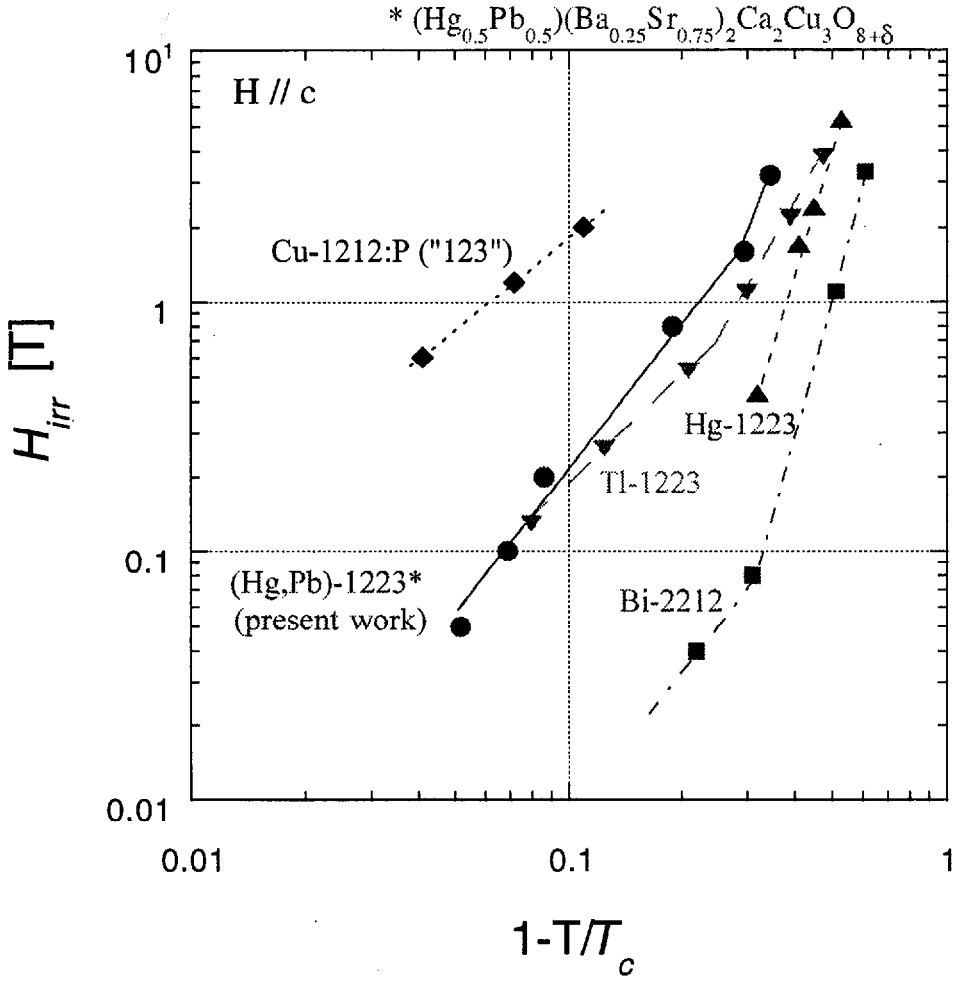

Fig. 2.17 Irreversibility field vs. (1-T/T_c) characteristics for for (Hg,Pb)(Ba,Sr)-1223 single cryatal, being compared to other conventional HTSC's.

2-4 Conclusion

The irreversibility field characteristics was investigated for the second member of the Hg-12(n-1)n homologous series having various hole density distributions. In order to control the hole density distribution, solid solutions of $HgBa_2(Ca_{1-x}Y_x)Cu_2O_{6+\delta}$ $(0 \leq x \leq 0.5)$ have been synthesized by an encapsulation technique and then post-annealed by a high-pressure oxidization (HPO) technique (5 GPa, 500°C, 2 hrs). All samples were found to successfully change their doping state from the under to the over-doped region. The best H_{irr}-vs.-$(1-T/T_c)$ characteristics was obtained by excess oxygen doping solely, reflecting that the fact the samples entered the most over-doped state. On the other hand, the samples simultaneously doped with both small amount of Y and oxygen, showed remarkably improved H_{irr} characteristics without large suppression of the T_c value. Consequently the optimized H_{irr}-vs.-T characteristics was achieved by controlling the hole density distribution in the Hg-1212.

The magnetic irreversibility study for Hg-1223 single crystals substituted by Pb and Sr, (Hg,Pb)(Ba,Sr)-1223 was carried out. A large enhancement was found in the (Hg,Pb)(Ba,Sr)-1223 compound, comparing with the pure Hg-1223 [67]. This means that such substitution is quite effective to improve the magnetic behavior, in other word utilized above, such substitutions lead a better electronic anisotropy reflecting the hole density distribution homogenized more by the cation substitutions (especially by Sr).

Chapter III Elucidation of the Mechanism for Peak Effect in (Hg,Pb)(Ba,Sr)-1223

3-1 Introduction

The members of mercury based homologous series $HgBa_2Ca_{n-1}Cu_nO_{2(n+1)+\delta}$ have been intensively investigated because of their higher critical temperatures (T_c) compared with other isostructural superconductors [7, 8]. Particularly, for the third member (Hg-1223) the highest T_c~135.4 K has been recorded under ambient pressure [9]. However the value of critical current density (J_c) and the magnetic field dependence of J_c are not so attractive from points of view of applications. Generally, in order to improve the J_c property and to raise irreversibility line in H-T space, introduction of effective pinning centers is required. Indeed, defects produced by heavy-ions, proton [147] or electron irradiation drastically improved J_c property, however, the T_c suppressed proportionally to density of defects [149]. Moreover, the depression of T_c is accompanied with a broadening of superconducting transition due to the local damages in CuO_2 planes.

Recently, cation substitutions, for example, Re or Pb for Hg site [37, 41, 42] and/or Sr for Ba site [37, 56] in Hg-1223 phase, were found to be very effective for improving J_c and irreversibility field characteristics. In addition, the enhanced "peak effect" was observed in these substituted compounds [172].

The presence of peak effect on the magnetization hysteresis loop is one of the common properties of type-II superconductors which is very attractive for the applications in terms of enhancement of J_c in strong magnetic fields [67, 155, 159]. Several explanations of this phenomenon have been proposed [155, 159-161], though its origin is still uncertain. According to some of them, the presence of weakly pinning defects in the superconducting matrix is crucial to get the pronounced peak effect [159-161]. If so, the magnitude of peak effect should mainly reflect a total number of weak pinning centers, while the position of secondary peak upon a H-T plane, so-called a "fishtail" line, $H_{s.p}$(T) show a good correlation with electronic anisotropy [155, 172]. For the case of (Y,*RE*)-123 such a defects like oxygen vacancy, oxygen vacancy clusters, impurity and antiphase defects were proposed as the candidates for weak pinning centers, however, no effective vortex pinning have been established for the mercury cuprate superconductors so far.

Recently, single crystals with substitution of Pb for Hg and Sr for Ba were obtained by means of an encapsulation technique [63] with better irreversible properties than those for other (Hg and Tl)-1223 compounds [172, 173]. The peak effect was observed not only in (Hg,Pb)(Ba,Sr)-1223 single crystals, but in the polycrystalline samples as well [173].

Moreover, we found that substitution of Sr for Ba markedly decrease the electronic anisotropy [172] and "fishtail" line in H-T space located higher than those for all reported (Hg and Tl)-1223 single crystals. However, the nature of the defects, that could be responsible for peak effect in these compounds is still unknown.

3-2 Experimental

(Hg,Pb)(Ba,Sr)-1223 polycrystalline samples were synthesized by encapsulation technique at 875 °C for 15 hours. The synthesis was essentially similar to the procedure which was invented previously by Colson *et al.*[61], except for the relatively high heating temperature. The single crystals were mechanically extracted from the bulk samples with nominal composition of $(Hg_{0.8}Pb_{0.2})(Ba_{0.25}Sr_{0.75})_2Ca_2Cu_3O_{8+\delta}$. The obtained single crystals have rectangle and regular shape and sizes ~ 100×100×30 μm^3 as shown in Fig. 3.7(a). The experimental details and the possible mechanism of the crystal growth are described in the reference [63].

For varying the doping state of the single crystals, some portions of a single crystal were post annealed under several conditions. An oxygenating anneal was performed under 150 bar of oxygen gas at 320 °C for 50 hrs. Reducing anneals were performed in 5%H_2/Ar gas flow at 350 and 300 °C for 0.5 hr and 20 hrs, respectively.

For comparison between two samples with and without peak effect, a high-pressure annealing was performed in order to depress the peak effect. A part of the powdered sample was heat treated under a pressure of 5 GPa at 1000 °C for 1 hr and then annealed in Ar gas flow at 350 °C for 10 hrs to obtain an optimal T_c value.

Phase composition of the samples was studied by X-ray diffraction (XRD) with Cu K_α radiation (M18XHF, MAC Science). Microstructure was observed by means of a field emission scanning electron microscope (FE-SEM) operating at 15 kV (S-4500, Hitachi). High-resolution electron microscopy (HREM), selected-area electron diffraction (SAED) and local compositional analyses were carried out by means of a field emission transmission electron microscope (FE-TEM) operating at 300 kV (JEM-3000F, JEOL) and equipped with an energy dispersive x-ray spectrometry detector (EDX; Series II, Noran). Note, that this TEM-EDX combination enables us to analyze the chemical composition of a local region with probing beam diameter of less than 1 nm and distance between each point of 3 nm. Furthermore a compositional analyses for the each point were based on the calibration with standard materials, which gave more correct value within an accuracy of about 2 %.

Magnetic studies were performed by a DC SQUID magnetometer (MPMS-5S, Quantum Design) under applied field up to 5 T. For the case of single crystals measurements, 25 single crystals were mechanically aligned on a surface of an epoxy-resin sample holder.

3-3 Results and Discussion

3-3-1 Aspects in the peak effect

1. Angular dependence

The magnetization hysteresis loops for the single crystals measured with the applied field parallel to c-axis and a-axis are shown in Figs. 2.16 (a), (b), respectively. In the figure, the hysteresis parallel to c-axis shows an obvious peak effect, while no peaks appear on that parallel to a-axis. The angular dependence of the peak effect is commonly observed in other superconductors [169, 170]. As an interpretation for the angular dependent, Klein *et al.* pointed out as follows. When the curve are plotted as a function of the component of the field along the c direction, $H_{\perp}$, and taking into account that the actual magnetization, m written by;

$$m = M / \cos\theta \ , \qquad (3\text{–}1)$$

where, θ is angle between applied magnetic field and c-axis and M the magnetization at $\theta = 0$. The magnetization curves in which involving a peak effect for various angles, $M(\theta, H)$-vs.-$H\cdot\cos\theta$ become completely overlapping each other. This indicates that the peak effect is basically related to critical currents in the CuO_2 planes [169].

2. Temperature dependence of peak field, $H_{s.p}$

The temperature dependence of peak field, $H_{s.p}$ in which the magnetization curve makes a maximum point was investigated. Figures 3.1(a) and (b) respectively shows the magnetization curves for as-grown and strongly reduced single crystals with applied field parallel to c-axis. Judging from Fig. 3.1(b), the magnitude of hysteresis width of the reduced single crystal is generally smaller than that of the as-grown crystals, for example, the ratio among them is four times at 60 K in 1 T. More noteworthy is the temperature dependencies of value $H_{s.p}$ for both the as-grown and the reduced single crystals are different. Figure. 3.2 shows the temperature dependence for several single crystals which were subjected to different annealing conditions, first the strong reduction (5%H_2/Ar flow at 350 °C for 20 hrs), secondly the short time reduction (5%H_2/Ar flow 300 °C for 0.5 hr), finally the oxidation annealing (150 bar of oxygen at 320 °C 50 hrs). In Fig. 3.2, the temperature dependence of magnetic susceptibility for these single crystal samples is shown. The reduced samples show increase of the T_c value from 115 K to 122 K, whereas the high-pressure oxidized sample shows an almost same curve as as-grown one. This result indicates the as-grown sample was

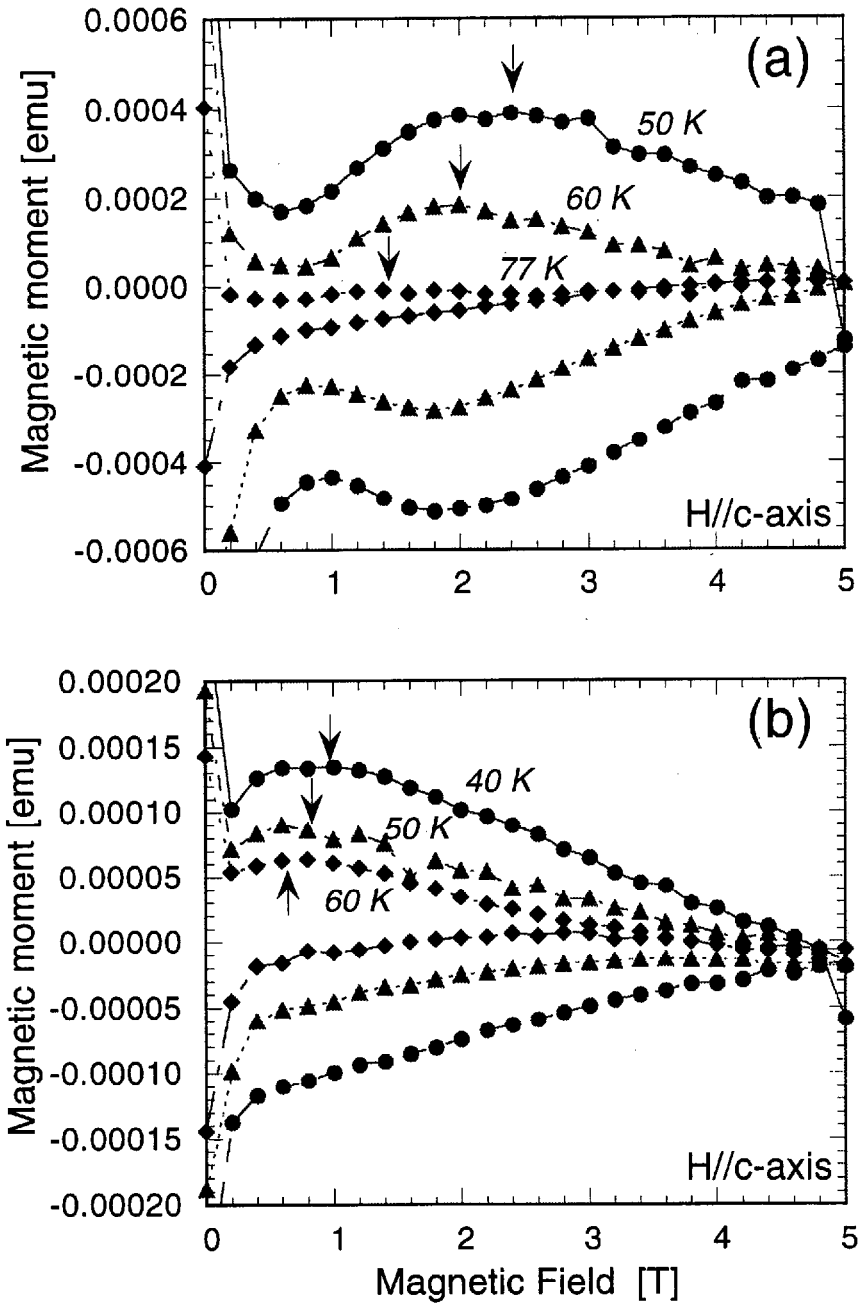

Fig. 3.1 Magnetization hysteresys loops with applied field parallel to c-axis for (Hg,Pb)(Ba,Sr)-1223 singles crystals (a) as-grown in encapsulation technique and (b) reduced in 5%H_2/Ar 350°C 20hrs.

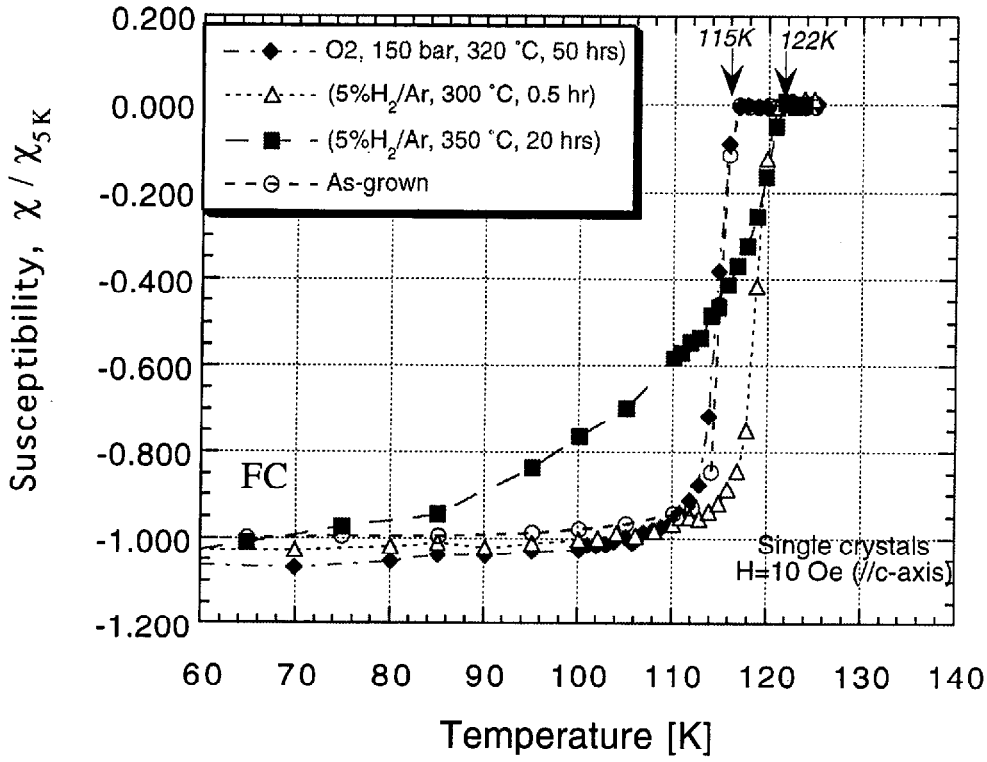

Fig. 3.2. Temperature dependence of susceptibility for single crystals with various annealing conditions

in over-doped state. Furthermore, oxygen content of the high-pressure oxidized sample has not changed even in the highly oxygenating condition. The most reduced sample showed almost same T_c as the sample with short time reduction, however, the transition was broadened. From this result indicates that the strongly reduced sample has started to decompose during the annealing process. Thus, we supposed that it is hard to further reduce an oxygen content than short time reduction in present single crystal.

These single crystals whose oxygen content must be altered by annealings clearly show different temperature dependence of $H_{s.p}$. As shown in Fig. 3.3, the single crystal with higher oxygen content generally indicates the higher $H_{s.p}$, except for the crystal oxygenated under high-oxygen-pressure showing slightly lower position from the as-grown crystal. From the susceptibility measurement, it was likely that the doping level of high-pressure oxidized single crystals must not far from the as-grown single crystals. Thus the temperature dependence of $H_{s.p}$ for high-pressure oxidized single crystals was consistent with the result of susceptibility measurement. As mentioned above, it is clear that the stronger reduction makes the $H_{s.p}$ more reduced. This result is consistent with the results previously reported for $TlBa_{0.8}Sr_{1.2}Ca_2Cu_3O_{9-\delta}$ [174], $(Tl_{0.6}Pb_{0.4})(Ba_{0.3}Sr_{1.7})CaCu_2O_y$ [175], $HgBa_2Ca_2Cu_3O_{8+\delta}$ samples [67]. Furthermore, what revealed here is that the temperature dependence of $H_{s.p}$ mainly correlates to the degree of hole doping, suggesting that the peak effect is reflecting not only extrinsic properties (*e.g.* vortex pinning by defects) but also intrinsic properties such as hole doping state.

3. Particle size effect

Furthermore the size effect of the peak effect was studied since the well pronounced peak effect on magnetization hysteresis loop has been observed in the $(Hg,Pb)(Ba,Sr)_2Ca_2Cu_3O_{8+\delta}$ poly-crystalline sample synthesized by encapsulation technique as well as single crystals. Figs. 3.4 (a), (b), (c) show the temperature dependence of the magnetization hysteresis loops for the samples with different forms, such as single crystal (average grain size, $d \sim 100$ μm), sintered bulk ($d \sim 40$ μm), compacted powder ($d \sim 10$ μm), respectively. Comparing these temperature dependencies, two significant characters are distinguished. First one is that the hysteresis shape changes subsequently from symmetric to asymmetric about horizontality. This asymmetry is most likely to be induced by the existence of surface barrier which generally makes the shape of magnetization hysteresis asymmetric. Note that the strong surface barrier has been often seen in the superconducting mercury copper oxides [84, 141, 176-181]. The same observation applies to this study, that is the behavior of sample with small grain size clearly shows the surface-barrier-induced asymmetry, since the portion of surface per a unit volume increases with decreasing the grain

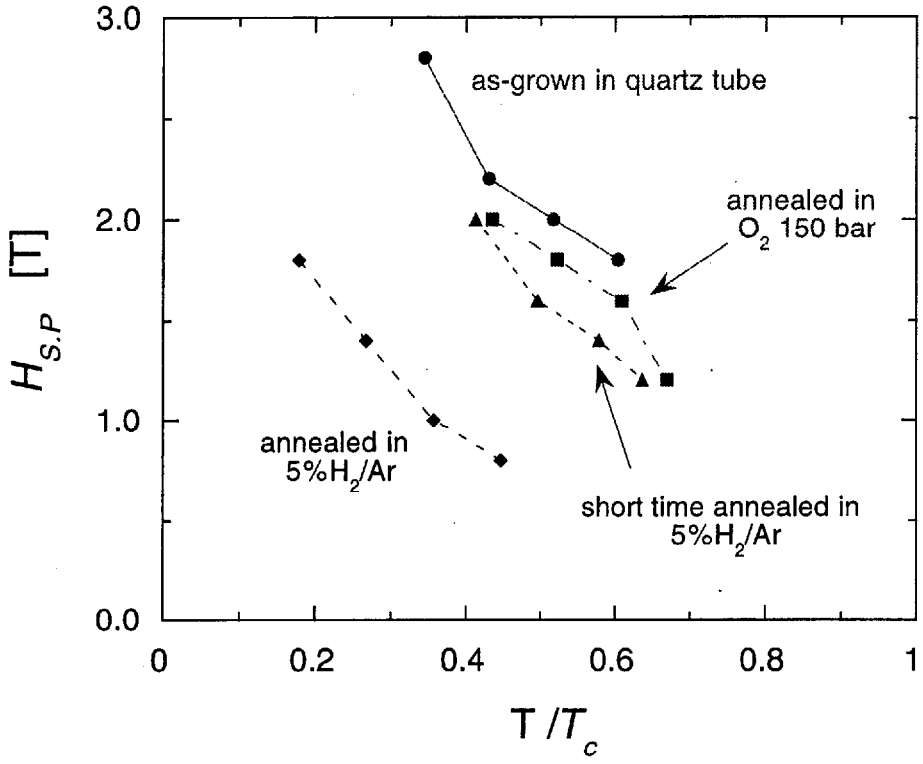

Fig. 3.3 Temperature dependence of peak field ,$H_{s.p}$ for (Hg,Pb)(Ba,Sr)-1223 single crystal with a various annealing condotions.

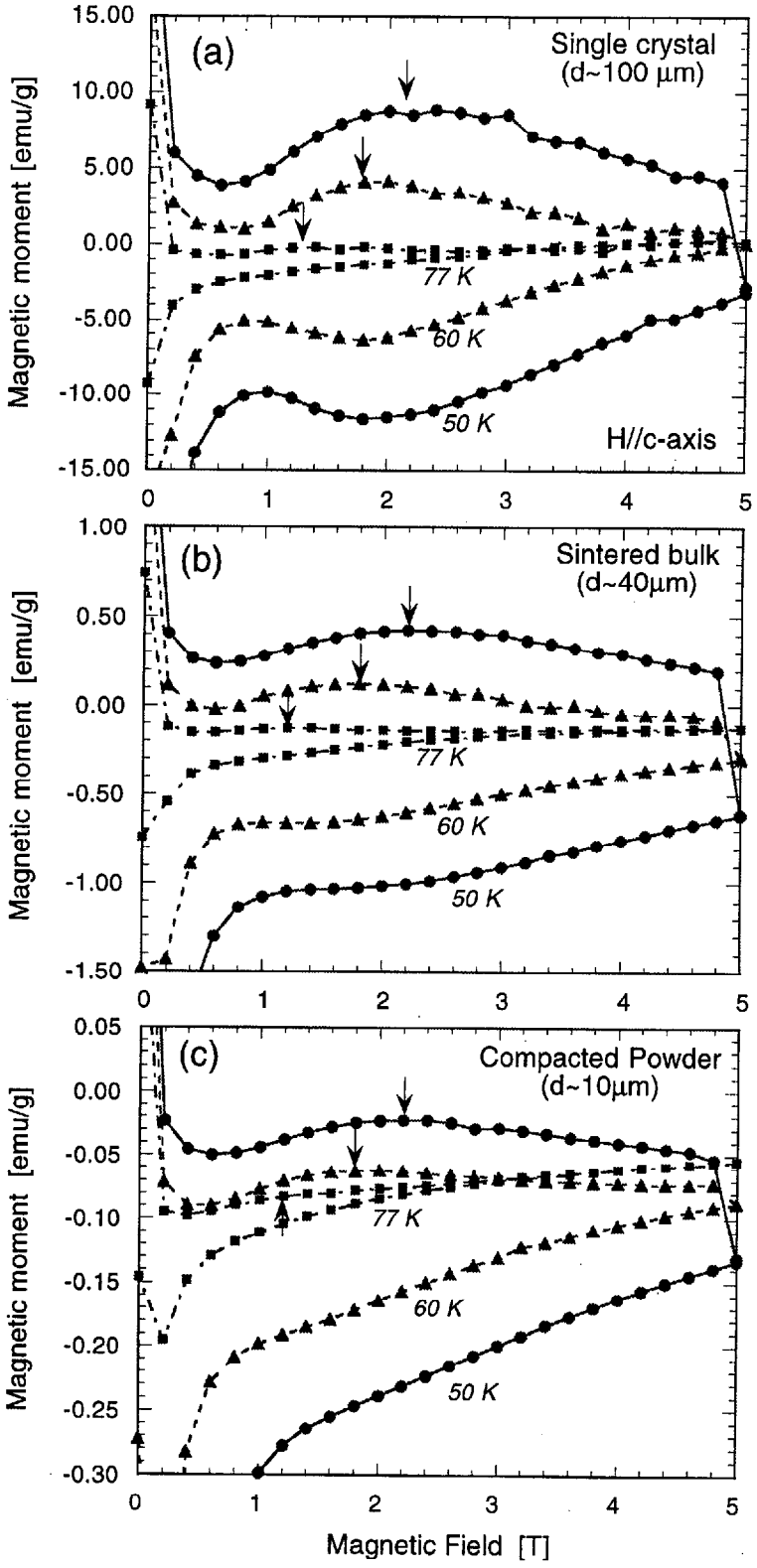

Fig. 3.4 Magnetization hysteresis loops for (a) singles crystals, (b) sintered bulk and (c) compacted powder samples of (Hg,Pb)(Ba,Sr)-1223 compouns.

size. The other apparent feature can be extracted from the $H_{s.p}$ behavior which emphasized by arrows in Figs. 3.4 (a), (b), (c). The result shows that the $H_{s.p}$ is not sensitive to grain size, besides the $H_{s.p}$ lines for the samples with different state (*i.e* strongly reduced or fully Sr substituted sample) are located in considerably different positions as shown in Fig. 3.5. On the other hand the magnitude of the magnetization hysteresis is reduced by decreasing the grain size. This result is quite consistent with our qualitative understanding, that is, the quantity $H_{s.p}$ is rather an intrinsic parameter as suggested above. The smaller grain size makes a large fraction of surface barrier in the magnetization resulting the peak effect which is originally a bulk property should be less pronounced. Here, it is worthwhile to note that the single crystal shows inadequately large magnetization signal compared with other two samples as shown in Fig. 3.4 (a), originated from a demagnetizing effect caused by the plate-like shape of the single crystals and/or from the angular dependence of the peak effect which reduces the magnetization hysteresis with certain amount, especially in the peak position.

4. Correlation with anisotropy

The above mentioned discussion of the size effect allows us to compare the samples through different forms, such as single crystal, sintered bulk, compacted powder. Thus, some typical $H_{s.p}$ lines are shown in Fig. 3.6 with those for other reported materials. Generally, the peak effect concerns, at least, a cross-over of the dimensionality of vortices. In this sense, the peak field, $H_{s.p}$ can be correlated to 2D - 3D cross-over field, H_{cr} [85, 155]

$$H_{cr} \propto \Phi_0 / \gamma^2 s^2 \ , \qquad (3\text{-}2)$$

where Φ_0 is flux quantum, γ the electronic anisotropy ($\gamma = \lambda_c/\lambda_{ab} = \xi_{ab}/\xi_c$), and the s inter-layer spacing. From this stand, the $H_{s.p}$ represents the both electronical and structural properties. If we compare the $H_{s.p}$'s among different materials with similar structure, the value of the $H_{s.p}$ may be roughly proportional to the anisotropy. Therefore, from Fig. 3.6, we can conclude the Ba-free (Hg,Pb)-1223 sample possessing the lowest anisotropy than any other samples subjected to compare. Furthermore, it is important to point out that the Sr substitution seems to work well for reduction of the anisotropy of present materials. This means the great advantage of the Sr substitution for providing the engineered materials.

3-3-2 Origin of the peak effect

1. Samples

As-sintered sample made by conventional method typically has smaller grains of 10 μm size in average as shown in Fig. 3.7(b). A part of the sample was heat treated under a pressure of 5 GPa and at 1000 °C for 1 hr and then annealed in Ar gas flow at 350 °C for 10 hrs to obtain an optimal T_c value. The high pressure treated poly-crystalline samples are

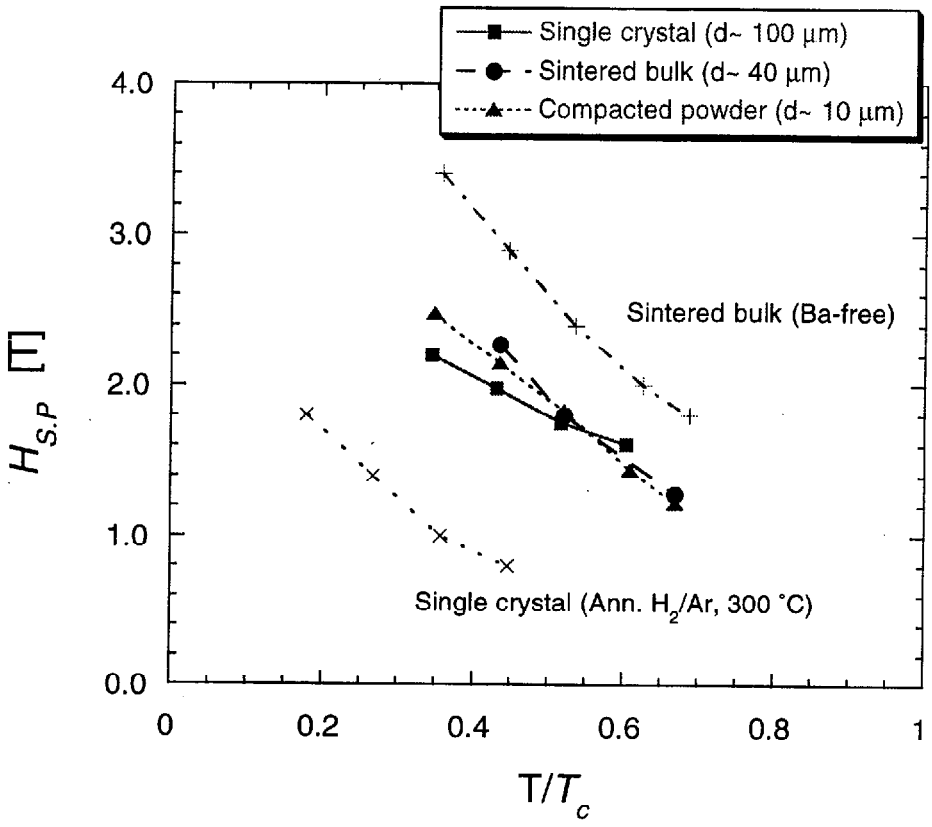

Fig. 3.5 Temperature dependence of peak field ,$H_{s.p}$ for (Hg,Pb)(Ba,Sr)-1223 single crystals with different particle size, being compared to strongly reduced (in 5%H_2/Ar 350°C 20hrs) single crystals and as-sintered bulk with Ba-free (Hg,Pb)(Sr)-1223 composition.

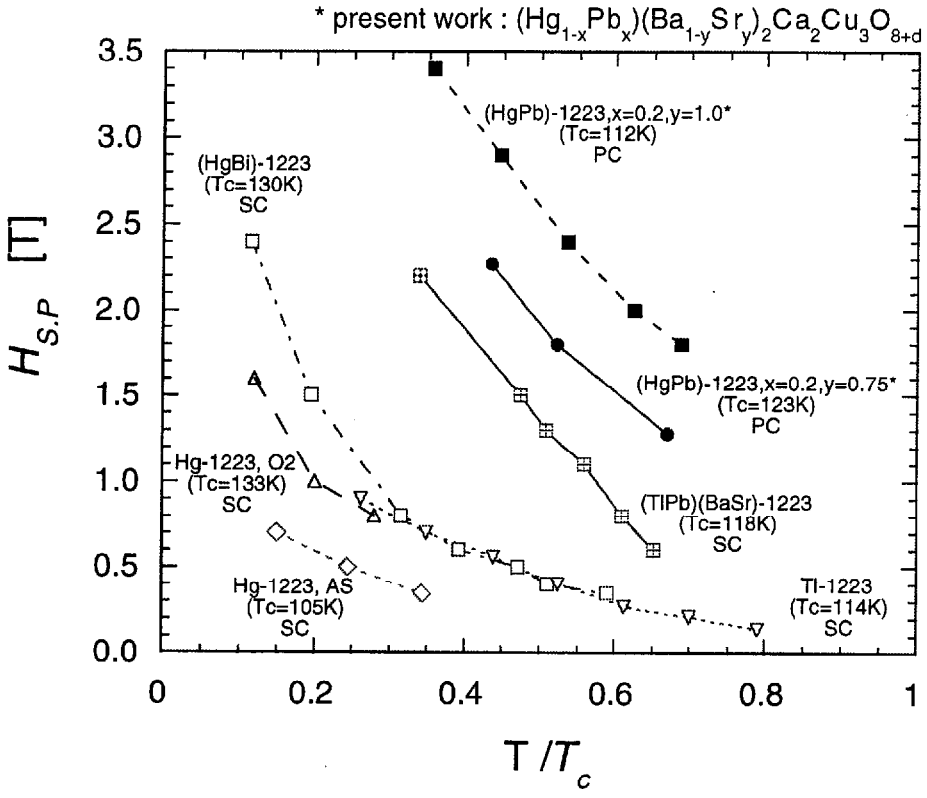

Fig. 3.6 Temperature dependence of peak field ,$H_{s.p}$ for (Hg,Pb)(Ba,Sr)-1223 poly-crystalline samples with different Sr contents, being compared to other conventional HTSC's.

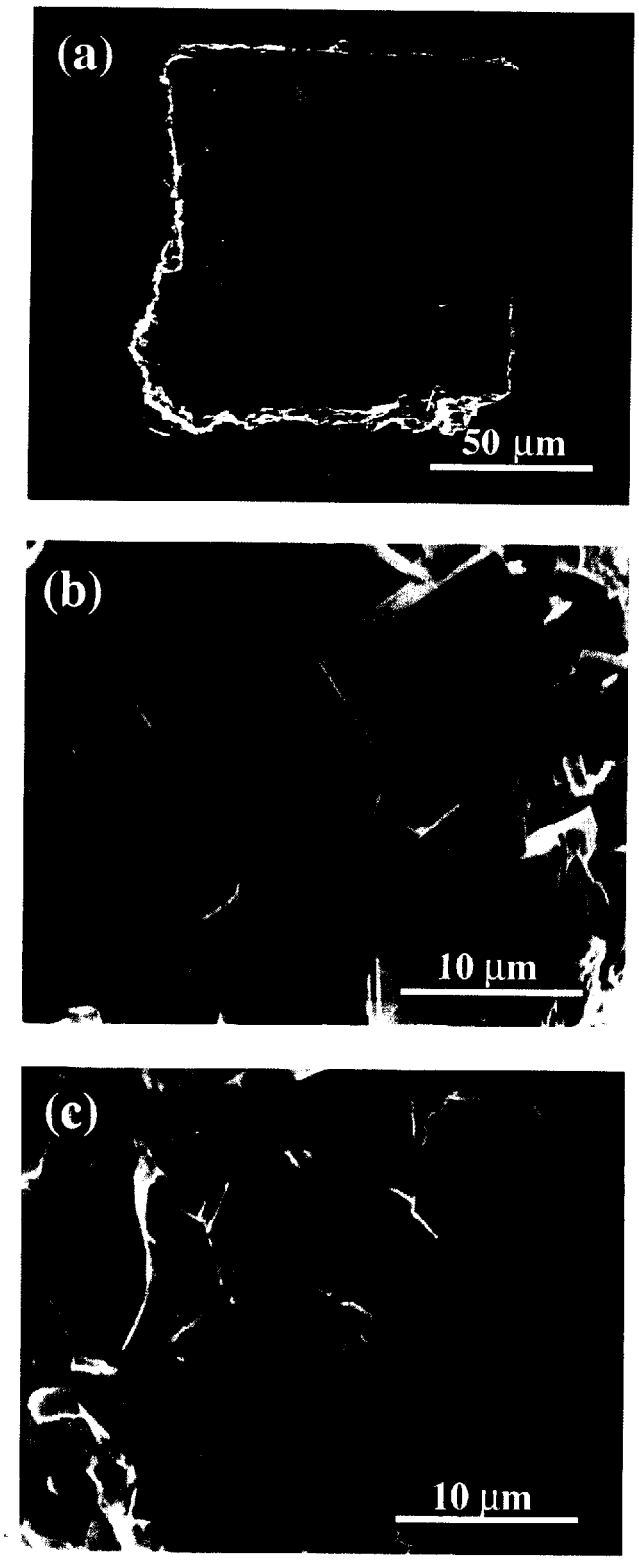

Fig. 3.7 Typical SEM images of (Hg,Pb)(Ba,Sr)-1223 samples: (a) singles crystals and polycrystalline samples (b) synthesized by encapsulation technique and (c) high-pressure technique

more dense and their grains are strongly linked each other as seen in Fig. 3.7(c), however, the size itself was not so affected during the high-pressure treatment.

Figure 3.8 shows the normalized temperature dependence of DC magnetic susceptibility in the field cooled mode for the samples prepared by the encapsulation and the high-pressure techniques. The onset T_c of these samples were 116 K, 123 K and 120 K, respectively. The magnetization hysteresis loops at 60 K for those samples are presented in Fig.3.9. The inset shows the similar data for single crystals in H//c geometry. Obviously, single crystal sample has a clear peak effect on both increasing and decreasing branches of hysteresis loop, seems like that of the (Y,*RE*)-123 single crystals. However, a well pronounce peak effect can be define also in the polycrystalline sample prepared by the encapsulation technique, in contrast to the high-pressure synthesized one. Generally, large scale defects such as precipitation of secondary phases or weak links could depress the peak effect [182, 183]. In our case, more pronounced peak effect was observed not for the high-pressure synthesized polycrystalline sample with less weak links but for the encapsulation sample which should have the large scale defects more than the former one. The other hand, the irreversibility field characteristics for both samples were not so different each other as shown in Fig.3.10, where the values of irreversibility field were determined as the field at which the difference between increasing and decreasing branches of magnetization hysteresis loops are extrapolated to be zero [121, 124]. Thus these samples should be possessing almost same electronic anisotropy characteristics. Therefore, judging from the width of hysteresis loops in Fig.3.9 and their comparable values of T_c and average grain size, the high-pressure sample is much inferior compared with the encapsulation sample only in terms of vortex pinning properties under moderate field.

2. Microstructural study

In order to clarify the difference between these polycrystalline samples in terms of peak effect characteristics in the moderate field, microstructural studies were carried out as follows.

The typical SAED patterns with the incident beam parallel to [001] are presented in Figs.3.11 (a), (b) for both encapsulation and high-pressure samples, respectively. The fine streaks along <110> are clearly observed on the each spot of higher order reflections for encapsulation sample. We estimated that these streaks are corresponding to a crystalline modulation with wavelength of tens nm order in the real space. In contrast, there is no trace of such structure in the high-pressure sample.

The corresponding HREM images in (001) plane for both encapsulation and high-pressure samples are shown in Figs.3.12 (a), (b), respectively. Distorted regions are visible in the case of encapsulation sample, whereas no such a distortions can be observed in the high-

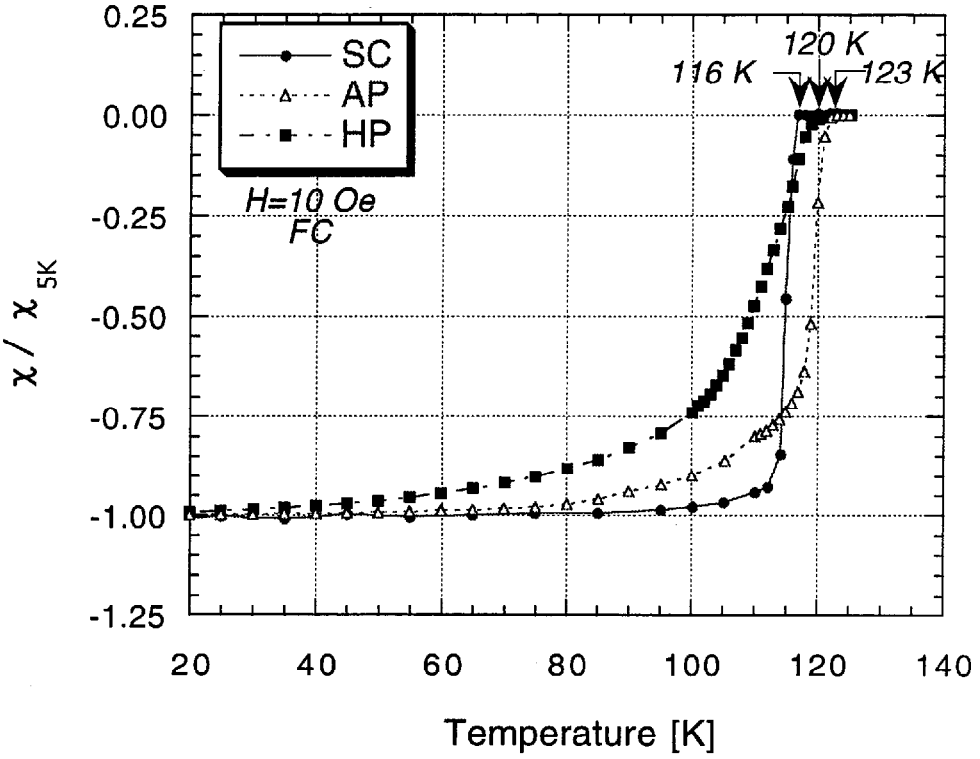

Fig. 3.8 Normalized temperature dependence of DC susceptibility for singles crystals (SC), polycrystalline samples as-prepareed by encapsulation technique (AP), and high-pressure technique (HP).

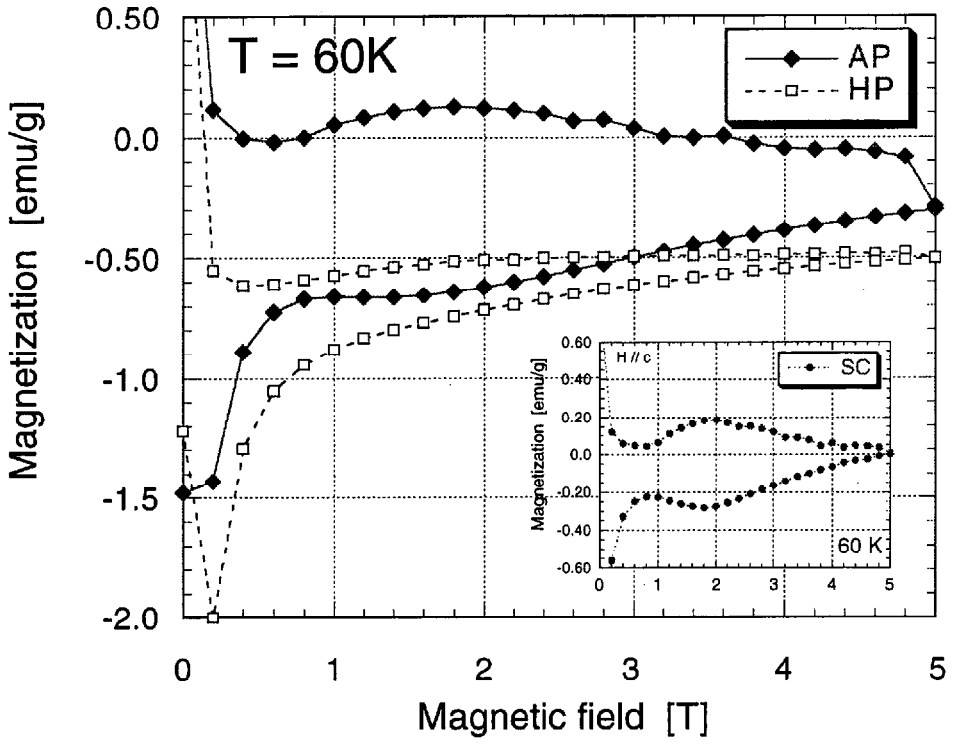

Fig. 3.9 Magnetization hysteresis loop at 60 K for the as-prepared bulk (AP), high-pressure synthesized bulk (HP). Inset shows the same data for single crystals (SC) samples.

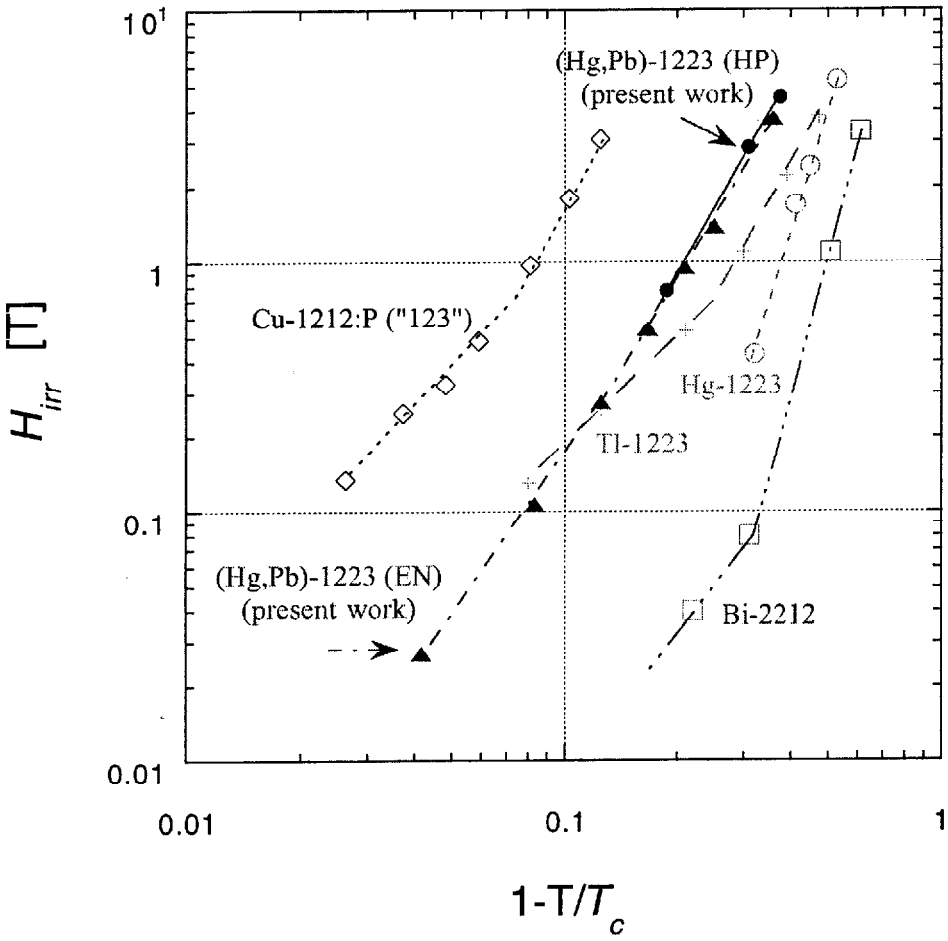

Fig. 3.10. The log-log plot of temperature dependence of Irrversibility field for encapsulation (EN) and high-pressure (HP) samples of (Hg,Pb)(Ba,Sr)-1223 compound, being compared to those for other conventional HTSC's.

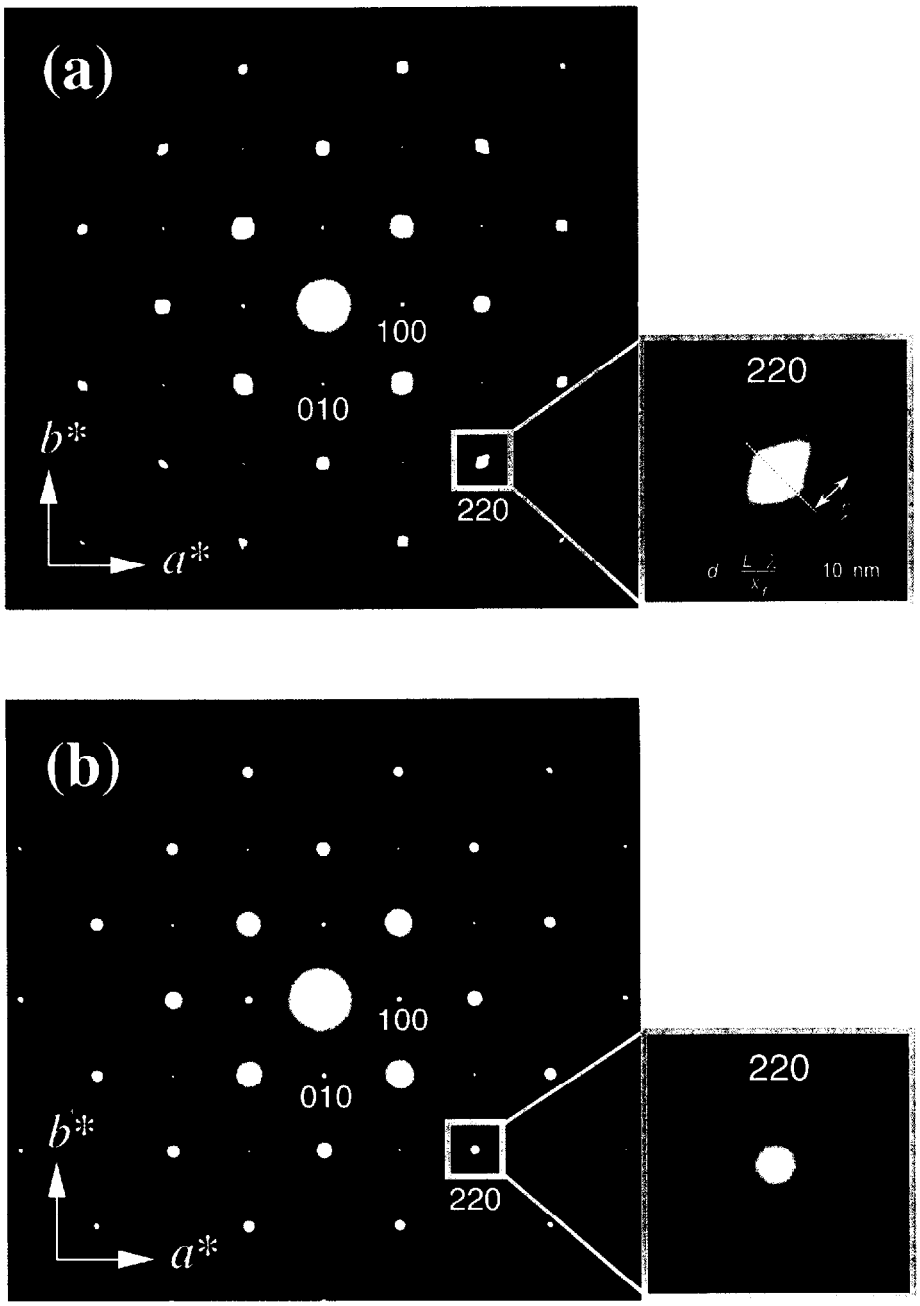

Fig. 3.11 The SAED pattern with incident beam parallel to [001] for (a) the as-preapred sample by encapsulation and (b) prepared under high-pressure tequnique. Inset shows the magnified image of 220 spot.

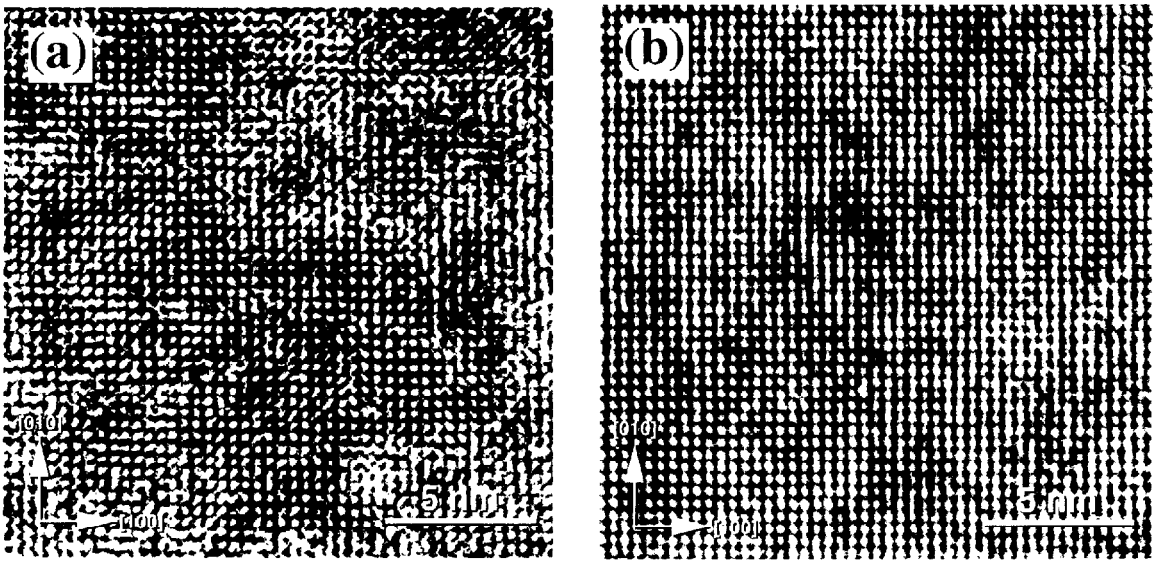

Fig. 3.12 HREM image for (001) plane of (a) the as-preapred sample by encapsulation and (b) prepared under high-pressure tequnique.

pressure synthesized one. Furthermore, both images have some dark regions probably reflected by an existing of strain fields. To extract the distinct features from these HRTEM images, the images were examined further. The HRTEM images were processed via Fourier filtering in which the Fourier transformed pattern was masked to select systematic reflections in order to improve the lattice images. The Fourier filtered HRTEM images for both encapsulation and high-pressure samples are shown in Figs. 3.13 (a), (b), respectively. In the figure for encapsulation sample, apparently, the regions with severely distorted lattice are visible.

3-3-3 Compositional analysis

Using the combination of TEM-EDS, the distribution of cations in the matrix of the single crystal and in the sample prepared under high-pressure was studied along with the <110> direction. During the EDS measurement, we took account into that the thickness of the illuminated region should be comparable in order to avoid a serious deviation of absorption coefficients for each element. The results for encapsulation and high-pressure samples are shown in Figs.3.14 (a), (b), respectively. Remarkably, in the case of the encapsulation sample there is an obvious alternative fluctuation of Hg and Pb ratio from 4% to 8% around, without any specific variation of other elements. This compositional fluctuation could be considered as a substantial modulation of atomic concentration because it was beyond the accuracy of EDX analysis. The other hand, less fluctuated compositions for each element were found in the high-pressure sample. In detail, there are certain fluctuations for each element. However, the physical properties should be more sensitive to the substitution for the Hg site than for other sites. The distribution of Hg and Pb in the region can be extrapolated by sinusoidal curves with the periodic length of ~ 20 nm. This value is roughly in agreement with the wave length of crystalline modulation (tens nm), estimated from the SAED data Fig.3.11(a). Note that each diffraction spot accompanies streaks rather than the extra spots that correspond to a certain superstructure. This implies that there are many waves of the modulation on the <110> direction with different periods of tens nm.

The average compositions were estimated as $Hg_{0.46}Pb_{0.46}Ba_{0.54}Sr_{1.14}Ca_{1.68}Cu_{3.08}O_y$ and $Hg_{0.70}Pb_{0.21}Ba_{0.48}Sr_{1.08}Ca_{1.83}Cu_{3.09}O_y$ for crystals of both encapsulation and high-pressure sample, respectively. These data show that both samples have slightly Cu rich and Sr and Ca poor composition. However, it is important to note that a strong enrichment of Pb in the encapsulation sample is found, whereas the high-pressure sample has less Pb. This should be requested by a solubility limit under the condition of 5 GPa.

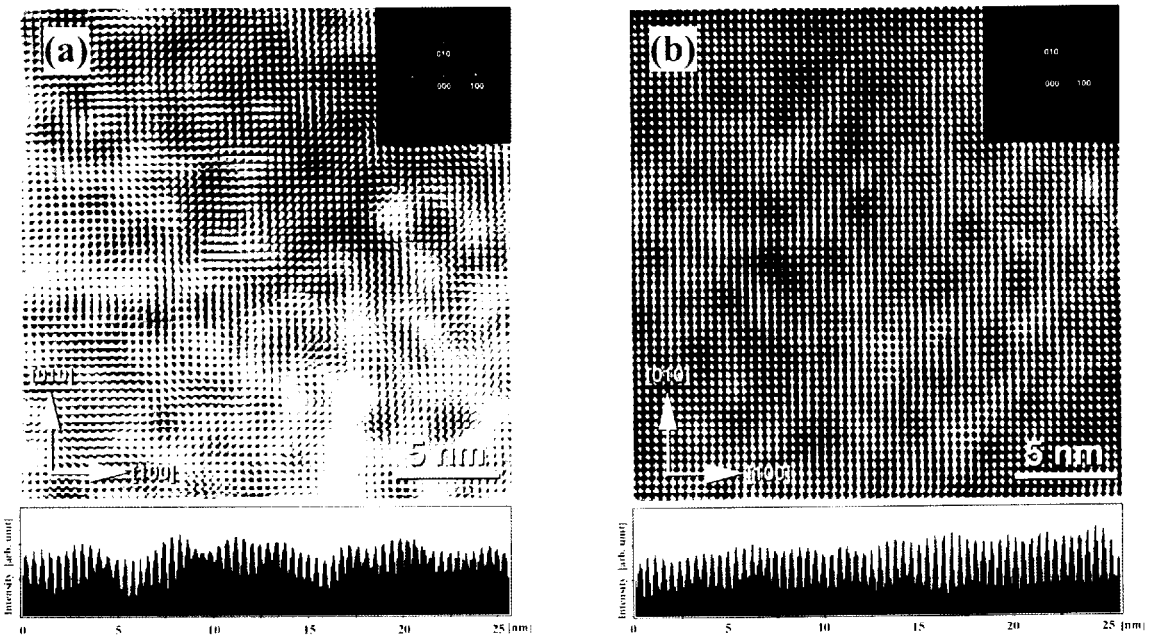

Fig. 3.13 Fourier filtered HREM images (from Fig. 3.12) for (001) plane of (a) the as-preapred sample by encapsulation and (b) prepared under high-pressure tequnique. Inset shows a Fourier diffractogram. Bottom is a cross-sectional intensity along [100].

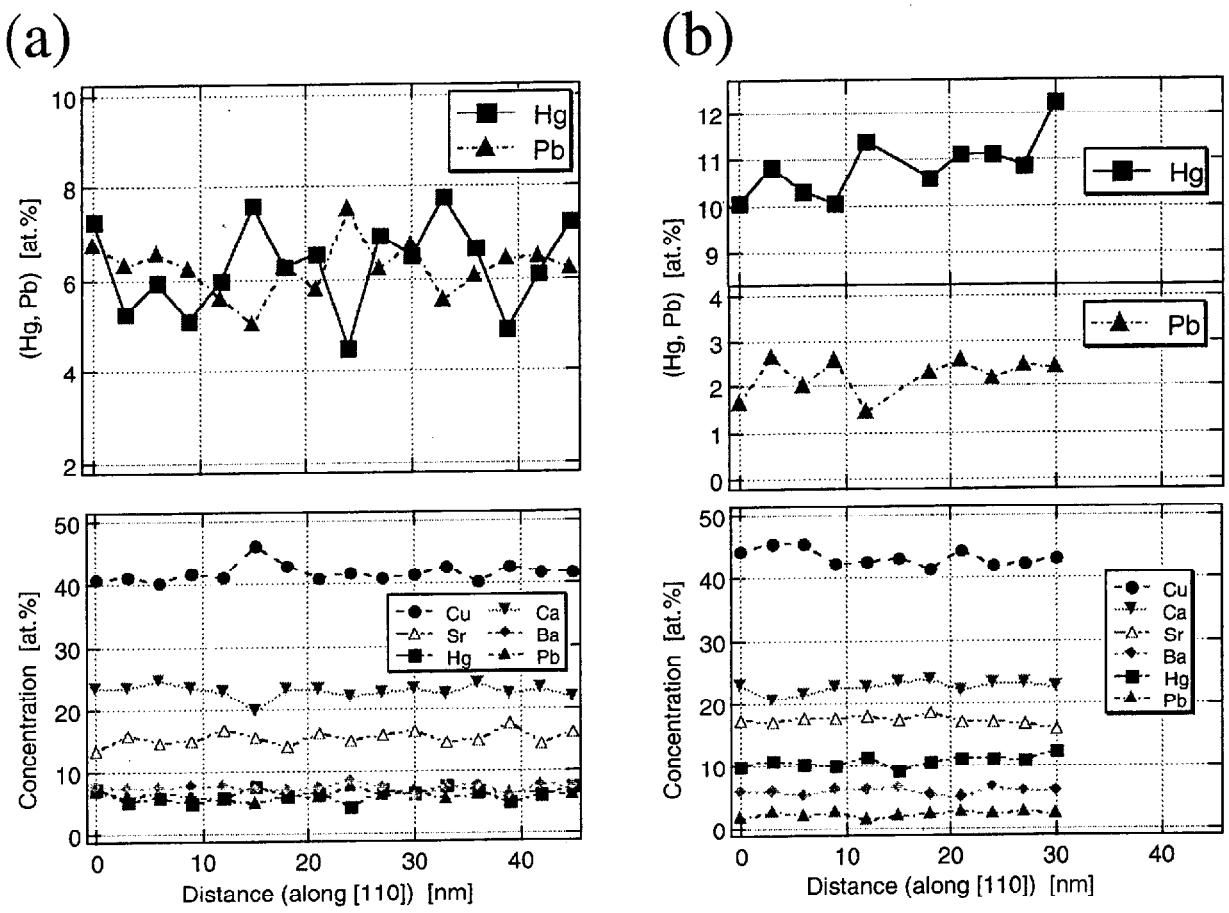

Fig. 3.14 Compositional distribution along with <110> of (a) the as-preapred sample by encapsulation and (b) prepared under high-pressure tequnique. Probing beam size was 1 nm and a distance between each points was fixed at 3 nm.

3-3-4 Compositional modulation

(1) Previous works:

A few reports concerning a correlation between the inherent disorder of crystal structure and J_c property for HTSC compounds were published [42, 64, 184]. The compositional modulations for Nb/Ba was reported in Nd-123 single crystals resulted by spinodal decomposition [185, 186]. The lamellar structures of Pb rich phase, as the result of eutectoid decomposition was observed in the heavily Pb doped Bi-2212 single crystals possessing a large enhancement on J_c [187, 188]. For the mercury based compounds, a chemical pressure-induced compositional modulation with a periodic length of 3 nm in <110> direction was assumed from high-resolution lattice imaging coupled with structural simulations for the (Hg,Pb)-1223 compound [42]. The model with clustering of Pb^{4+} was proposed for single crystal structure refinement of (Hg,Pb)-1234 [64]. Our result presented here is in well agreement with this model.

(2) Present work:

The compositional modulations in the studied single crystal can be interpreted in frame of spinodal decomposition mechanism. This is in a good agreement with the existence of diffused interface between the regions of different chemical compositions, that is one of the feature of this process. For example, the same diffused interface was observed on the early stage of ordering in CuAu alloy reported as a possible product of spinodal decomposition [189]. Furthermore, the ratio of Hg:Pb equals to 1:1, estimated for the encapsulation sample, is quite favorable for occurring of the spinodal decomposition. Judging from these facts, a possible origin for the formation of modulated structure in (Hg,Pb)(Ba,Sr)-1223 phase is spinodal decomposition mechanism, however, more detailed experiments such as a determination of the spinodal temperature and/or the temperature dependence of modulated period are required.

3-3-5 Possible mechanism of pinning

Considering the T_c value for the Pb-1223 phase is equal up to 123 K [190], the local Pb rich region in the encapsulation (Hg,Pb)(Ba,Sr)-1223 sample should have a lower T_c than that of the matrix. Consequently, the lattice disorder resulted from compositional modulation could suppress the superconducting order parameter moderately and may act as δT_c type pinning centers [191, 192]. Figure. 15 shows the schematic illustration of a vortex in high-κ (κ is GL parameter) material, the order parameter is repelled just around the vortex resulting the vortex gains a energy just corresponding to the repelled order parameter. The model for pinning induced by the modulation of local-order-parameter has been suggested by Tachiki et al. [193] for interpretation of intrinsic pinning related with layered structures. If the modulation of local order parameter which relates to local T_c (t_c) on the ab plane, a vortex on

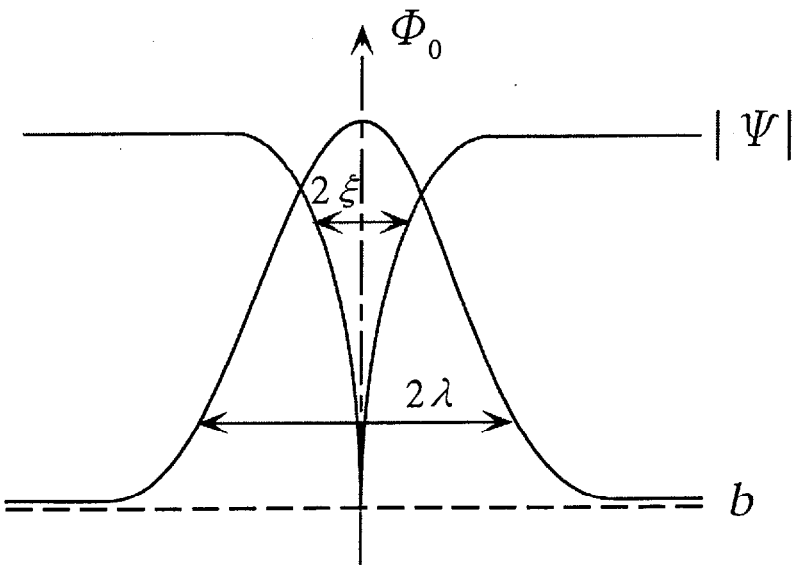

Fig. 3.15. Cross-sectional view of the structure of an isolated fluxon (Φ_0) in a "high-κ" material with a larger penetration length (λ) than a coherence length (ξ).

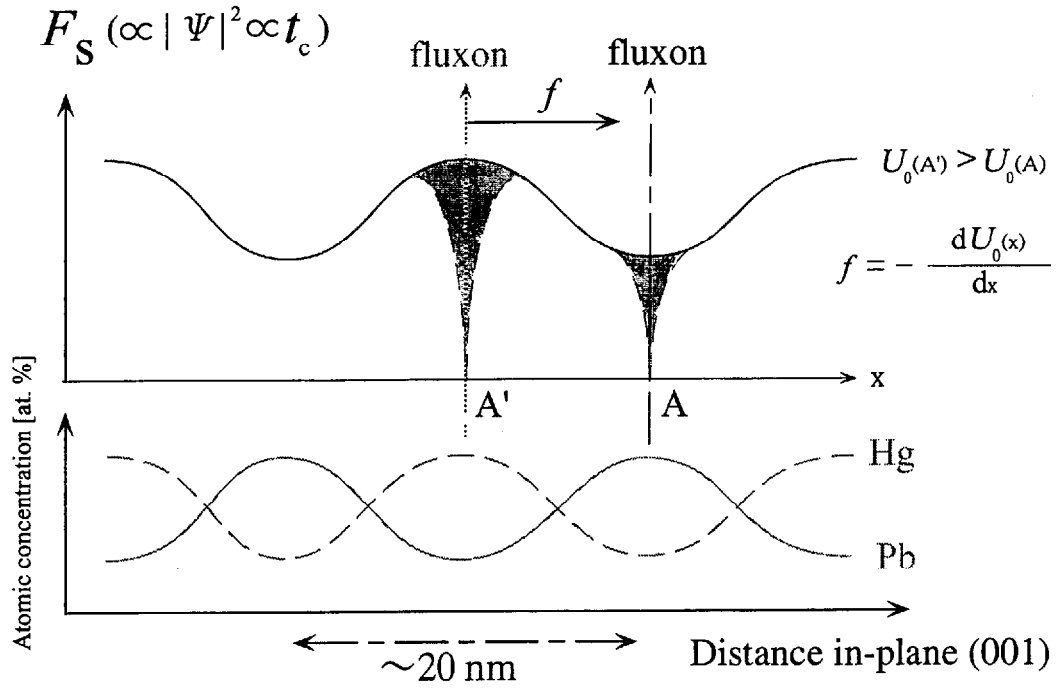

Fig. 3.16. Schematic picture of flux pinnig in a material with spatial variation of superconducting order parameter (Ψ) along the (001) plane (upper). The shaded portion represents a region where the order parameter repelled by the fluxons (at A and A' position). Bottom shows a corresponding compositional modulation in a (001) plane of (Hg,Pb)-1223, which possibly provides a spatial variation of local t_c, *i.e.* ΔT_c.

the plane should be stabilized at the region with lower t_c which is possibly provided by the compositional modulation as mentioned above. The schematic illustration for such a situation is shown in Fig.3.16. Here, the fluxon at the position A is more unstable than that at the position A' since the former has higher loss of superconducting condensation energy than the latter. On the other hand, another explanation for the pinning effect derived by such spatial inhomogeniety of t_c comes from kinetic energy of the fluxon [194]. The deviation of superconducting coherence length between two regions such as Nb and Nb-Ti layers causes the repulsive force to each fluxon crossing through an interface of the regions. Such kind of pinning would also occur in present compound.

Therefore we can deduce that such inhomogeneites could be responsible for the peak effect in studied samples.

3-4 Conclusion

The pronounced 'peak effect' on magnetization hysteresis loop has been observed in the $(Hg,Pb)(Ba,Sr)_2Ca_2Cu_3O_{8+\delta}$ poly-crystalline sample synthesized by an encapsulation technique as well as single crystals. In the encapsulation sample which shows the clear 'peak effect', we found the alternative Hg/Pb compositional modulations in the <110> direction with the period of ca. 20 nm between Hg-rich and Pb-rich regions. Less pronounce fluctuation of such Hg/Pb ratio observed in the sample synthesized under high-pressure. Electron diffraction studies allow us confirm a presence of long-range disorder along <110> direction with the characteristic length of tens nm and coherent diffused interface between the regions. Observed compositional modulation most likely to be a kind of vortex pinning responsible for the peak effect in the studied samples and produced via spinodal decomposition. The possible candidate for vortex pinning which is responsible for the peak effect was proposed based on the δT_c pinning model.

Chapter IV General Discussions and Remarks for Future Studies

4-1 Enhancement in the irreversibility field of Hg-12(n-1)n (n = 2, 3)

The irreversibility field characteristics was investigated for the second and third members of the Hg-12(n-1)n homologous series.

In the case of Hg-1212:

(1) The best H_{irr}-vs.-(1-T/T_c) characteristics was obtained for the sample with the highest doping state that was induced solely by excess oxygen solely among the samples prepared in the present work. However, the T_c value was lowered considerably (from 120 K to ~70 K), as compared with that of an optimally doped sample.

(2) In the H_{irr}-vs.-T plot, the most enhanced characteristics was obtained for the sample in which holes were doped from multiple sites by means of not only high-pressure oxidization but also light substitution of Y for Ca (by~10 %). Note that such samples doped with holes from multi-sites would have an optimized hole-density distribution compared with those doped with holes induced by excess oxygen only.

Result (1) is consistent with previously reported results that significant enhancement in the H_{irr}-vs.-(1-T/T_c) characteristics was achieved in highly oxidized samples of both Hg-1201 [83] and Hg-1223 [120]. The most probable explanation for this is that given by Yamauchi *et al.* [121] based on the concept of hole density distribution. From this point of view, the less confined hole-density distribution induced by an over-doped state provides the better H_{irr}-vs.-(1-T/T_c) characteristics. However, one may hardly overlook the large depression of T_c in the case of less confined hole density distribution.

In practical applications, optimally engineered materials in terms of both T_c and H_{irr} characteristics would be demanded. Usually, the requirements for high-T_c and high-H_{irr} are rather contradictory to be realized in a same HTSC material [13]. Previously, Nakane *et al.* [122] studied the correlation between the H_{irr} characteristics and hole density distribution in the Cu-1212:P compound in detail. They claimed that it was possible to obtain the optimization of both T_c and H_{irr} characteristics by controlling the hole density distribution which had been estimated from neutron powder diffraction data by BVS method.

Thus, controlling hole density distribution becomes important since the hole-density distribution governs most of the superconducting properties of HTSC. In fact, aforementioned result (2) indicates possible tailoring of HTSC materials by controlling the hole-density distribution. In practice of material tailoring, simultaneous cation substitution techniques at multiple sites would be useful. Figure 4.1(a) shows the a schematic image of

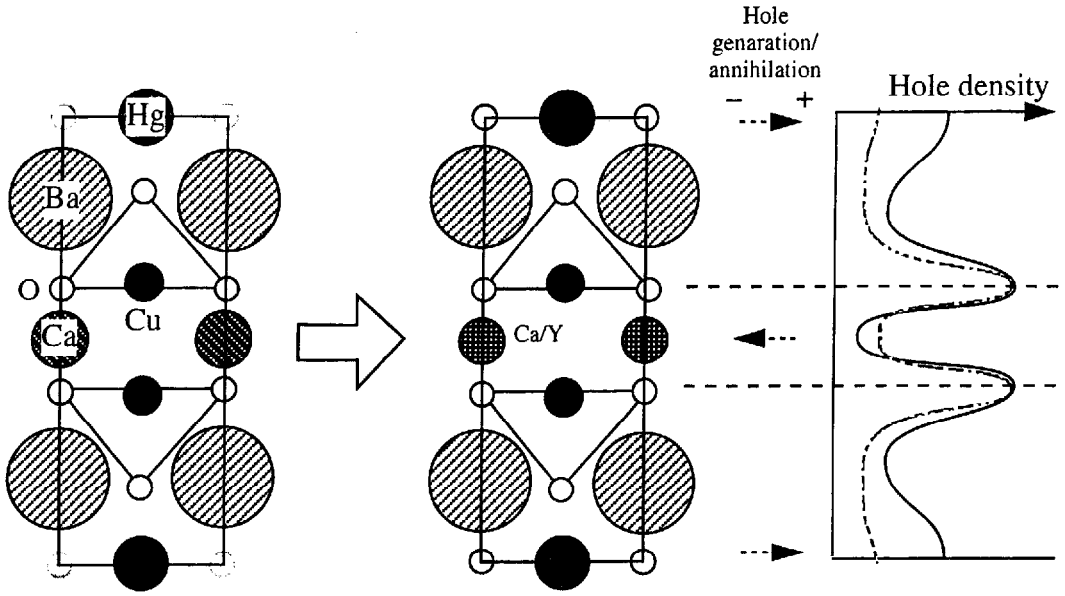

Fig. 4.1 (a). Schematic image of relation between crystal structure and the hole density distribution in Hg-1212. Left structure is for the pristine phase, and right, for the Ysubstituted and high-pressure oxidized phase. Far right shows the hole density distribution, where dotted and solid lines are for the pristine and the substituted ones, respectively, Middle arrows represent site specific hole genaration/annihilations.

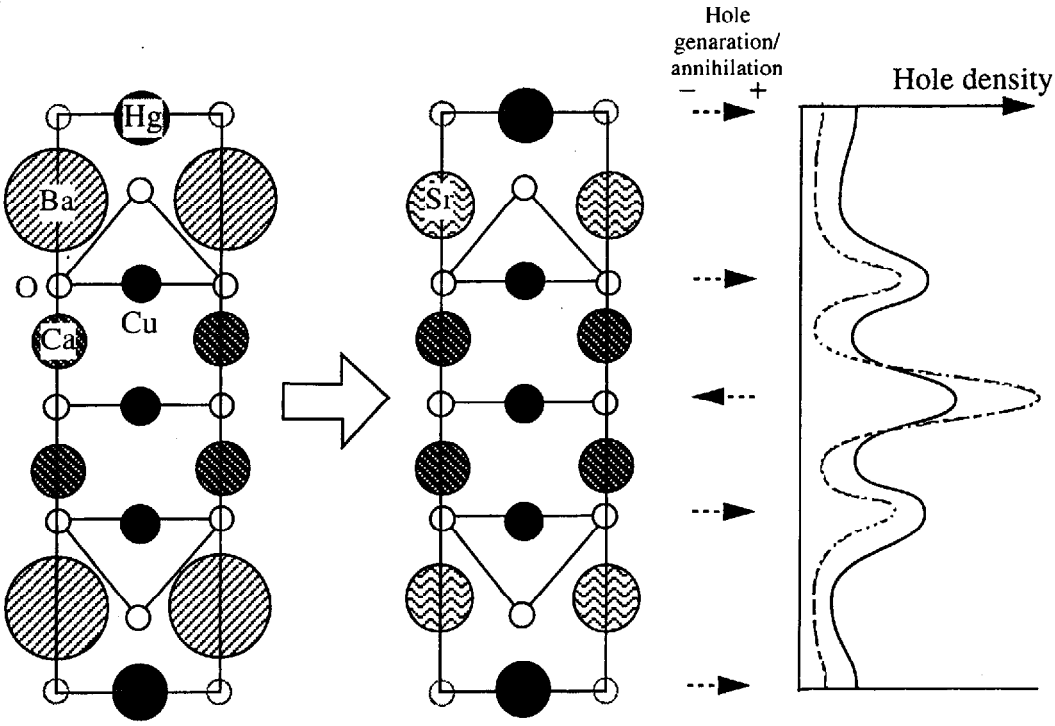

Fig. 4.2 (b). Schematic image of relation between crystal structure and the hole density distribution in Hg-1223. Left structure is for the pristine phase, and right, for the Sr substituted phase. Far right shows the hole density distribution, where dotted and solid lines are for the pristine and the substituted ones, respectively, Middle arrows represent site specific hole genaration/annihilations.

controlling the hole density distribution of Hg-1212 compound. In the figure, the multi-sites doping realizes a moderately tailored hole density distribution thereby both T_c and H_{irr} characteristics may be optimized.

In the case of Hg-1223, the magnetic irreversibility was studied for the samples in which Hg and Ba were substituted by Pb and Sr, *i.e.* (Hg,Pb)(Ba,Sr)-1223. Significant enhancement in the H_{irr}-vs.-(1-T/T_c) characteristics was confirmed for the (Hg,Pb)(Ba,Sr)-1223 compounds, as compared with the Hg-1223 compound without cation partial substitutions [67]. This result is in good agreement with previous reports for the samples with cation substitutions: Re for Hg and Sr for Ba [37, 142]. It was claimed that the main factors for the enhancement in the magnetic irreversibility characteristics were the Re doping which had provided the oxygen-octahedron clusters acting as strong pinning centers [142]. and/or the metallization induced by the octahedral ReO_3 clusters [37, 81, 145, 195]. However, it was recently reported that such Re doping was not effective for enhancing the magnetic irreversibility characteristics except that in a low temperature region (~40 K) [140, 196]. This indicates that the Sr substitution for Ba is effective to improve the magnetic irreversibility characteristics as compared with any other kinds of substitution for Hg. Nevertheless the cation substitutions for Hg are indispensable to stabilize a phase with the Sr substitution for Ba during the sintering under ambient-pressure [54, 140, 195].

The best H_{irr}-vs.-(1-T/T_c) characteristics in the present study was resulted for the sample which had the highest degree of Sr substitution, *i.e* Ba-free (Hg,Pb)(Sr)-1223. This fact is in good agreement with previous works [37, 56, 197, 198]. Thus, it is most likely that the main factor responsible for such enhancement is the Sr substitution for Ba. So far, many researchers have explained the function of Sr substitution based on the enhancement of "inter-layer" coupling caused by the reduction in the "inter-layer" distance as the Sr ionic size is smaller than that of Ba. An explanation of this type is based on the "inter-layer" coupling model proposed by Kim *et al.* [143]. Here, "inter-layer" means a correlation among the two blocks of stacked CuO_2 planes via "blocking" block. In this "inter-layer" coupling model, the most crucial point is the distance between two superconducting blocks of stacked CuO_2 planes. That is, the shorter the "inter-layer" distance is the stronger would be the Josephson-coupling between CuO_2 stacks to enhance the irreversibility-field characteristics. This simple explanation scheme seems to have paid the less attention to the hole/carrier distribution over the crystal. Note that the hole/carrier density distribution is the key in understanding the superconducting properties as mentioned above. In fact, in some cases, the magnetic irreversibility was mainly determined by the hole density distribution rather than the "inter-layer" distance [122, 199]. Thus, the effect of hole density distribution change due to the Sr

substitution for Ba must be taken into account. The Sr substitution would yield a more homogeneous hole density distribution over the crystal. One possible evidence for such hole density distribution change due to the Sr substitution for Ba may be obtained through bond valence sum calculations. The degree of "hole confinement" (Eq.1.5) for our (Hg,Pb)(Ba,Sr)-1223 single crystal (T_c = 115 K) was calculated by structural data determined from single crystal study by Yamawaki *et al.* [200]. The value of "hole confinement" was ~ 0.43, this value is smaller than the value of 0.53 for Sr-free Hg(Ba)-1223 (T_c = 133 K) [92]. This would mean that the (Hg,Pb)(Ba,Sr)-1223 compound has more homogeneous hole density distribution compared with than the Sr-free Hg(Ba)-1223 compound. Figure 4.1(b) shows a schematic image of the effect of Sr substitution for Ba on the hole distribution, where the "hole confinement" is reduced by the cation substitution according to the bond valence sum calculation.

4-2 Elucidation of the mechanism for peak effect in (Hg,Pb)(Ba,Sr)-1223

The mechanism for peak effect in (Hg,Pb)(Ba,Sr)-1223 was investigated. Firstly, the temperature dependence of the peak field, $H_{s.p}$, was revealed to be sensitive to the degree of hole doping. This result is consistent with the those previously reported for $TlBa_{0.8}Sr_{1.2}Ca_2Cu_3O_{9-\delta}$ [174], $(Tl_{0.6}Pb_{0.4})(Ba_{0.3}Sr_{1.7})CaCu_2O_y$ [175], $HgBa_2Ca_2Cu_3O_{8+\delta}$ [67]. The dependence of $H_{s.p}$ on the hole doping state suggests that the peak effect is related not only to the extrinsic factors (*e.g.* vortex pinning by defects) but also to the intrinsic factors such as the hole doping state.

It has been generally believed that peak effect could be observed only in single crystals. However, the well pronounced peak effect in the magnetization hysteresis loop had been observed even for poly-crystalline samples of $(Hg,Pb)(Ba,Sr)_2Ca_2Cu_3O_{8+\delta}$ synthesized by an encapsulation technique as well as for single crystals. Therefore the dependence of peak effect on the particle size was studied. The result shows that $H_{s.p}$ was not sensitive to the grain size, while the peak height in the magnetization curve was reduced by decreasing the grain size. This result is consistent with the view that quantity $H_{s.p}$ is largely an intrinsic parameter as suggested above. The smaller grain size means the larger fraction of the surface barrier in the total magnetization. Since the peak effect is essentially a bulk property, it should be less pronounced for the smaller grains.

On the other hand, the temperature dependence of $H_{s.p}$ revealed that the Sr substitution is effective to raise the value of $H_{s.p}$. According to the large enhancement in the irreversibility field, this material should have a high degree of homogeneity in the hole density distribution along the c-axis. Furthermore, the magnitude of $H_{s.p}$ was also increased in the over-doped

materials as previously pointed out. Thus it is clear that Sr substitution is effective to increase the hole density in the charge-reservoir and accordingly yield the more homogeneous hole density distribution. This at the same time indicates the validity of the manipulation of the hole density distribution in order to on-demand tailor the magnetic field dependence of peak effect at practical temperature.

Single crystals were utilized in order to elucidate the origin of peak effect for various electron microscopic analyses and spectroscopy. As shown in a typical HRTEM image of the (001) plane (Fig. 3.11), somewhat distorted structure was observed. A selected area electron diffraction (SAED) pattern with the incident beam parallel to [001] for the region corresponding to the HRTEM image (Fig. 3.10) shows sharp streaks along <110> at all the spots. From the dimension of the streaks, some long-period irregularities of tens nanometer order can be expected to exist. Compositional analysis on the (001) plane was carried out by TEM-EDS with a probing beam of 1 nm diameter along a <110> direction. A compositional modulation, i.e. periodic fluctuation in the Hg and Pb ratio was observed, while no significant spatial variations were seen for other cations. The distribution of Hg and Pb may be approximated by a sinusoidal curve with the period of ~ 20 nm. This value is in good agreement with the irregularity dimension (of tens nm) previously estimated from the SAED data. If there are vortex pinning centers with inter-centers distance of ~ 20 nm, the matching field would equal to be ~ 6 T, which disagrees with the experimental peak field for this material.

Previously, a number of reports concerning the correlation between the "inherent disorder" of crystal structure and the J_c property in the HTSC compounds were published [42, 64, 184]. Compositional modulations for Nd/Ba was reported in "Nd-123" single crystals [185, 186]. A lamellar structure of Pb rich phase, as the result of eutectoid decomposition, was observed in heavily Pb doped Bi-2212 single crystals which possessed a high J_c characteristics [187, 188]. For the mercury based compounds, a chemical pressure-induced compositional modulation with a periodicity of ~ 3 nm along <110> direction was resulted from high-resolution lattice images coupled with the resulted structural simulations for the (Hg,Pb)-1223 compound [42]. A model with clustering of Pb^{4+} was proposed from a single-crystal structure refinement of (Hg,Pb)-1234 [64]. Our present result is in reasonable agreement with this model in terms of the dimension of modulation.

Taking into account the observed facts that (1) the ratio of Hg and Pb was nearly 1:1, that (2) the distributions of both Hg and Pb were approximated by a simple sinusoidal curve and that (3) the streaks in the [001] SAED pattern indicated long-range modulations of tens nanometers, the observed modulated structure may be considered to have yielded via spinodal decomposition .

A vortex pinning mechanism was proposed for this compound based on the "δT_c" pinning mechanism [191, 192]. Since the T_c value for the Pb-1223 phase is up to 123 K [190], locally Pb riched region would have a lower T_c than that of the matrix. Consequently, the lattice disorder resulted from a compositional modulation would suppress the superconducting order parameter moderately and causes the δT_c-type vortex pinning. Furthermore, recently it was suggested that periodic (or ordered) defect-like structures are more favorable for the peak effect according to both experimental results [201] and numerical simulation results [202]. This idea is consistent with our present results. Therefore such compositional inhomogeneity is most likely to be responsible for the peak effect observed in the samples studied in this work.

4-3 Suggestions for future work

In this work, only a few ways of altering the hole density distribution in the mercury copper oxides have been employed , *i.e.* Y substitution and oxygen doping for Hg-1212; Pb and Sr substitutions for Hg-1223. What must be carried out next is the Pb and Sr substitutions for Hg-1212. The Pb substitution for Hg is likely to cause compositional modulation in the crystal. This might induce a pronounced peak effect owing to enhanced weak pinning. Moreover the Pb substitution would also cause a decrease of the melting temperature during the synthesis, which is favorable to the growth of large single crystals. The Sr substitution for Ba might result in an optimized hole density distribution even in Hg-1212 in terms of the H_{irr} characteristics.

In this work, no direct information about the real hole density distribution was obtained. Thus experimental tools for detecting the real distribution are looked for. One of the candidates is bond-valence-sum calculation based on the structural data obtained from the neutron powder diffraction or the single crystal study.

On the other hand, the holes are detectable in the energy space. Generally an energy region for pre-peak (*i.e.* 525-530 eV) of O-*K* edge is the most informative region for detecting the holes [168]. If it is possible to take a [100] electron diffraction (ED) pattern for the present samples with an energy window of 525-530 eV by means of a TEM with a high-resolution energy filter such as the FE-TEM with an Omega-filter, the Patterson function of hole distribution would be obtained by inverse-Fourier transformation for the ED pattern. Furthermore, an angular dependence of such image can provide an image of real hole density distribution in principle. However, it is difficult to gain enough signal intensity for such purpose. More development in detection of the signal is required.

The origin of the compositional modulations in present (Hg,Pb)(Ba,Sr)-1223 samples, *i.e.* the spinodal decomposition mechanism, is not still beyond speculation. Thus, further confirmations for evidences of such mechanism are required. If a phase separation occurs through during the synthesis, the spinodal decomposition phenomenon should take place in a cooling stage. To detect the spinodal temperature should be a first step for investigation the phenomenon. Firstly, a sample is sintered in an ordinary way. At the end of sintering, the sample is quenched from the sintering temperature to room temperature. The sample should not have the phase-separation through the quenching process. This phase-separation-free sample is heated again at several temperatures. After the heat treatment, the sample is checked by magnetization measurement and TEM-EDX analysis. By scanning the heating temperature, a considerable temperature at which the spinodal decomposition phenomenon would occur, can be detected. Moreover, if further experiments mentioned above with different compositions are carried out, the spinodal curve would be drawn. This curve must help us to tailor the peak effect through the phase separation in present compound.

Chapter V Summary

Chapter I: The basis of the present study was presented. Firstly, the history of high-T_c superconductors (HTSC) was briefly overviewed. Then, some general features of HTSC with which this work was concerned were mentioned. Finally the objectives of this study was stated.

Chapter II: Firstly, the irreversibility field characteristics was investigated for sample of the second member of the Hg-12(n-1)n homologous, *i.e.* Hg-1212. In order to control the hole density distribution, solid solutions of $HgBa_2(Ca_{1-x}Y_x)Cu_2O_{6+\delta}$ ($0 \le x \le 0.5$) were synthesized by an encapsulation technique and then post-annealed utilizing a high-pressure oxidization (HPO) technique (5 GPa, 500°C, 2 h). All the samples were able to be varied in terms of the hole doping state from the under to the over-doped region. The best H_{irr}-vs.-(1-T/T_c) characteristics was obtained for the sample with the highest doping state that was induced solely by excess oxygen doping. On the other hand, in the H_{irr}-vs.-T plot, the most enhanced characteristics was obtained for the sample in which holes were doped from multiple sites by means of not only high-pressure oxidization but also light substitution of Y for Ca (by~10 %). Accordingly, these results indicate possible tailoring of HTSC materials by controlling the hole-density distribution.

The magnetic irreversibility study was carried out for the Hg-1223 single crystals with Hg and Ba partially substituted by Pb and Sr, *i.e.* (Hg,Pb)(Ba,Sr)-1223. Significant enhancement in the irreversibility-field characteristics was achieved for a (Hg,Pb)(Ba,Sr)-1223 compound as compared with the Sr-free (Hg)(Ba)-1223 compound. The Sr substitution for Ba worked effectively to improve the magnetic irreversibility. This was in good agreement with previous works [37, 56, 197, 198]. Furthermore the bond valence calculation [92] suggested the hole density distribution in a (Hg,Pb)(Ba,Sr)-1223 compound was more homogeneous than that in the Sr-free Hg(Ba)-1223 compound. This revealed that the hole density distribution is most likely responsible for the significant enhancement in the magnetic irreversibility field characteristics of the present sample in which Sr was partially substituted for Ba.

Chapter III: The mechanism for the peak effect in (Hg,Pb)(Ba,Sr)-1223 was investigated. The temperature dependence of the peak field, $H_{s.p}$ was revealed to be sensitive to the degree of hole doping. The dependence of $H_{s.p}$, on the hole doping state suggests that the peak effect is related not only to extrinsic factors (*e.g.* vortex pinning by defects) but also to intrinsic factors such as the hole doping state. Furthermore the dependence of peak effect

on the particle size was studied since the well pronounced peaks had been observed in the magnetization hysteresis loops for not only poly-crystalline samples of $(Hg,Pb)(Ba,Sr)_2Ca_2Cu_3O_{8+\delta}$ synthesized by an encapsulation technique but also single crystals. The $H_{s.p}$ was found to be insensitive to the grain size, while the peak height in the magnetization curve was reduced by decreasing the grain size. On the other hand, the most enhanced temperature dependence of $H_{s.p}$ was found in the sample with the highest degree of Sr substitution i.e $(Hg,Pb)Sr_2Ca_2Cu_3O_{8+\delta}$.

In order to investigate the origin of vortex pinning effect which may be responsible to Hg-1223 samples. Observations and analyses were performed for two different (Hg,Pb)(Ba,Sr)-1223 samples. The first sample was synthesized by an encapsulation technique and exhibit a peak effect (sample I). Another was prepared by an by a high-pressure technique and no peak effect (sample II). An SAED pattern with incident beam parallel to [001] for sample I, showed sharp streaks along <110> at each diffraction spot. From the dimension of the streaks, some long-period super-structures of tens nanometer order were expected. On the other hand, in sample II, there were no anomalous features measured upon the shape of diffraction spots. From HRTEM images of the (001) plane, somewhat distorted structure was observed for sample I, whereas no such distortions were seen for sample II. Furthermore, compositional analysis in the (001) plane was carried out by TEM-EDS with probing beam of 1 nm diameter along a <110> direction. For sample I, alternative Hg/Pb compositional modulations waves were detected along a <110> direction with periodicity of ~ 20 nm yielding alternative Hg-rich and Pb-rich regions. Such compositional modulations were much less pronounced in sample II. Therefore as a candidate for the vortex pinning mechanism which may be responsible for the peak effect, a model was considered based on the "δT_c" pinning model. Thus the observed compositional modulation is most likely responsible for the peak effect in the present compound.

References

[1] J. Bardeen, L. N. Cooper and J. R. Schrieffer, "Theory of Superconductivity", *Phys. Rev.* **108** (1957) 1175-1204.

[2] G. J. Bednorz and K. A. Müller, "Possible High T_c Superconductivity in the Ba-La-Cu-O System", *Z. Phys. B* **64** (1986) 189-193.

[3] M. K. Wu, J. R. Ashburn, C. J. Torng, P. H. Hor, R. L. Meng, L. Gao, Z. J. Huang, Y. Q. Wang and C. W. Chu, "Superconductivity at 93 K in a New Mixed-Phase Y-Ba-Cu-O compound System at Ambient Pressure", *Phys. Rev. Lett.* **58** (1987) 908-910.

[4] H. Maeda, Y. Tanaka, M. Fukutomi and T. Asano, "A New High-T_c Oxide Superconductor without a Rare Earth Element", *Jpn. J. Appl. Phys.* **27** (1988) L209-L210.

[5] Z. Z. Sheng and A. M. Hermann, "Superconductivity in the Rare-Earth-Free Tl-Ba-Cu-O System above Liquid-Nitrogen Temperature", *Nature* **332** (1988) 55-58.

[6] Z. Z. Sheng and A. M. Hermann, "Bulk Superconductivity at 120K in the Tl-Ca/Ba-Cu-O System", *Nature* **332** (1988) 138-139.

[7] S. N. Putilin, E. V. Antipov, O. Chmaissem and M. Marezio, "Superconductivity at 94 K in $HgBa_2CuO_{4+\delta}$", *Nature* **362** (1993) 226-228.

[8] A. Schilling, M. Cantoni, J. G. Guo and H. R. Ott, "Superconductivity Above 130 K in the Hg-Ba-Ca-Cu-O system", *Nature* **363** (1993) 56-58.

[9] K. Isawa, A. Tokiwa-Yamamoto, M. Itoh, S. Adachi and H. Yamauchi, "Encapsulation Method for the Synthesis of Nearly Single-Phase Superconducting $HgBa_2Ca_2Cu_3O_{8+\delta}$ with $T_c \geq 135$ K", *Physica C* **222** (1994) 33-37.

[10] H. Takahashi, A. Tokiwa-Yamamoto, N. Mori, S. Adachi, H. Yamauchi and S. Tanaka, "Large Enhancement of T_c in the 134 K Superconductor $HgBa_2Ca_2Cu_3O_y$ under High Pressure", *Physica C* **218** (1993) 1-4.

[11] H. Yamauchi, M. Karppinen and S. Tanaka, "Homologous Series of Layered Cuprates", *Physica C* **263** (1996) 146-150.

[12] H. Yamauchi and M. Karppinen, "Structural Classification of Superconducting Cuprates", *Superlatt. Microstructr.* **21A** (1997) 146.

[13] M. Karppinen and H. Yamauchi, "Control of The Charge Inhomogeneity and High-T_c Superconducting Properties in Homologous Series of Multi-Layered Copper Oxides", *Mater. Sci. Engineer. : R* **26** (1999) 51-96.

[14] H. Yamauchi and M. Karppinen, "Net Holes and Superconductivity in the Members with n≥3 of Homologous Sreies, Tl- and Hg-m2(n-1)n", *J. Supercond.* **11** (1998) 43-46.

[15] S. N. Putilin, I. Bryntse and E. V. Antipov, "New Compex Copper Oxides: $HgBa_2RCu_2O_7$ (R = La, Nd, Eu, Gd, Dy, Y)", *Mat. Res. Bull.* **26** (1991) 1299-1307.

[16] S. F. Hu, D. A. Jefferson, R. S. Liu and P. P. Edwards, "Superconductivity up to 90 K in a New Family of the (Pb,Hg)Sr_2(Ca,Y)Cu_2O_7 System", *J. Solid State Chem.* **103** (1993) 280-286.

[17] M. A. Subramanian, J. Gopalakrishnan, C. C. Torardi, P. L. Gai, E. D. Boyes, T. R. Askew, R. B. Flippen, W. E. Farneth and A. W. Sleight, "Superconductivity Near Liquid Nitrogen Temperature in the Pb-Sr-R-Ca-Cu-O System (R = Y or Rare Earth)", *Physica C* **157** (1988) 124-130.

[18] S. Adachi, H. Adachi, K. Setsune and K. Wasa, "Study on Annealing Treatment and Sr/Ca Ratio for Pb-Sr-Y-Ca-Cu-O Ceramics with "1212" Structure", *Jpn. J. Appl. Phys.* **30** (1991) L690-L693.

[19] B. A. Scott, E. Y. Suard, C. C. Tsuei, D. B. Mitzi, T. R. McGuire, B.-H. Chen and D. Walker, "Layer Dependence of the Superconducting Transition Temperature of $HgBa_2Ca_{n-1}Cu_nO_{2n+2+\delta}$", *Physica C* **230** (1994) 239-245.

[20] S. N. Putilin, E. V. Antipov, A. M. Abakumov, M. G. Rozova, K. A. Lokshin, D. A. Pavlov, A. M. Balagurov and D. V. Sheptyakov, "Effect of Fluorination and High Pressure on the Structure and Properties of the Hg-bearing Superconductors", *Physica C* (submitted) .

[21] E. V. Antipov, S. N. Putilin, E. M. Kopnin, J. J. Capponi, C. Chaillout, S. M. Loureiro and M. Marezio, "Mercury-Based Copper Mixed-Oxide Superconductors", *Physica C* **235-240** (1994) 21-24.

[22] S. N. Putilin, E. V. Antipov and M. Marezio, "Superconductivity above 120 K in $HgBa_2CaCu_2O_{6+\delta}$", *Physica C* **212** (1993) 266-270.

[23] S. Lee, O. A. Shlyakhtin, M.-O. Mun, M.-K. Bae and S.-I. Lee, "A Freeze-Drying Approach to the Preparation of $HgBa_2Ca_2Cu_3O_{8+x}$ Superconductor", *Supercond. Sci. Technol.* **8** (1995) 60-64.

[24] S. Lee, M.-O. Mun, M.-K. Bae and S.-I. Lee, "Synthesis and Superconducting Properties of $HgBa_2Ca_2Cu_3O_{8+x}$", *J. Mater. Chem.* **4** (1994) 991-992.

[25] I. Bryntse and A. Kareiva, "Sol-gel Synthesis and Superconduction Properties of $HgBa_2CaCu_2O_{6+\delta}$", *Physica C* **251** (1995) 115-125.

[26] A. Kareiva and I. Bryntse, "A Novel Synthesis Route to the Mercury-Containing Superconductor $HgBa_2CaCu_2O_{6+\delta}$ Partly Based on the Sol-Gel Technique", *J. Mater. Chem.* **5** (1995) 885-887.

[27] P. G. Radaelli, J. L. Wanger, B. A. Hunter, M. A. Beno, G. S. Knapp, J. D. Jorgensen and D. G. Hinks, "Structure, Doping and Superconductivity in $HgBa_2CaCu_2O_{6+\delta}$ ($T_c \leq 128$ K)", *Physica C* **216** (1993) 29-35.

[28] A. Tokiwa-Yamamoto, K. Isawa, M. Itoh, S. Adachi and H. Yamauchi, "Composition, Crystal Structure and Superconducting Properties of Hg-Ba-Cu-O and Hg-Ba-Ca-Cu-O Superconductors", *Physica C* **216** (1993) 250-256.

[29] R. Usami, S. Adachi, M. Itoh, T. Tatsuki, A. Tokiwa-Yamamoto and K. Tanabe, "Synthesis of $HgBa_2Ca_3Cu_4O_y$ under Ambient Pressure", *Physica C* **262** (1996) 21-26.

[30] E. V. Antipov, S. M. Loureiro, C. Chaillout, J. J. Capponi, P. Bordet, J. L. Tholence, S. N. Pitilin and M. Marezio, "The Synthesis and Characterization of the $HgBa_2Ca_2Cu_3O_{8+\partial}$ and $HgBa_2Ca_3Cu_4O_{10+\partial}$ Phases", *215* (1993) 1-10.

[31] M. Hirabayashi, K. Tokiwa, H. Ozawa, Y. Noguchi, M. Tokumoto and H. Ihara, "High-Pressure Synthesis of Single-Phase "1223" Mercury-Based Superconductors", *Physica C* **219** (1994) 6-8.

[32] K. A. Lokshin, I. G. Kuzemskaya, L. F. Kulikova and E. V. Antipov, "High Pressure Synthesis of Hg-1234 and Strongly-Overdoped Hg-1223 Phases", *Physica C* **279** (1997) 11-17.

[33] J. Karpinski, G. I.Meijer, H. Schwer, R. Molinski, E. Kopnin, K. Conder, M. Angst, J. Jun, S. Kazakov, A. Wisniewski, R. Puzniak, J. Hofer, V. Alyoshin and A. Sin, "High-Pessure Synthsis, Crystal Growth, Phase Diagram, Structural and Magnetic Properties of $Y_2Ba_4Cu_nO_{2n+x}$, $HgBa_2Ca_{n-1}Cu_nO_{2n+2+\partial}$ and Qusi-One-Dimensional Cuprates", *Supercond. Sci. Technol.* **12** (1999) R153-R181.

[34] E. M. Kopnin, E. V. Antipov, J. J. Capponi, P. Bordet, C. Chaillout, S. d. Brion, M. Marezio, A. P. Bobylev and G. V. Tendeloo, "Suppression of Superconductivity in Hg-1223 and Hg-1234 by Partial Replacement of Hg by Carbon", *Physica C* **243** (1995) 222-232.

[35] P. Bordet, S. Loureiro, S. L. Floch, J. J. Capponi, C. C. Chaillout, J. Chenavas, J. L. Tholence, E. V. Antipov, P. G. Radaelli and M. Marezio, "High Pressure Synthesis and Structure of the Superconducting Mercury Cuprates $(Hg_{1-x}M_x)Ba_2Ca_{n-1}Cu_nO_{2+2n+\partial}$ with M=C, S.", *Physica C* **282-287** (1997) 65-68.

[36] J. Q. Li, C. C. Lam, J. Feng and K. C. Hung, "Effect of In Doping in $Hg_{1-x}In_xBa_2CaCu_2O_{6+\partial}$", *Supercond. Sci. Technol.* **11** (1998) 217-222.

[37] J. Shimoyama, K. Kishio, S. Hahakura, K. Kitazawa, K. Yamaura, Z. Hiroi and M. Takano, "Chemical Stabilization and Irreversible Magnetic Behavior of $HgM_2Ca_{n-1}Cu_nO_y$ with M=Sr(Ba) and n=1 to 3", in: *Advances in Superconductivity* **VII**, K. Yamafuji and T. Morishita (eds.) (Springer-Verlag, Tokyo, 1995), pp. 287-290.

[38] P. Bordet, S. L. Floch, J. J. Capponi, C. C. Chaillout, M. F. Gorius, M. Marezio, J. L. Tholence and P. G. Radaelli, "Gold Substitution in Mercury Cuprate Superconductors", *Physica C* **262** (1996) 151-158.

[39] P. Dai, B. C. Chakoumakos, G. F. Sun, K. W. Wong, Y. Xin and D. F. Lu, "Synthesis and Neutron Powder Diffraction Study of the Superconductor $HgBa_2Ca_2Cu_3O_{8+\delta}$ by Tl Substitution", *Physica C* **243** (1995) 201-206.

[40] A. K. Pandey, G. D. Verma and O. N. Srivastava, "Investigation on the Tl-Doped Hg-Ba-Ca-Cu-O High Temperature Superconductors in Regard to Hole Doping and Microstructure Characteristics", *Physica C* **306** (1998) 47-57.

[41] K. Isawa, A. Tokiwa-Yamamoto, M. Itoh, S. Adachi and H. Yamauchi, "The Effect of Pb Doping in the $HgBa_2Ca_2Cu_3O_{8+\delta}$ Superconductor", *Physica C* **217** (1993) 11-15.

[42] Z. Iqbal, T. Dotta, D. Kirven, A. Lungu, J. C. Barry, F. J. Owens and A. G. Reidinger, "Superconductivity Above 130 K in the Hg-Pb-Ba-Ca-Cu-O system", *Phys. Rev. B* **49** (1994) 12322-12325.

[43] K. Isawa, A. Tokiwa-Yamamoto, M. Itoh, S. Adachi and H. Yamauchi, "Synthesis of Neary Single-phase $(Hg,Pb)Ba_2Ca_2Cu_3O_{8+\delta}$ Superconductors", *Physica C* **235-240** (1994) 913-914.

[44] C. Michel, H. Hervieu, A. Maignan, D. Pelloquin, V. Badri and B. Raveau, "Stabilization of Mercury Cuprates by Bismuth The Superconductors $Hg_{1-x}Bi_xBa_2Ca_{m-1}Cu_mO_{2m+2+\delta}$", *Physica C* **241** (1995) 1-9.

[45] D. Pelloquin, V. Hardy and A. Maignan, "Synthesis and Characterization of Single Crystals of the Superconductors $Hg_{0.8}Bi_{0.2}Ba_2Ca_{n-1}Cu_nO_{2n+2+\delta}$ (n=2,3)", *Phys. Rev. B* **54** (1996) 16246-16253.

[46] G. Villard, D. Pelloquin and A. Maignan, "Structure of New $Hg_{0.75}V_{0.25}Ba_2CuO_{4+\delta}$ Superconducting Single Crystals. Effect of Overdoping on the Magnetization Second Peak", *Physica C* **307** (1998) 128-136.

[47] J. Shimoyama, S. Hahakura, K. Kitazawa, K. Yamafuji and K. Kishio, "A New Mercury-Based Superconductor: $(Hg,Cr)Sr_2CuO_y$", *Physica C* **224** (1994) 1-5.

[48] O. Chmaissem, T. Z. Deng and Z. A. Sheng, "Synthesis and Study of (Hg,Cr)-Based 1201-Type Superconducting Cuprate $(Hg,Cr)Sr_2CuO_{4+\delta}$", *Physica C* **242** (1995) 17-22.

[49] O. Chmaissem and Z. Z. Sheng, "Enhancement of $T_{c\ onset}$ in $(Ga,Hg)Sr_2(Y,Ca)Cu_2O_7$ by Hg Doping", *Physica C* **242** (1995) 228-232.

[50] S. Hahakura, J. Shimoyama, O. Shiino and K. Kishio, "New Barium-Free Mercury-Based High-T_c Superconductors $(Hg,Mo)Sr_2(Ca,Y)_{n-1}Cu_nO_y$ and $HgSr_2(Ca,Y)_{n-1}(Cu,Re)_nO_y$ (n=1 and 2)", *Physica C* **233** (1994) 1-7.

[51] K. Tang, Y. Qian, Z. Chen, L. Yang, L. Wang and Y. Zhang, "$(Hg,Mo)Sr_2Y_{1-x}Ca_xCu_2O_{6+\delta}$. A New Series of Mercury-Based High-T_c Superconductor", *Physica C* **242** (1995) 216-220.

[52] K. Yamaura, J. Shimoyama, S. Hahakura, Z. Hiroi, M. Takano and K. Kishio, "High-Pressure Synthesis and Superconductivity of a Ba Free Mercury-Based Superconductor $(Hg_{0.75}Re_{0.25})Sr_2Ca_2Cu_3O_y$", *Physica C* **246** (1995) 351-356.

[53] R. S. Liu, D. S. Shy, S. F. Hu and D. A. Jefferson, "Superconductivity Up to 32 K in a New Family of the Hg-Containing $(Pb,Hg)(Sr,La)_2CuO_{5-\delta}$ (1201) System", *Physica C* **216** (1993) 237-242.

[54] S. Lee, M. Kuznetsov, N. Kiryakov, D. Emelyanov and Y. Tretyakov, "Synthesis and Properties of $Hg_{0.7}Pb_{0.3}(BaSr)_2Ca_2Cu_3O_{8+x}$ Superconductors", *Physica C* **290** (1997) 275-280.

[55] J. Shimoyama, S. Hahakura, R. Kobayashi, K. Kitazawa, K. Yamafuji and K. Kishio, "Interlayer Distance and Magnetic Properties of Hg-Based Superconductors", *Physica C* **235-240** (1994) 2795-2796.

[56] S. Lee, N. Kiryakov, D. Emelyanov, M. S. Kuznetsov, Y. Tretyakov, V. Petrykin, M. Kakihana, H. Yamauchi, Y. Zhuo, M. S. Kim and S. I. Lee, "Effect of Sr Substitution on Irreversibility Line, Lattice Dynamics and Formation of Hg,Pb-1223 Superconductors", *Physica C* **305** (1998) 57-67.

[57] G. Nilsson and I. Bryntse, "Synthesis and Characterization of $HgBs_2Ca_{0.7}Dy_{0.3}Cu_{6+\delta}$", *J. Alloys Comp.* (1997) 200-207.

[58] N. R. Khasanova, I. Bryntse and E. V. Antipov, "Synthesis and Structure Investigation of Sm Containing Hg-1212 Phases", *Physica C* **247** (1995) 197-205.

[59] A. Maignan, C. Michel, G. v. Tendeloo, M. Herview and B. Raveau, "Superconductivity up to 110 K in the 1212-Hg Based Cuprate $Nd_{1-x}Ca_xBa_2Hg_{1-x'}Cu_{2+x'}O_{6+y}$", *Physica C* **216** (1993) 1-5.

[60] M. G. Rozova, M. V. Lobanov, E. M. Kopnin, M. L. Kovba, O. I. Lebedev, S. N. Putilin and E. V. Antipov, "Synthesis and Characterization of $HgBa_2RCu_2O_{6+\delta}$ (R=Eu, Gd, Ho, Er, Tm, Yb and Y)", *J. Alloys Comp.* **234** (1996) 207-210.

[61] D. Colson, A. Bertinotti, J. Hammann, J. F. Marucco and A. Pinatel, "Synthesis and Characterization of Superconducting Single Crystals of $HgBa_2Ca_2Cu_3O_{8+\delta}$", *Physica C* **233** (1994) 231-236.

[62] A. Bertinotti, V. Viallet, D. Colson, J.-F. Marucco, J. Hammann, G. L. Bras and A. Forget, "Synthesis, Crystal Structure and Magnetic Properties of Superconducting Single Crystals of $HgBa_2CuO_{4+\delta}$", *Physica C* **268** (1996) 257-265.

[63] S. Lee, T. Akao, H. Suematsu, H. Yamauchi, N. P. Kiryakov and D. A. Emelyanov, "Growth, Characterization and Superconducting Properties of Sr-Based (Hg,Pb)-1223 Single Crystals", (to be submitted) .

[64] H. Schwer, J. Karpinski, K. Conder, L. Lesne, C. Rossel, A. Morawski, T. Lada and A. Paszewin, "X-Ray Single-Crystal Structure Refinement of the 129 K Superconductor $Hg_xPb_{1-x}Ba_2Ca_3Cu_4O_{10+\delta}$", *Physica C* **243** (1995) 10-18.

[65] H. Schwer, J. Karpinski, L. Lesne, C. Rossel, A. Morawski, T. Lada and A. Paszewin, "X-Ray Single Crystal Structure Analysis of the 1245 Type Superconductor $Hg_{0.5}Pb_{0.5}Ba_2Ca_4Cu_5O_{12+\delta}$", *254* (1995) 7-14.

[66] R. Gatt, E. Olsson, A. Morawski, T. Lada, A. Paszewin, I. Bryntse, A. M. Grishin, Y. Eeltsev, P. Berastegui and L.-G. Johansson, "Hg-1212 and Hg-1223 Single Crystals: Synthesis and Characterization", *Physica C* **276** (1997) 270-276.

[67] A. Maignan, S. N. Putilin, V. Hardy, C. Simon and B. Raveau, "Magnetic Study of $HgBa_2Ca_2Cu_2O_{8+\delta}$ Single Crystals: Effect of Doping on Irreversibility and Fishtail lines", *Physica C* **266** (1996) 173-177.

[68] M. Pissas, C. Mitros, G. Kallias, V. Psycharis, A. Simopoulos, A. Kostikas and D. Niarchos, "Irreversibility Line in Superconducting $HgBa_2CuO_{4+\delta}$ Single Crystals", *Phys. Rev. B* **58** (1998) 9536-9542.

[69] J. B. Torrance, Y. Tokura, A. I. Nazzal, A. Bezinge, T. C. Huang and S. S. P. Parkin, "Anomalous Disapperance of High-T_c Superconductivity at High Hole Concentration in Metallic $La_{2-x}Sr_xCuO_4$", *Phys. Rev. Lett* **61** (1988) 1127-1130.

[70] Y. Tokura, J. B. Torrance, T. C. Huang and A. I. Nazzal, "Broader Perspective on the High-Temperature Superconducting $YBa_2Cu_3O_y$ System: The Real Role of the Oxygen", *Phys. Rev. B* **38** (1988) 7156-7159.

[71] M.-H. Whangbo and C. C. Torardi, "Hole Density Dependence of the Critical Temperature and Coupling Constant in the Cuprate Superconductors", *Science* **249** (1990) 1143-1146.

[72] M. Karppinen, A. Fukuoka, and H. Yamauchi, "Determination of Oxygen Content and Metal Valence in Oxide Superconductors by Chemical Method", *Supercond. Sci. Technol.* **9** (1996) 121-135.

[73] I. D. Brown and D. Altermatt, "Bond-Valence Parameters Obtained from a Systematic Analysis of the Inorganic Crystal Structure Database", *Acta Cryst. B* **41** (1985) 244-247.

[74] I. D. Brown, "A Determination of the Oxidation States and Internal Stresses in $Ba_2YCu_3O_x$, x = 6-7 Using Bond Valences", *J. Solid State Chem.* **82** (1989) 122-131.

[75] I. D. Brown, "The Influence of Internal Strain on the Charge Disribution and Superconducting Transition Temperature in $Ba_2YCu_3O_x$", *J. Solid State Chem.* **90** (1989) 155-167.

[76] D. M. d. Leeuw, W. A. Groen and L. F. Feiner, "Correlation between the Superconducting Transition Temperature and Crystal Structure of High-T_c Cuprate Compounds", *Physica C* **166** (1990) 133-139.

[77] J. Tallon, "The relationship between Bond-Valence Sums and Tc in Cuprate Superconductors", *Physica C* **168** (1990) 85-90.

[78] M.-H. Whangbo, D. B. Kang and C. C. Torardi, "Correlations between the Superconducting Transition Temperatures and the In-plane Copper-Oxygen Bond Lengths in the Copper-oxide Superconductors", *Physica C* **158** (1989) 371-376.

[79] Y. J. Uemura, G. M. Luke, B. J. Sternlieb, J. H. Brewer, J. F. Carolan, W. N. Hardy, R. Kadono, J. R. Kempton, R. F. Kiefl, S. R. Kreitzman, P. Mulhern, T. M. Riseman, D. L. Williams, B. X. Yang, S. Uchida, H. Takagi, J. Gopalakrishnan, A. W. Sleight, M. A. Subramanian, C. L. Chien, M. Z. Cieplak, G. Xiao, V. Y. Lee, B. W. Statt, C. E. Stronach, W. J. Kossler and X. H. Yu, "Universal Correlations between T_c and n_s/m^* (Carrier Density over Effective Mass) in High-T_c Cuprate Superconductors", *Phys. Rev. Lett.* **62** (1989) 2317-2320.

[80] X. Zhao, X. Sun, X. Fan, W. Wu, X.-G. Li, S. Guo and Z. Zhao, "Correlation between T_c and n_s/m^* in $Bi_2Sr_2CaCu_2O_{8+\delta}$ Single Crystals", *Physica C* **307** (1998) 265-270.

[81] J. L. Tallon, C. Bernhard, C. Niedermayer, J. Shimoyama, S. Hahakura, K. Yamaura, Z. Hiroi, M. Takano and K. Kishio, "A New Approach to Design of High-T_c Superconductors: Metallised Interlayers.", *J. Low Temp. Phys.* **105** (1996) 1379-1383.

[82] L. Fàbrega, A. Calleja, A. Sin, S. Piñol, X. Obradors and J. Fontcuberta, "Muon Spin Relaxation in Re-substituted $HgA_2Ca_{n-1}Cu_nO_{2n+2+x}$ (A=Sr,Ba;n=2,3) Superconductors", *Phys. Rev. B* **60** (1999) 7579-7584.

[83] R. Usami, A. Fukuoka, H. Kubota and H. Yamauchi, "The Oxygen-Content Dependence of the Magnetization Anisotropy of $HgBa_2CuO_{4+\delta}$", *Physica C* **243** (1995) 19-23.

[84] S. Tochihara, M. Mashino, H. Yasuoka, H. Mazaki, M. Osada and M. Kakihana, "Effect of Ca Doping on the Lower Critical Field of $YBa_2Cu_3O_{7-\delta}$ Single Crystals", in: *Advances in Superconductivity* **XI**, N. Koshizuka and S. Tajima (eds.) (Springer-Verlag, Tokyo, 1999), pp. 267-270.

[85] M. Tinkham, "Introduction to Superconductivity" , 2 nd. ed. (McGrraw-Hill, Inc, 1996).

[86] C. Sulkowski, T. Plackowski and W. Sadowski, "Thermopower Anisotropy of High Underdoped and Slightly Overdoped $RBa_2Cu_3O_{7-\delta}$ Single Crystals", *Phys. Rev. B* **57** (1998) 1231-1235.

[87] C. N. R. Rao, T. V. Ramakrishnan and N. Kumar, "Systematics in the Thermopower Behavior of Several Series of Bismuth and Thallium Cuprate Superconductors: An

Interpretation of the temperature variation and the sign of the thermopower", *Physica C* **165** (1990) 183-188.

[88] C. Bernhard and J. L. Tallon, "Thermoelectric Power of $Y_{1-x}Ca_xBa_2Cu_3O_{7-\delta}$: Contributions from CuO_2 Plane and Chains", *Phys. Rev. B* **54** (1996) 10201-10209.

[89] K. Fujinami, T. Ito, H. Suematsu, K. Matsuura, M. Karppinen and H. Yamauchi, "Establishment of Strongly Over-doped State in the Hg-1223 Superconductor", *Phys. Rev. B* **56** (1997) 14790-14796.

[90] A. Fukuoka, A. Tokiwa-Yamamoto, M. Itoh, R. Usami, S. Adachi and K. Tanabe, "Dependence of T_c and Transport Properties on the Cu Valence in $HgBa_2Ca_{n-1}Cu_nO_{2(n+1)+\delta}$ (n=2,3) Superconductors", *Phys. Rev. B* **55** (1997) 6612-6620.

[91] M. Karppinen and H. Yamauchi, "Metal Valences and Hole-doping Routes in Tl- and Hg-based Superconducting Cuprates", *J. Supercond.* **11** (1998) 39-42.

[92] M. Karppinen and H. Yamauchi, "The Doping Routes and Distribution of Holes in Layered Cuprates: a Novel Bond-Valence Approach", *Philos. Mag. B* **79** (1999) 343-366.

[93] K. Kubo and H. Yamauchi, "Transport Properties of Infinite-Layer p-Type Cuprates", *Phys. Rev. B* **49** (1994) 1289-1293.

[94] K. Kubo, M. Ichikawa, N. Sugii, K. Yamamoto and H. Yamauchi, "Synthesis of the Infinite-Layer Compounds $Ca_{1-x}Li_xCuO_2$ ($0.15 \leq x \leq 0.45$) Doped p-Type Carriers", *Phys. Rev. B* **49** (1994) 6919-6926.

[95] K.-I. Magishi, Y. Kitaoka, G.-q. Zheng, K. Asayama, K. Tokiwa, A. Iyo and H. Ihara, "Spin Correlation in High-T_c Cuprate $HgBa_2Ca_2Cu_3O_{8+\delta}$ with T_c=133 K -An Origin of T_c-Enhancement Evidenced by ^{63}Cu-NMR Study-", *J. Phys. Soc. Jpn.* **64** (1995) 4561-4565.

[96] K. Magishi, Y. Kitaoka, G.-q. Zheng, K. Asayama, K. Tokiwa, A. Iyo and H. Ihara, "^{63}Cu NMR Probe of Superconducting Properties in $HgBa_2Ca_2Cu_3O_{8+\delta}$: A Possible Reason for T_c=133 K", *Phys. Rev. B* **53** (1996) R8906-8909.

[97] R. Dupree, Z. P. Han, A. P. Howes, D. M. Paul, M. E. Smith and S. Male, "^{17}O NMR Characterisation of Oxygen Sites in the $Bi_2Sr_2Ca_{n-1}Cu_nO_{4+2n}$ (n=1,2,3) High Temperature Superconductors", *Physica C* **175** (1991) 269-278.

[98] A. P. Howes, R. Dupree, D. M. Paul and S. Male, "An ^{17}O NMR Study of the Cu-O Planes of $Bi_2Sr_2Ca_2Cu_3O_{10}$", *Physica C* **193** (1992) 189-195.

[99] G.-Q. Zheng, Y. Kitaoka, K. Asayama, K. Hamada, H. Yamauchi and S. Tanaka, "NMR Study of Local Hole Distribution, Spin Fluctuation and Superconductivity in $Tl_2Ba_2Ca_2Cu_3O_{10}$", *Physica C* **260** (1996) 197-210.

[100] R. F. Egerton, "Electron Energy Loss Specroscopy in the Electron Microscope" (Plenum Press, New York, 1986).

[101] N. Nücker, J. Fink, J. C. Fuggle, P. J. Durham and W. M. Temmerman, "Evidence for Holes on Oxygen Sites in the High-T_c Superconductors $La_{2-x}Sr_xCuO_4$ and $YBa_2Cu_3O_{7-\delta}$", *Phys. Rev. B* **37** (1988) 5158-5163.

[102] J. Zaanen, M. Alouani and O. Jepsen, "X-ray Absorption of $YBa_2Cu_3O_7$: A Band Picture", *Phys. Rev. B* **40** (1989) 837-840.

[103] H. Romberg, M. Alexander, N. Nücker, P. Adelmann and J. Fink, "Electronic Structure of the System $La_{2-x}Sr_xCuO_{4+\delta}$", *Phys. Rev. B* **42** (1990) 8768-8771.

[104] H. Romberg, N. Nücker, M. Alexander, J. Fink, D. Hahn, T. Zetterer, H. H. Otto and K. F. Renk, "Density and Symmetry of Unoccupied Electronic States of $Tl_2Ba_2CaCu_2O_8$", *Phys. Rev. B* **41** (1990) 2609-2611.

[105] N. Nücker, H. Romberg, X. X. Xi, J. Fink, B. Gegenheimer and Z. X. Zhao, "Symmetry of Holes in High-T_c Superconductors", *Phys. Rev. B* (1989) 6619-6629.

[106] A. Bianconi, M. Santis, A. D. Cicco, A. M. Flank, A. Fontaine, P. Lagarde, H. Katayama-Yoshida, A. Kotani and A. Marcelli, "Symmetry of the $3d^9$ Ligand Hole Induced by Doping in $YBa_2Cu_3O_{7-\delta}$", *Phys. Rev. B* **38** (1988) 7196-7199.

[107] N. Nücker, E. Pellegrin, P. Schweiss, J. Fink, S. L. Molodtsov, C. T. Simmons, G. Kaindl, W. Frentrup, A. Erb and G. Müller-Vogt, "Site-Specific and Doping-dependent Electronic Structure of $YBa_2Cu_3O_x$ Probed by O 1*s* and Cu *2p* X-ray-Absorption Spectroscopy", *Phys. Rev. B* **51** (1995) 8529-8542.

[108] B. R. Sekhar, F. Studer, K. B. Garg, Y. Moriwaki, C. Gasser and K. Tanabe, "Increase Density of the In-plane and Out-plane Doping Holes in the Superconducting State of $HgBa_2Ca_2Cu_3O_y$", *Phys. Rev. B* **56** (1997) 14809-14814.

[109] M. Merz, N. Nücker, P. Schweiss, S. Schuppler, C. T. Chen, V. Chakarian, J. Freeland, Y. U. Idzerda, M. Kläser, G. Müller-Vogt and T. Wolf, "Site-Specific X-ray-Absorption Spectroscopy of $Y_{1-x}Ca_xBa_2Cu_3O_{7-y}$: Overdoping and Role of Apical Oxygen for High Temperature Superconductivity", *Phys. Rev. Lett.* **80** (1998) 5192-5195.

[110] A. Q. Pham, N. Merrien, A. Maignan, F. Studer, C. Michel and B. Raveau, "Origin of the Metal-Insulator Transition in the Superconducting Series $Bi_2Sr_2Ca_{1-x}Y_xCu_2O_{8+\delta}$", *Physica C* **210** (1993) 350-358.

[111] F. Studer, D. Bourgault, C. Martin, R. Retoux, C. Michel, B. Raveau, E. Dartyge and A. Fontaine, "Valence States of Lead, Thallium and Copper in Superconducting Cuprates by XANES", *Physica C* **159** (1989) 609-615.

[112] S.-J. Hwang, J.-H. Choy and N. H. Hur, "*In situ* Temperature-Dependent X-ray-Absorption Spectroscopy Studies for the Mercury-based Superconductors", *Phys. Rev. B* **57** (1998) 1259-1265.

[113] M. A. v. Veenendaal and G. A. Sawatzky, "Intersite Interaction in Cu *L*-edge XPS, XS, XES of Doped andUndoped Cu Compounds", *Phys. Rev. B* **1994** (1994) 3473-3482.

[114] J. M. Tranquada, S. M. Heald, W. Kunnmann, A. R. Moodenbaugh, S. L. Qiu, Y. Xu and P. K. Davies, "Comparative Study of Cu *K*-edge X-ray-Absorption nad Cu 2*p* X-ray Photoelectron Spectra in Copper Oxide compounds", *Phys. Rev. B* **44** (1991) 5176-5189.

[115] M. Takemoto, H. Ikawa, N. Ohashi, T. Ohyama, T. Tsurumi, O. Fukunaga, J. Tanaka and A. Watanabe, "Cu *K* Edge X-ray Absorption Spectra of $La_2SrCu_2O_6$-type Superconductor", *Physica C* **302** (1998) 151-158.

[116] K. Gjønnes, N. Bøe and J. Taftø, "Distribution of Holes in $YBa_2Cu_3O_7$ from Convergent Beam Electron Diffraction", *Ultramicroscopy* **48** (1993) 37-41.

[117] Y. Zhu and J. Tafto, "Measurement of Charge Transfer in $YBa_2Cu_3O_7$ Using Novel Electron Diffraction", *Philos. Mag. B* **75** (1997) 785-791.

[118] L. Wu, Y. Zhu and J. Tafto, "Test of First-Principle Calculations of Charge Transfer and Electron-Hole Distribution in Oxide Superconductors by Precise Measurements of Structure Factors", *Phys. Rev. B* **59** (1999) 6035-6038.

[119] M. Werner, G. Brandstätter, F. M. Sauerzopf, H. W. Webner, A. Hoekstra, R. Surdeanu, R. J. Wijngaarden, R. Griessen, Y. Abulafia and Y. Yeshurun, "Comparative Study of Global and Local Magnetization Measurements on Single Crystalline High-T_c Superconductors", *Physica C* **303** (1998) 191-201.

[120] K. Fujinami, H. Suematsu, M. Karppinen and H. Yamauchi, "Effect of Overdoping on the Irreversibility Field and Critical Current Density of the $HgBa_2Ca_2Cu_3O_{8+z}$ Superconductor", *Physica C* **307** (1998) 202-208.

[121] H. Yamauchi, M. Karppinen, K. Fujinami, T. Ito, H. Suematsu, K. Matsuura and K. Isawa, "Strongly Overdoped States and Irreversibility-Field Characteristics of the Hg-1223 and Cu-1223:P Superconducting Cuprates", *Supercond. Sci. Technol.* **11** (1998) 1006-1010.

[122] T. Nakane, K. Fujinami, M. Karppinen and H. Yamauchi, "Magnetic-Field Irreversibility in Superconducing $Cu(Ba_{0.8}Sr_{0.2})_2(Yb_{1-x}Ca_x)Cu_2O_{6+z}$ with Controlled Distribution of Holes", *Supercond. Sci. Technol.* **12** (1999) 242-247.

[123] C. P. Bean, "Magnetization of High-Field Superconductors", *Rev. Mod. Phys.* **36** (1964) 31-39.

[124] F. Supple, A. M. Campbell and J. R. Cooper, "An Investigation of the Irreversibility Line in $Bi_2Sr_2CaCu_2O_8$ Single Crystals", *Physica C* **242** (1995) 233-245.

[125] N. Ihara and T. Matsushita, "Effect of Flux Creep on Irreversibility Lines in Superconductors", *Physica C* **257** (1996) 223-231.

[126] Q. Li, M. Suenaga, Q. Li and T. Freltoft, "Sample Size Effect on the Determination of the Irreversibility line of High-T_c Superconductors", *Appl. Phys. Lett.* **64** (1994) 250-252.

[127] M. P. A. Fisher, "Vortex-Grass Superconductivity: A Possible New Phase in Bulk High-T_c Oxides", *Phys. Rev. Lett.* **62** (1989) 1415-1418.

[128] T. Matsushita and T. Kiss, "Thermal Depinning of Flux Lines in Superconductors", *Physica C* **315** (1999) 12-22.

[129] A. Gupta, P. Esquinanzi, H. F. Braun and H.-W. Neumüller, "Thermally Activated Depinning in Polycrystalline Bi-Based High-T_c Superconductors", *Phys. Rev. Lett.* **63** (1989) 1869-1872.

[130] T. Matsushita, "On the Origin of the Irreversibility Line in Superconductors — Depinning or Melting of Fluxoids", *Physica C* **214** (1993) 100-106.

[131] M. Suenaga, A. K. Ghosh, Y. Xu and D. O. Welch, "Irreversibility Temperatures of Nb_3Sn and Nb-Ti", *Phys. Rev. Lett.* **66** (1991) 1777-1780.

[132] Y. S. Song, M. Hirabayashi, H. Ihara and M. Tokumoto, "Anisotropy of the Irreversibility Lines for c-Axis-Aligned $HgBa_2Ca_2Cu_3O_{8+\delta}$ Powders", *Phys. Rev. B* **50** (1994) 16644-16648.

[133] Z. J. Huang, Y. Y. Xue, R. L. Meng and C. W. Chu, "Irreversibility Line of the $HgBa_2CaCu_2O_{6+\delta}$ High-Temperature Superconductors", *Physica C* **49** (1994) 4218-4221.

[134] H. Kumakura, H. Kitaguchi, K. Togano, H. Maeda, J. Shimoyama, S. Okayasu and Y. Kazumata, "Effect of High-Energy Ion Irradiation and Electron Irradiation on Textured $Bi_2Sr_2CaCu_2O_x$ — 180-MeV Cu^{11+} and Br^{11+} Irradiations and 3-MeV Electron Irradiation", *J. Appl. Phys.* **74** (1993) 451-457.

[135] A. Umezawa, W. Zhang, A. Gurevich, Y. Feng, E. E. Hellstrom and D. C. Larbalestier, "Flux Pinning, Granulality and the Irreversibility Line of the High-T_c Superconductor $HgBa_2CuO_{4+x}$", *Nature* **364** (1993) 129-131.

[136] U. Welp, G. W. Crabtree, J. L. Wagner, D. G. Hinks and P. G. Radaelli, "The Irreversibility line of $HgBa_2CuO_{4+\delta}$", *Appl. Phys. Lett.* **63** (1993) 693-695.

[137] U. Welp, G. W. Crabtree, J. L. Wagner and D. G. Hinks, "Flux Pinning and the Irreversibility lines in the $HgBa_2CuO_{4+\delta}$, $HgBa_2CaCu_2O_{6+\delta}$, $HgBa_2Ca_2Cu_3O_{8+\delta}$ compounds", *Physica C* **218** (1993) 373-378.

[138] K. Isawa, A. Tokiwa-Yamamoto, M. Itoh, S. Adachi and H. Yamauchi, "Pb-Doping Effect on Irreversibility Fields of $HgBa_2Ca_2Cu_3O_{8+\delta}$ Superconductors", *Appl. Phys. Lett.* **65** (1994) 2105-2107.

[139] K. Isawa, T. Higuchi, T. Machi, A. Tokiwa-Yamamoto, S. Adachi, M. Murakami and H. Yamauchi, "Irreversibility Line for a Pb-Doped Hg-Ba-Ca-Cu-O Superconductor", *Appl. Phys. Lett.* **64** (1994) 1301-1303.

[140] O. Chmaissem, P. Guptasarma, U. Welp, D. G. Hinks and J. D. Jorgensen, "Effect of Re Substitution on the Defect Structure, and Superconducting Properties of $(Hg_{1-x}Re_x)Ba_2Ca_{n-1}Cu_nO_{2n+2+\delta}$ (n=2,3,4)", *Physica C* **292** (1998) 305-314.

[141] J. Krelaus, M. Reder, J. Hoffmann and H. C. Freyhardt, "Magnetization and Relaxation in Hg-1223: Bulk vs. Surface Irreversibility, Anisotropy and Influence of Re-Doping", *Physica C* **314** (1999) 84-92.

[142] O. Chmaissem, J. D. Jorgensen, K. Yamaura, Z. Hiroi, M. Takano, J. Shimoyama and K. Kishio, "Crystal Structure of Hg-Sr-Ca-Cu-O Superconductors with Enhanced Flux Pinning: $Hg_{1-x}Re_xSr_2Ca_{n-1}Cu_nO_{2n+2+\delta}$ (n = 2, 3; x ≈ 0.2-0.25)", *Phys. Rev. B* **53** (1996) 14647-14655.

[143] D. H. Kim, K. E. Gray, R. T. Kampwirth, J. C. Smith, D. S. Richeson, T. J. Marks, J. H. Kang, J. Talvacchio and M. Eddy, "Effect of Cu-O Layer Spacing on the Magnetic Field Induced Resistive Broadening of High-Temperature Superconductors", *Physica C* **177** (1991) 431-437.

[144] K. Kishio, J. Shimoyama, T. Kimura, Y. Kotaka, K. Kitazawa, K. Yamafuji, Q. Li and M. Suenaga, "Carrier Doping and Interlayer Coupling in HTSC Single Crystals", *Physica C* **235-240** (1994) 2775-2776.

[145] J. L. Tallon, V. M. Williams, C. Bernhard, D. M. Pooke, M. P. Staines, J. D. Johnson and R. H. Meinhold, "Interplaner Coupling, Induced Superconductivity, and van Hove Singularity in High-T_c Cuprates", *Phys. Rev. B* **53** (1996) R11972-R11975.

[146] J. Schwartz, S. Nakamae, J. G. W. Raban, J. K. Heuer, S. Wu, J. L. Wagner and D. G. Hinks, "Large Critical Current Density in Neutron-irradiated Polycrystalline $HgBa_2Cu0_{4+\delta}$", *Phys. Rev. B* **48** (1993) 9932-9934.

[147] R. Usami, M. Itoh, A. Fukuoka, X.-J. Wu and K. Tanabe, "Microstructure of Proton-Irradiated $HgBa_2Ca_{(n-1)}Cu_nO_y$ (n= 2,3)", *Physica C* **269** (1996) 193-197.

[148] Y. Kazumata, H. kumakura and K. Togano, "Vortex Pinning in $Bi_2Sr_2CaCu_2O_8$ Tapes Irradiated by Ions", *Phys. Rev. B* **54** (1996) 16206-16210.

[149] G. P. Summers, E. A. Burke, D. B. Chrisey, N. Nastasi and J. R. Tesmer, "Effect of Particle-induced Displacements on the Critical Temperature of $YBa_2Cu_3O_{7-\delta}$", *Appl. Phys. Lett.* **55** (1989) 1469-1471.

[150] K. Kishio, "Anisotropy on HTSC Oxides: Its Chemical Control and Flux Pinning" in *Coherence in Superconductors*, edited by G. Deutscher and A. Revcolevschi (World Scientific Pub., Singapore, 1996), pp. 212-225.

[151] J. R. Waldram, "States with internal flux" in *Superconductivity of Metals and Cuprates* (Institute of Physics Publishing, Bristol and Philadelphia, 1996), pp. 85-86.

[152] M. Baert, V. V. Metlushko, C. D. Potter, E. Rosseel, R. Jonckheere, V. V. Moshchalkov and Y. Bruynseraede, "Critical Currents and Flux Phases in Superconducting MultiLayers with a Lattice of Submicrometer holes", *Physica C* **235-240** (1994) 2789-2790.

[153] M. Baert, V. V. Metlushko, C. D. Potter, E. Rosseel, K. Temst, R. Jonckheere, A. Gilabert, V. V. Moshchalkov and Y. Bruynseraede, "Enhanced Pinning and Matching Effects in Superconducting Films with a Lattice of Submicrometer holes", *Physica C* **235-240** (1994) 2791-2792.

[154] G. Yang, P. Shang, S. D. Sutton, I. P. Jones, J. S. Abell and C. E. Gough, "Competing pinning mechanism in Bi2Sr2CaCu2Oy Single Crystals by Magnetic and Defect Structural Studies", *Phys. Rev. B* **48** (1993) 4054-4060.

[155] V. Hardy, A. Wahl, A. Ruyter, A. Maignan, C. Martin, L. Coudrier, J. Provost and C. Simon, "The Fishtail Effect in Different Tl Based Single Crystals. A Pssible Interplay with the Electronic Anisotropy", *Physica C* **232** (1994) 347-358.

[156] M. Kawano, K. Fujinami, H. Suematsu, T. Onda, M. Hayakawa, M. Karppinen, H. Ogiwara and H. Yamauchi, "Peak Effect in Stoichiometric $SmBa_2Cu_3O_y$", *Mater. Sci. Engineering B* **54** (1998) 123-127.

[157] P. D. Panetta, J. E. Ostenson and D. K. Finnemore, "Pinning mechanisms in $YBa_2Cu_3O_{7-\delta}$ Single Crystals", *Phys. Rev. B* **52** (1995) 15570-15574.

[158] A. I. Larkin and Y. V. Ovchinnikov, "Pinning in Type II Superconductors", *J. Low Temp. Phys.* **34** (1979) 409-428.

[159] M. Daeumling, J. M. Seuntjens and D. C. Larbalestier, "Oxygen-Defect Flux Pinning, Anomalous Magnetization and Intra-Grain Granularity in $YBa_2Cu_3O_{7-d}$", *Nature* **346** (1990) 332-335.

[160] J. L. Vargas and D. C. Larbalestier, "Flux Pinning by Ordered Oxygen-Deficient Phases in Nearly Stoichiometric $YBa_2Cu_3O_{7-\delta}$ Single Crystals", *Appl. Phys. Lett.* **60** (1992) 1741-1743.

[161] A. E. Koshelev and V. M. Vinokur, "Pinning-Induced Transition to Disordered Vortex Phase in Layered Superconductors", *Phys. Rev. B* **57** (1998) 8026-8033.

[162] A. Tokiwa-Yamamoto, S. Adachi, K. Isawa, X. Wu, M. Itoh and H. Yamauchi, "Synthesis and Superconductivity of Hg-Ba-Ca-Cu-O Superconductors", in: *Advances in Superconductivity* **VI**, T. Fujita and N. Koshizuka (eds.) (Springer-Verlag Tokyo, 1994), pp. 247-250.

[163] T. Ito, H. Suematsu, M. Karppinen and H. Yamauchi, "Oxygen Content in High-Pressure Synthesized $CuBa_2Ca_3Cu_4O_{10+\delta}$ (Cu-1234:P) Superconductor", *Physica C* **308** (1998) 198-202.

[164] C. S. Gopinath, N. H. Hur and S. Subramanian, "Oxidation State of Mercury in $HgBa_2(Ca_{0.86}Sr_{0.14})_2Cu_3O_{8+\delta}$ Studied by X-ray Photoelectron Spectoroscopy", *Phys. Rev. B* **52** (1995) R9879-R9881.

[165] D. J. Singh and W. E. Pickett, "Electronic Structure Studies of Doped and Undoped Hg-Ba-Ca-Cu-O", *Physica C* **235-340** (1994) 2113-2114.

[166] S. M. Loureiro, E. T. Alexandre, E. V. Antipov, J. J. Capponi, S. d. Brion, B. Souletie, J. L. Tholence, M. Marezio, Q. Huang and A. Santoro, "Suppression of Superconductivity and the Overdoped Region in $HgBa_2CuO_{4+\delta}$", *Physica C* **243** (1995) 1-9.

[167] T. Matsushita, E. S. Otabe, T. Nakane, M. Karppinen and H. Yamauchi, "Evaluation of Irreversible Property in superconducting $Cu(Ba_{0.8}Sr_{0.2})_2YbCu_2O_{6+z}$ powder", *Physica C* **322** (1999) 100-104.

[168] R. S. Liu and J. M. Chen, "The Study of the Hole Distribution in High-T_c 1212-Type Cuprates via X-ray Absorption Spectrocopy", *Supercond. Sci. Technol.* **11** (1998) 1028-1031.

[169] L. Klein, E. R. Yacoby, Y. Yeshurun, A. Erb, G. Müller-Vogt, V. Breit and H. Wühl, "Peak Effect and Scaling of Irreversible Properties in Untwinned Y-Ba-Cu-O Crystals", *Phys. Rev. B* **49** (1994) 4403-4406.

[170] N. Kobayashi, K. Hirano, T. Nishizaki, H. Iwasaki, T. sasaki, S. Awaji, K. Watanabe, H. Asaoka and H. Takei, "Anisotopic Properties of the Anomalous Second Peak in the Magnetization Curves and the Irreversibility Field of $YBa_2Cu_3O_y$ ($6.6 \leq y \leq 6.9$) Single Crystals", *Physica C* **251** (1995) 255-262.

[171] A. Wahl, V. Hardy, A. Maignan, C. Martin and B. Raveau, "Irreversibility Line and Critical Current Densities of '1223' Cuprates $TlBa_2Ca_2Cu_3O_9$: A Single Cystal Study", *Cryogenics* **34** (1994) 941-945.

[172] S. Lee, T. Akao, H. Suematu, H. Yamauchi, N. P. Kiryarov, D. A. Emelyanov and M. S. Kuzunetsov, "Enhanced Pinning and Peak Effect in Overdoped $(Hg,Pb)(Sr,Ba)_2Ca_2Cu_3O_{8+\delta}$ Superconductors", *Appl. Phys. Lett.* **73** (1998) 3586-3588.

[173] T. Akao, S. Lee, N. Kiryakov, D. Emelyanov, H. Suematu and H. Yamauchi, "Single Crystal Study of Enhanced Flux Pinning in $(Hg,Pb)(Ba,Sr)_2Ca_2Cu_3O_{8+\delta}$ and $(Hg,Pb)Sr_2Ca_2Cu_3O_{8+\delta}$", in: *Advances in Superconductivity* **XI**, N. Koshizuka and S. Tajima (eds.) (Springer-Verlag, Tokyo, 1999), pp. 393-396.

[174] A. Wahl, A. Maignan, V. Hardy, J. Provost, C. Simon and B. Raveau, "Magnetic Study of an Overdoped "1223" System: $TlBa_{0.8}Sr_{1.2}Ca_2Cu_3O_{9-\delta}$ Single Cystals", *Physica C* **244** (1995) 341-348.

[175] S. Kokkaliaris, S. N. Godeev, P. A. J. d. Groot, X. M. Yang and M. T. Weller, "Magnetization stydies of $Tl_{0.6}Pb_{0.4}Ba_{0.3}Sr_{1.7}CaCu_2O_y$ Single Crystals", *Physica C* **309** (1998) 49-55.

[176] M.-K. Bae, M. S. Choi, M.-O. Mun, S. Lee, S.-I. Lee and W. C. Lee, "Surface Barrier Effect of Isothermal Magnetization of Grain-aligned $HgBa_2Ca_2Cu_3O_8$", *Physica C* **234** (1994) 207-210.

[177] M. Reissner, "Surface versus Bulk Pinning in a $HgBa_2Ca_2Cu_3O_{8+x}$ Ceramics", *Physica C* **290** (1997) 173-187.

[178] Y. C. Kim, J. R. Thompson, D. K. Christen, Y. R. Sun, M. Paranthaman and E. D. Specht, "Surface Barriers, Irreversibility Line, and Pancake Vortices in an Aligned $HgBa_2Ca_2Cu_3O_{8+\delta}$ Superconductor", *Phys. Rev. B* **52** (1995) 4438-4444.

[179] G. C. Kim and Y. C. Kim, "Surface-barrier Effect for Irreversible Properties in the Grain-aligned $HgBa_2Ca_2Cu_3O_{8+\delta}$ Superconductor", *Physica C* **259** (1996) 218-221.

[180] Y. R. Kim, J. R. Thompson, J. Schwartz, D. K. Christen, Y. C. Kim and M. Paranthaman, "Surface Barrier in Hg-based Polycrystalline Superconductors", *Phys. Rev. B* **51** (1995) 581-588.

[181] J. A. Lewis, V. M. Vinokur, J. Wagner and D. Hinks, "Surface-barrier Effect in the Grain-aligned $HgBa_2CuO_{4+\delta}$, $HgBa_2CaCu_2O_{6+\delta}$ and $HgBa_2Ca_2Cu_3O_{8+\delta}$ Compounds", *Phys. Rev. B* **52** (1995) R3852-3855.

[182] H. Küpfer, A. A. Zhukov, R. Kresse, R. Meier-Hirmer, W. Jahn, T. Wolf, T. Matsushita, K. Kimura and K. Salama, "Comparison of Pinning Parameters Between Low-T_c Superconductors and $YBa_2Cu_3O_{7-\delta}$", *Phys. Rev. B* **52** (1995) 7689-7700.

[183] M. R. Koblischka, A. J. J. v. Dalen, T. Higuchi, K. Sawada, S. I. Yoo and M. Murakami, "Observations of Multiple peaks in the Magnetization Curves of $NdBa_2Cu_3O_7$ single crstals", *Phys. Rev. B* **54** (1996) R6893-R6896.

[184] R. S. Liu, S. F. Hu, D. H. Chen, D. S. Shy and D. A. Jefferson, "Crystal Structure of the $(Pb,Hg)Sr_2(Ca,Y)Cu_2O_{7-\delta}$ Superconductor", *Physica C* **222** (1994) 13-18.

[185] M. Nakamura, T. Hirayama, Y. Yamada, Y. Ikuhara and Y. Shiohara, "Correlation between Anomalous Peak Effect in Magnetic Hysteresis Loop and Nanoscale Structure for $NdBa_2Cu_3O_{7-\delta}$ Single-Crystal Superconductor", *Jpn. J. Appl. Phys.* **35** (1996) 3882-3886.

[186] T. Hirayama, Y. Ikuhara, M. Nakamura, Y. Yamada and Y. Shiohara, "Periodic Fluctuation of Ba/Nd ratio in Single Crystals of High-J_c $NdBa_2Cu_3O_{7-\delta}$ Superconductor", *J. Mater. Res.* **12** (1997) 293-295.

[187] I. Chong, Z. Hiroi, M. Izumi, J. Shimoyama, Y. Nakayama, K. Kishio, T. Terashima, Y. Bando and M. Takano, "High Critical-Current Density in the Heavily Pb-Doped $Bi_2Sr_2CaCu_2O_{8+\delta}$ Superconductor: Generation of the Efficient Pinning Centers", *Science* **276** (1997) 770-773.

[188] Z. Hiroi, I. Chong and M. Takano, "Two-Phase Micro structure Generating Efficient Pinning Centers in the Heavily Pb-sbstituted $Bi_2Sr_2CaCu_2O_{8+\delta}$ Single Crystals", *J. Solid State Chem* **138** (1998) 98-110.

[189] Y. Tanaka, K.-I. Udoh, K. Hisatsune and K. Yasuda, "Early Stage of Ordering in Stoichiometric AuCu Alloy", *Materials Transactions, JIM* **39** (1998) 87-94.

[190] T. Tamura, S. Adachi, X.-J. Wu, C.-Q. Jin, T. Tatsuki and H. Yamauchi, "115 K Superconductivity in the Pb-Sr-Ca-Cu-O System and Formation of a New Homologous Series Consisting of Pb-based Layered Cuprates", *Physica C* **249** (1995) 111-116.

[191] R. Griessen, W. Hai-hu, A. J. J. v. Dalen, B. Dam, J. Rector, H. G. Schnack, S. Libbrecht, E. Osquiguil and Y. Bruynseraede, "Evidence for Mean Free Path Fluctuation Induced Pinning in the $YBa_2Cu_3O_7$ and $YBa_2Cu_4O_8$ Films", *Phys. Rev. Lett.* **72** (1994) 1910-1913.

[192] H. H. Wen, Z. X. Zhao, Y. G. Xiao, B. Yin and J. W. Li, "Evidence for Flux Pinning Induced by Spatial Fluctuation of Transition Temperatures in the Single Domain $(Y_{1-x}Pr_x)Ba_2Cu_3O_{7-\delta}$ samples", *Physica C* **251** (1995) 371-378.

[193] M. Tachiki and S. Takahashi, "Strong Vortex Pinning Intrinsic in High-T_c Oxide Superconductors", *Solid State Communications* **70** (1989) 291-295.

[194] T. Matsushita, M. Iwakuma, K. Funaki, K. Yamafuji, K. Matsumoto, O. Miura and Y. Tanaka, "Flux Pinning property of Artificially Introduced Nb in Nb-Ti Superconductors", in: *Advances in Cryogenic Engineering* **42**, L. T. Summers (eds.) (Plenum Press, New York, 1996), pp. 1103-1108.

[195] L. Fàbrega, B. Martínez, J. Fontcuberta, A. Sin, S. Piñol and X. Obradors, "The Re-doped High T_c Superconductor $HgBa_2Ca_2Cu_3O_x$: Magnetic Irreversibility Versus Anisotropy", *J. Appl. Phys.* **83** (1998) 7309-7311.

[196] R. Puzniak, J. Karpinski, A. Wisniewski, R. Szymczak, M. Angst, H. Schwer, R. Molinski and E. M. Kopnin, "Influence of Re Substitution on the Flux Pinning in $(Hg,Re)Ba_2Ca_2Cu_3O_{8+\delta}$ Single Crystals", *Physica C* **309** (1998) 161-169.

[197] A. Maignan, C. Martin, V. Hardy and C. Simon, "Magnetic Properties of a $Tl_{0.5}Pb_{0.5}Sr_2CaCu_2O_7$ Single Crystal", *Physica C* **228** (1994) 323-330.

[198] Y. C. Kim, J. R. Thompson, D. K. Christen, M. Paranthaman and E. D. Specht, "Enhanced Irreversibility Field and Current Stabilitzation by Pb Substitution in Aligned Tl-1223 High-T_c Superconductor", *Physica C* **253** (1995) 357-366.

[199] T. Hosomi, H. Suematsu, M. Karppinen and H. Yamauchi, "Magnetic Irreversibility Characteristics of Highly Unstable Superconducting $Ba_2Ca_2Cu_3O_y$ and its Derivative Phase", *Physica C* **324** (1999) 65-70.

[200] K. Yamawaki, S. Sasaki, S. Lee and H. Yamauchi, "Single-crystal Study of (Hg,Pb)-1223 Superconductor at Low Temperature", *Physica C* (submitted) .

[201] H. Suematsu, H. Okamura, S. Lee, S. Nagaya and H. Yamauchi, "A Possible Cause of Peak Effect in Y-Ba-Cu-O Melt-Grown Bulks : Modulation in Oxygen Distribution", *Physica C* (submitted) .

[202] K. Takase, K. Demachi and K. Miya, "Numerical Simulation of Fluxoid Behaviors in Bi2212 Single Crystal", in: *Advances in Superconductivity* **XI**, N. Koshizuka and S. Tajima (eds.) (Springer-Verlag, Tokyo, 1999), pp. 509-512.

Acknowledgements

This thesis is based on the study which I have been carried out as a member of Yamauchi group in Materials and Structures Laboratory of Tokyo Institute of Technology.

First of all, my special thanks are due to my supervisor, professor Hisao Yamauchi for his stimulation, encouragement and significant advices during the whole work written in this thesis, although, I am solely responsible for any errors. I am most grateful to Dr. Sergey R. Lee for his helpful suggestions and comments especially in sample preparations. It was my great experience that I could collaborate with him for even only two years. I am indebted to professor Maarit Karppinen for valuable suggestions and critical reading the original form of this thesis. Dr. Hisayuki Suematsu who has been kindly taking care of me in my whole study life is highly appreciated. I would like to thank Dr. Johan Lindén who patiently revised my poor English partly in Chapter II.

I gratefully acknowledge his helpful discussions with Professor Teruo Matsushita of Kyushu Institute of Technology on electromagnetic study in this work. I am grateful to professor Yoshitsugu Tomokiyo of Kyushu University for his instructive suggestions to our TEM study. Special thanks are due to Mr. Keiji Kurashima and Dr. Yoshio Bando of National Institute for Research in Inorganic Materials (NIRIM) for their helps in operations of FE-TEM (JEM-3000F). I wish to express my gratitude to Mr. Kunio Kobayashi for his assistance in TEM operations. Mr. Kouji Yamawaki and Prof. Satoshi Sasaki are appreciated for providing me with the result of single crystal study.

I am obliged to all my colleagues, Mr. T. Ito, Mr. M. Kawano, Mr. M. Nagase, Mr. K. Fujinami, Mr. H. Okamura, Mr. T. Hosomi, Mr. N. Kiryakov, Mr. M. Kochi, Mr. T. Suzuki, Mr. Y. Takahama, Mr. T. Nakane, Mr. J. Nakamura, Mr. Y. Morita, Mr. T. Yamamoto, Ms. Morooka and Mr. S. Ichikawa and other students in Yamauchi Group. Useful ideas and precious information were given from them during daily life. Especially. I would like to express my special gratitude to Mr. Tomonori Nagashima and Mr. Kohei Mizogami who has worked together with me on a common subject.

I wish to thank Ms. A. Takahashi who is a secretary of our Lab. for her support and hospitality.

14th March, 2000

Takahiro Akao

Curriculum Vitae

Name : Takahiro Akao

Born : December. 28, 1969
Tokyo, Japan

Education :

B. Engineering, 1994, Department of Electrical and Imformation Engineering, Faculty of Engineering, Yamagata Univ., Yamagata, Japan

M. Engineering, 1996, Department of Electrical and Imformation Engineering, Graduate School of Engineering, Yamagata Univ., Yamagata, Japan

Professional Experience :

Staff member in Department of Reserch and Develoment, Fuji electric, Ltd., Matsumoto, Japan, 1996-1997

Publication list :

S. Kambe, T. Akao, S. Ohshima and K. Okuyama,"Structure and physical property of $(Bi_{1-x}Cu_x)Sr_2YCu_2O_y$", in *Advances in Superconductivity* ***VI***, T. Fujita and Y. Shiohara (eds.), (Springer-Verlag, Tokyo, 1994) pp. 339-342.

S. Kambe, T. Akao, S. Ohshima and K. Okuyama, "Preparation of a single phase sample of $(Bi_{1-x}Cu_x)Sr_2YCu_2O_y$ and its physical properties", *Materials Science and Engineering* B **32** (1995) 57-61.

S. Kambe, T. Akao, S. Ohshima and K. Okuyama, "Preparation and physical properties of superconductor : $[(Bi_{1-x}Mo_x)_{0.33}Cu_{0.67}]Sr_2YCu_2O_y$ ", *Physica* C **255** (1995) 151-156.

S. Lee, T. Akao, H. Suematsu, H. Yamauchi, N. P. Kiryakov, D. A. Emelyanov and M. S. Kuzunetsov, "Enhanced pinning and peak effect in overdoped $(Hg,Pb)(Ba,Sr)_2Ca_2Cu_3O_{8+\delta}$ superconductors", *Appl. Phys. Lett.* **73** (1998) 3586-3588.

H. Yamauchi, M. Karppinen, K. Fujinami, T. Itoh, T. Akao, Sergey Lee and H. Suematsu, "The over-doped state in M-1223 (M = Hg, Cu) superconducting cuprates", in *Abstracts: 5th International workshop on High-Temperature Superconductors and novel Inorganic Materials Engeneering (MSU-HTSC V)* (Moscow State University, Moscow, 1998) pp.OR34.

Sergey Lee, T. Akao, H. Suematsu, N. P. Kiryakov, M. S. Kuznetsov, D. A. Emelyanov and Yu D.Tretyakov, "Effect of Pb and Sr substitutions on irreversibility and fishtail lines of Hg-1223 phase: powder, ceramic and single crystal studies", in *High-Temperature Superconductors and Novel Inorganic Materials*, G.van Tendeloo (ed.), (1999) pp.193-198.

T. Akao, S. Lee, N. Kiryakov, D. Emelyanov, H. Suematsu and H. Yamauchi, "Single crystal study of enhanced flux pinning in $(Hg,Pb)(Ba,Sr)_2Ca_2Cu_3O_{8+\delta}$ and $(Hg,Pb)Sr_2Ca_2Cu_3O_{8+\delta}$", in *Advances in Superconductivity* ***XI***, N. Koshizuka and S. Tajima (eds.), (Springer-Verlag, Tokyo, 1999) pp. 393-396.

H. Yamauchi, T. Akao and H. Suematsu, "Peak effect in the High T_c Superconductors", in *Proceedings of 2nd International Synposium on Electronic Component Materials,* (KAIST, Taejon , Korea, 1999) pp. 81-86.

S. Kambe, E. Sato, T. Akao, S. Ohshima, K.Okuyama and R. Sekine, "Superconductivity above 30 K in $[(Bi_{1-x}Mo_x)_{0.33}Cu_{0.67}]Sr_2YCu_2O_y$ ~Appearance of superconductivity by transfer of holes from a block layer to a CuO_2 layer~", *Phys. Rev. B* **60** (1999) 687-697.

T. Akao, S. R. Lee, H. Suematsu, K. Kurashima, Y. Bando and H. Yamauchi, "Peak effect caused by compositional modulation in superconducting (Hg,Pb)(Ba,Sr)-1223 single crystals", in *Proceedings of Physics and Chemistry of Molecular and Oxide Superconductors, Stockholm Sweeden, 28 July-2 August 1999*, *J. Low Temp. Phys.* **117** (1999) 933-937.

T. Akao, S. R. Lee, K. Mizogami, H. Suematsu and H. Yamauchi, "Irreversibility-field enhancement by optimizing hole density distribution in the Hg-1212 Superconductor", *to appear in Physica C* .

T. Akao, S. R. Lee, H. Suematsu, K. Kurashima and H. Yamauchi, "Mesoscopic Modulation and Peak Effect Phenomenon in Superconducting (Hg,Pb)-1223 Single Crystal", to be submitted.

Conferences:

T. Akao, S. Kambe, I. Shime, S. Ohshima and K. Okuyama, "Synthesis and physical properties of $(Bi_{1-x}Cu_x)Sr_2YCu_2O_y$", The Japan Society of Applied Physics, (The 54th Autumn Meeting), Oct. 1993, Hokkaido Univ. (Sapporo).

S. Kambe, T. Akao, I. Shime, S. Ohshima and K. Okuyama, "Synthesis and physical properties of $(Bi_{1-x}Cu_x)Sr_2YCu_2O_y$: (II)", The Japan Society of Applied Physics, (The 55th Autumn Meeting), Aug. 1994, Meijo Univ. (Nagoya).

S. Kambe, T. Akao, S. Ohshima and K. Okuyama, "Synthesis and physical properties of (Bi,Mo,Cu)$Sr_2Y_1Cu_2O_y$ superconductor", The Japan Society of Applied Physics and Related Societies, (The 42th Spring Meeting), Mar. 1995, Tokai Univ. (Tokyo).

S. Kambe, T. Akao, R. Sekine, S. Ohshima and K. Okuyama, "A DV-X_α calculation study on electronic structure of CuO_2 plane in the $(Bi_{0.33}Cu_{0.67})Sr_2YCu_2O_y$", The Japan Society of Applied Physics, (The 56th Autumn Meeting), Sep. 1995, Kanazawa Univ. (Kanazawa).

T. Akao, S. R. Lee, H. Suematsu and H. Yamauchi, "Peak effect in $(Hg,Pb)(Ba,Sr)_2Ca_2Cu_3O_{8+\delta}$ superconductors", The Japan Society of Applied Physics and Related Societies, (The 45th Spring Meeting), Mar. 1998, Tokyo Engineering Univ. (Tokyo).

T. Akao, S. R. Lee, H. Suematsu and H. Yamauchi, "Microstructures and Peak Effect in Superconducting Cuprates I : Peak effect in $(Hg,Pb)(Ba,Sr)_2Ca_2Cu_3O_{8+z}$ single cristals", The Japan Society of Applied Physics, (The 59th Autumn Meeting), Sep. 1999, Hiroshima Univ. (Hiroshima).

T. Akao, S. R. Lee, H. Suematsu, K. Kurashima and H. Yamauchi, "Microstructures and Peak Effect in Superconducting Cuprates III : Compositional modulation and peak effect in $(Hg,Pb)(Ba,Sr)_2Ca_2Cu_3O_{8+\delta}$ single crystals", The Japan Society of Applied

Physics and Related Societies, (The 46th Spring Meeting), Mar. 1999, Tokyo Univ. of Science, (Tokyo).

T. Akao, H. Suematsu, S. R. Lee, K. Kurashima, Y. Bando and H. Yamauchi, "Obsevation of the Phase Separation in (Hg,Pb)(Ba,Sr)$_2$Ca$_2$Cu$_3$O$_{8+\delta}$ Superconductors using a Field Emission Analytical Electron Microscope", The Japanese Society of Electron Microscopy, (The 55th Annual Meeting), May 1999, Nagoya Congress Center (Nagoya).

T. Akao, S. R. Lee, H. Suematsu, K. Kurashima, Y. Bando and H. Yamauchi, "Peak effect caused by compositional modulation in superconducting (Hg,Pb)(Ba,Sr)-1223 single crystals", Physics and Chemistry of Molecular and Oxide Superconductors, 28 July-2 Aug. 1999, Stockholm, Sweeden.

T. Akao, K. Mizogami, S. R. Lee, H. Suematsu and H. Yamauchi, "Enhancement of H_{irr} with controlling of hole distribution in Hg-1212 superconductors", The Japan Society of Applied Physics, (The 60th Autumn Meeting), Sep. 1999, Konan Univ. (Kobe).

T. Akao, K. Mizogami, S. R. Lee, H. Suematsu and H. Yamauchi, "Irreversibility-field Enhancement by Optimizing Hole Distribution in the Hg-1212 Superconductor", International Workshop on Chemical Designing and Processing of High-T_c Superconductors V, Oct. 1999, Tokyo Inst. Tech. (Tokyo).